CHEMICAL REVIEWS

pubs.acs.org/CR

Review

Microfluidics for Neuronal Cell and Circuit Engineering

Rouhollah Habibey,[§] Jesús Eduardo Rojo Arias,[§] Johannes Striebel, and Volker Busskamp*

Cite This: *Chem. Rev.* 2022, 122, 14842−14880

Read Online

ACCESS | Metrics & More | Article Recommendations

ABSTRACT: The widespread adoption of microfluidic devices among the neuroscience and neurobiology communities has enabled addressing a broad range of questions at the molecular, cellular, circuit, and system levels. Here, we review biomedical engineering approaches that harness the power of microfluidics for bottom-up generation of neuronal cell types and for the assembly and analysis of neural circuits. Microfluidics-based approaches are instrumental to generate the knowledge necessary for the derivation of diverse neuronal cell types from human pluripotent stem cells, as they enable the isolation and subsequent examination of individual neurons of interest. Moreover, microfluidic devices allow to engineer neural circuits with specific orientations and directionality by providing control over neuronal cell polarity and permitting the isolation of axons in individual microchannels. Similarly, the use of microfluidic chips enables the construction not only of 2D but also of 3D brain, retinal, and peripheral nervous system model circuits. Such brain-on-a-chip and organoid-on-a-chip technologies are promising platforms for studying these organs as they closely recapitulate some aspects of in vivo biological processes. Microfluidic 3D neuronal models, together with 2D in vitro systems, are widely used in many applications ranging from drug development and toxicology studies to neurological disease modeling and personalized medicine. Altogether, microfluidics provide researchers with powerful systems that complement and partially replace animal models.

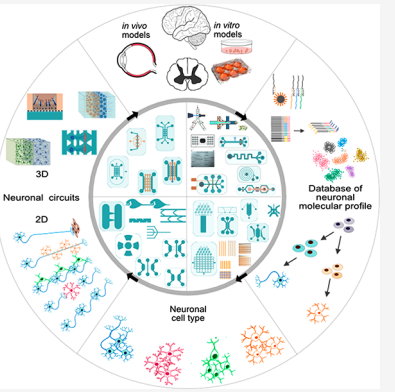

CONTENTS

Received: March 30, 2022
Published: September 7, 2022

https://doi.org/10.1021/acs.chemrev.2c00212
Chem. Rev. 2022, 122, 14842−14880

1. HIGHLIGHTS

(1) Microfluidics support a wide range of bottom-up neural engineering approaches, from the generation of neural cell types to the in vitro assembly of 2D and 3D neural circuits.
(2) Microfluidics enable the isolation of specific neuronal cell types, either from primary tissues, in vitro cultures, or brain organoids.
(3) Microfluidics-assisted sorting and molecular profiling of neurons facilitates creating comprehensive identity databases.
(4) Controlled delivery of diverse transcription factors and/or small molecule cocktails in microfluidic platforms enables high-efficiency forward programming of hiPSCs to specific neuronal cell types.
(5) Layered neural circuits with oriented connectivity are constructed by incorporating physicochemical cues in microfluidic platforms and controlling neuronal cell polarity.
(6) Microfluidic devices support brain-on-a-chip and organoid-on-chip technologies by enhancing control over 3D network structure, improving perfusion, and providing more longevous cultures.

2. INTRODUCTION

Human neural circuits within the central nervous system (CNS) are formed by various excitatory and inhibitory neuronal cell types with distinct biophysical and functional features.[1,2] Although additional cell types such as astrocytes and oligodendrocytes are also found in the brain, where they fulfill crucial support functions, neurons are the primary units of information processing and the building blocks of neural circuits. Given the complexity of neural circuits, mapping the anatomical and functional features of the brain remains a challenging task for neurobiologists.[3−6] From a clinical point of view, neuronal loss and dysfunction are both associated with a variety of neurological disorders.[2,7] Understanding the pathophysiology underlying such disorders at the cellular and circuit levels is key to developing novel and more effective therapeutic alternatives. Presently, the major approaches to understand brain function involve the use of native neural circuits within their environment in vivo, of brain slices ex vivo, and of in vivo−mimetic circuits assembled in vitro.[8−10] The latter enable to scale down the complexity of the in vivo system and to study circuit functionality under controlled experimental conditions.[5,11−14] However, conventional in vitro neuronal cultures on a flat substrate do not recapitulate the structure and organization of in vivo circuits and usually fail to mimic relevant microenvironmental cues. In this context, microfluidic devices constitute a powerful toolkit to engineer superior neuronal circuits that more closely resemble their in vivo counterparts.[15−17]

Microfluidics and microfabrication technologies have been extensively used to develop intricate devices with integrated neural cell-sized microchannels.[18−21] These devices operate with volumes in the micro- and nanoliter scales and incorporate pumps, valves, and electrokinetic elements.[22−24] Thereby, not only are they compatible with rapid and directed transport of fluids but also support the straightforward automation and parallel execution of multiple operational steps.[25−27] Further, by depositing chemical cues in the physically confined spaces of these devices, it is also possible to control neural circuit architecture and function in vitro.[13,26,28] In addition, many microfluidic devices are also compatible with optical and electrophysiological tools that enable individual neurons to be monitored, manipulated, and examined.[29−32] In the past decade, the use of microfluidics has deepened our understanding of neurons and the circuits they form by enabling the isolation and molecular profiling of single cells from primary tissues[33−35] by supporting the in vitro engineering of neural cells[36−38] and the construction of 2- and 3-dimensional neural circuits with defined spatial orientations.[16,39−41]

Advances in microfluidic technologies have been paralleled by progress in the stem cell field. Induced pluripotent stem cells (iPSCs)[42,43] offer, as embryonic stem cells (ESCs),[44,45] the possibility to produce any neuronal cell subtype in vitro. In contrast to ESCs, however, iPSCs can be created from somatic cells of any individual, thereby overcoming ethical limitations of ESCs such as depending on human embryos to obtain them.[46] iPSC-derived neurons serve as building blocks to form complex neural circuits.[47] Although there are still no protocols for the derivation of many neuronal subtypes, research on using neural stem cells (NSCs) for neural tissue engineering and repair has progressed at a steady pace,[48] with microfluidics supporting this progress by allowing to develop simplified on-a-chip models of brain circuitries.[13,49−51] Further, microfluidics have also been a major driver for omics (i.e., genomics, proteomics, transcriptomics), facilitating to extract in-depth molecular data from native brain tissues and organoids.[52] In this context, the increasing number of transcriptomic atlases characterizing the gene expression profiles of cells and/or nuclei from different brain regions represent extremely valuable databases for the field of neuronal cell engineering.[53] These databases serve as references to analyze and quality control the full spectrum of stem cell-derived neuronal subtypes.

In this review, we aim to link diverse microfluidic concepts related to the engineering of neuronal cell types with approaches for assembling simple or complex models of brain networks in vitro: the focus is set on neuroscientific applications. We cover major studies published over the last 20 years but focus primarily on the past decade due to the recent rapid progress of single-cell sequencing and organoid technologies. We feature advanced microfluidic platforms for sorting, classifying, profiling, and engineering neural cells, as well as for constructing neural circuits (Figure 1A). We also cover studies describing reprogramming, differentiation, and controlled polarization of neuronal cells through the engineering of niche-like compartments in microfluidic devices (Figure 1B,C). Finally, we review recent approaches for patterning, structuring, and engineering ordered/oriented 2D and 3D neural circuits by mimicking those found in the brain in vivo (Figure 1C,D).

3. MICROFLUIDIC PLATFORMS FOR SORTING AND CLASSIFYING NEURONAL CELL TYPES

Neurons exhibit highly variable morphological features, biophysical properties, and activity patterns in vivo.[54] However, once isolated from adult tissues, neurons are postmitotic and do not proliferate in culture. For this reason, the neurons most commonly used to engineer neural circuits in microfluidic platforms have historically been those obtained from embryonic or early postnatal animal brain tissues, which remain proliferative for a limited time before terminal differentiation

https://doi.org/10.1021/acs.chemrev.2c00212
Chem. Rev. 2022, 122, 14842−14880

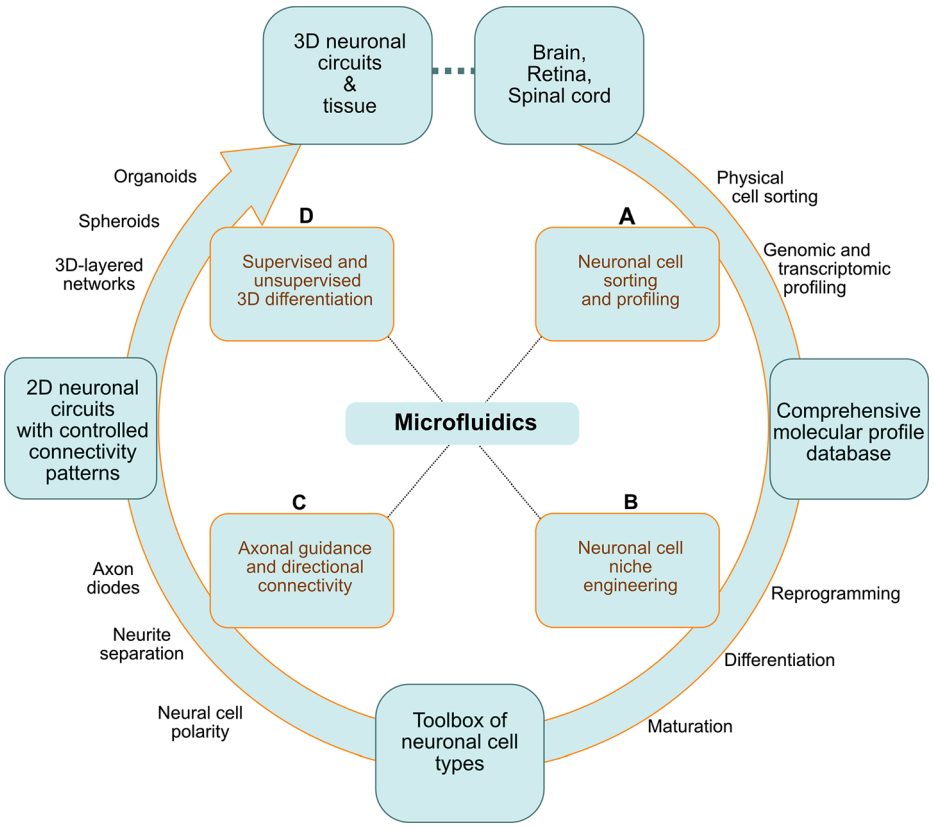

Figure 1. Diverse applications of microfluidic platforms: from molecular characterization of cells in the central nervous system to engineering neuronal cell types and neural circuits in vitro. (A) Neuronal cells extracted from native brain tissue are sorted based on their physical properties or surface markers and are classified based on their genomic or transcriptomic profile (qRT-PCR and single-cell RNA-Seq). (B) The information gathered on the molecular identity of the diverse neurons in the brain, retina, and spinal cord is useful for devising strategies to reprogram and differentiate hiPSCs into specific neuronal cell types. (C) HiPSC-derived neurons can be used to engineer 2D neural circuits or (D) be incorporated in physiologically relevant systems as 3D layered networks and organoids.

in culture (Table 3). Notwithstanding, the usefulness of these cells for the study of neural circuits is limited due to multiple factors, including: the challenging preparation and culturing procedures required, the heterogeneity of the cellular populations obtained upon isolation, and the limited number of available source tissues.[55]

NSCs represent a valuable alternative as they are capable of proliferating and differentiating into neurons, astrocytes, and oligodendrocytes.[56] NSCs can be derived either from ESCs or iPSCs.[57] These stem cells proliferate almost indefinitely and, in combination with appropriate differentiation protocols, can theoretically be differentiated into almost any human cell type.[58] Patient-specific hiPSCs are used for disease modeling and, in certain cases, in the clinical setting for autologous transplantation after gene repair.[59,60] HiPSCs can be differentiated into distinct cell types either by using specific media formulations and culturing protocols or by the introduction of genomic modifications.[61−63] Strategies for producing dopaminergic,[64−66] glutamatergic,[67,68] GABAergic,[69,70] serotonergic,[71] and cholinergic[72] neurons, as well as Schwann cells,[73] oligodendrocytes,[74] and astrocytes[75,76] from hiPSCs have been developed.

Microfluidics have been extensively used for separating and sorting both primary and cultured neurons, which have been subsequently used in single cell transcriptomic studies.[77−80] The findings of these studies are often the starting point for identifying molecular drivers of differentiation and can be used to produce neurons in vitro from ESCs or iPSCs.[81] In this sense, identifying the genetic mechanisms that drive neural stem cells toward particular neural fates (e.g., giving rise to excitatory or inhibitory phenotypes or to glutamatergic or cholinergic neurons) is essential to engineer specific neurons from stem cells with high precision.[3,72,82] Additionally, heterogeneous and polyclonal NSC- or iPSC-derived neural cultures often need to be dissociated and separated into a single-cell suspension to proceed with studies on clonal populations.[83] Here, sorting and separation steps enable the generation of high-purity neuronal cultures.[84]

3.1. Sorting Neuronal Cells by Microfluidic Platforms

Complex and heterogeneous cell mixtures derived either from a tissue or from an in vitro culture often need to be sorted to obtain pure populations of the cells of interest. Such purified cell populations can then be transcriptionally profiled to determine cellular identity or cultured for subsequent functional and morphological analyses.[85] Cell-sorting technologies separate cells based either on their biophysical properties or on the expression of cell-surface markers.[86] Conventional methods to separate and sort cells tend to be laborious and often require large sample sizes and reagent volumes.[84] In contrast, microfluidic platforms allow significant reduction of these parameters while offering tight control of flows. Numerous processing steps that further facilitate and accelerate cellular studies can be additionally incorporated into microfluidic devices. For example, sorting processes can be sped up in microfluidic devices by parallelization,[87] or reagents can be mixed and cells

https://doi.org/10.1021/acs.chemrev.2c00212
Chem. Rev. 2022, 122, 14842−14880

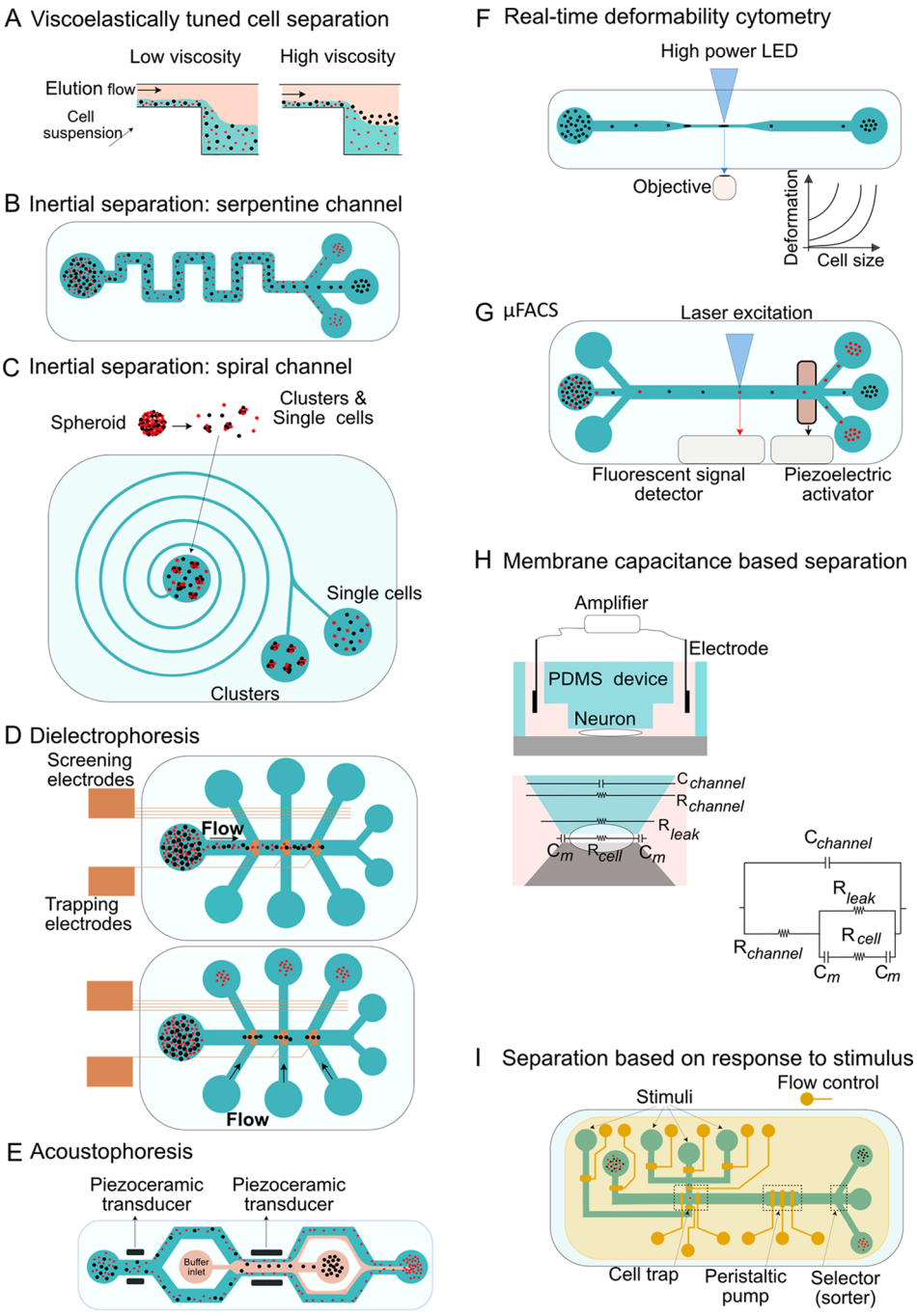

Figure 2. Different microfluidic cell-sorting strategies. (A) Cell separation using viscoelastically tuned hydrodynamic spreading. Depending on the viscosity of the elution flow and on cell size, specific cells can be separated.[94] (B) Inertial separation of neurons and glia in a serpentine microchannel. Large cells (neurons) tend to migrate to the center of the microchannel, while small glial cells that experience stronger inertial forces stay close to the sidewalls.[95] (C) Isolating single cells in neurospheres using inertial microfluidics. The curvature of the spiral microfluidic channel induces Dean's forces that push small particles and single cells toward the inner wall. Larger particles, as cell clusters, move toward the center.[83] (D) As whole cell membrane capacitance is a biomarker of stem cell fate potential and, conversely, of ongoing differentiation processes, label-free dielectrophoresis-assisted continuous sorters exploit this electrophysiological property of the plasma membrane for sorting more (e.g., neuron- or astrocyte-forming cells) or less differentiated cells (e.g., stem cells).[96,100] (E) Acoustophoresis-based separation of live neuroblastoma and human ESCs from apoptotic cells. A first piezoceramic transducer aligns the cells close to the wall, while a second one deflects their trajectory based on their acoustic properties and morphology.[97] (F) Real-time deformability cytometry enables on-the-fly analysis of cells deforming as they pass through narrow microchannels without exposing them to shear stresses or pressure gradients.[102] (G) Low-cost and simple microfluidic FACS (μFACS).[126] Label-based neuronal cell sorting can be performed in μFACS at a reduced cost. (H) Characterizing the differentiation state of neuronal stem cells based on specific membrane capacitance and cytoplasm conductivity. Cells are continuously aspirated into a constriction channel to measure these properties.[127] (I) Sorting cells based on their dynamic response to a chemical stimulus.[109] Cells are introduced to the sorting device through a flow line (depicted in green), and their movement and positions are adjusted by control lines (depicted in yellow). After trapping the cells, a stimulus is delivered through the appropriate flow line, and the cell response is measured based on calcium influx. As proof of principle, this method has been applied to separate olfactory sensory neurons that respond to specific odor cues.[109]

https://doi.org/10.1021/acs.chemrev.2c00212
Chem. Rev. 2022, 122, 14842−14880

counted, lysed, and analyzed within one single device. These systems operate as lab-on-a-chip platforms.

Microfluidics-based cell sorting techniques are broadly divided into label-free, fluorescent-based, and bead-based methods.[22,88−92] Several label-free cell-sorting microfluidic platforms have been designed to separate neuronal cell types based on their intrinsic biophysical properties[93] (Figure 2). For instance, by using viscoelastic tuning and adjusting liquid flow rate in microchannels, neuronal and glial cells derived from rat spinal cord have been separated (Figure 2A).[81,94] Similarly, an inertial microfluidic platform designed by Jin et al. separates dissociated primary neuronal and glial cells in a serpentine channel (Figure 2B), reaching purity levels above 80% at the outlet channel.[95] In this inertial platform, neuronal cells with large somas are shifted to the center of the microchannel, while small glial cells are pushed to the sides (Figure 2B). Inertial microfluidics with spiral-shaped channels (Figure 2C) have also been used to isolate neuronal cells from large cell clusters.[83]

Besides hydrodynamic-based cell-sorting methods that exploit fluid flow to separate cells, electrophoresis- and acoustophoresis-based approaches have also been tested in microfluidic platforms (Figure 2D,E).[96,97] Dielectrophoresis (DEP; Figure 2D) uses nonuniform electric field gradients to polarize and move or manipulate particles or cells.[98,99] Microfluidic-based DEP allows to sort cells according to their membrane capacitance in a label-free way, irrespective of their size. Murine neurogenic and astrogenic progenitor cells, for instance, have been successfully separated based on differences in their cell membrane capacitance by modulating the frequency of an alternating current (AC) applied through electrodes embedded in a microfluidic device.[100] The detailed characterization of these cells revealed that astrogenic progenitors experience a positive DEP at lower frequencies than neurogenic progenitors.[96,100] Acoustophoresis, on the other hand, separates cells within microfluidic channels using an ultrasound radiation force (Figure 2E). The acoustic radiation that cells absorb increases with their size, mass, and compressibility. The cells that absorb high levels of acoustic radiation move faster than the rest toward a central node.[97,101] With this method, Zalis et al. separated live neuroblastoma N2a cells from apoptotic cells in a mixed population of live and dead cells.[97] Further, cytometry strategies for characterizing the deformability of red blood cells can be extended for conducting measurements on stiff cells like neurons or retinal photoreceptors (Figure 2F).[93] Otto et al., for example, developed a real-time deformability cytometry method that allows tracking of neuronal cells differentiating from stem cells based on their mechanical fingerprints.[102] Besides conventional deformability cytometry, cells passing through constricted microfluidic channels also deform without being exposed to shear stresses and pressure gradients. This method demonstrated unique morphorheological properties of primary and mouse embryonic stem cell (mESC)-derived rod photoreceptors during development; the determination of such properties could be valuable for the prospective identification and label-free isolation of rod photoreceptors.[93]

Fluorescence-activated cell sorting (FACS), meanwhile, enables the sorting and isolation of diverse cell types based on their expression of specific markers and is now routinely used for a variety of applications. In this method, cells are labeled either by genomically engineering them to ectopically express fluorescent proteins under the control of specific promoters or in response to particular stimuli or by the use of fluorophore-conjugated antibodies that recognize specific epitopes characteristic of the cell type of interest. Once labeled, cells are guided one by one through a micrometric flow cell nozzle and a laser excites the fluorophores of interest. The detected signal is then used to identify the cells expressing the marker of interest and sort them into a collection vessel. Modern FACS systems are often built with several lasers and a large number of detectors that make them suitable for the identification and isolation of multiple cell types in parallel or of cells with complex phenotypes.[103] Although the sorting output of FACS is very precise, flow cytometry is expensive and often needs a trained operator.[104] Fortunately, such costs can be sharply reduced by the use of sample pumping, focusing, and sorting, as employed in microfluidic FACS platforms (μFACS; Figure 2G).[103] These elements can be additionally integrated with downstream analysis and processing steps in lab-on-a-chip devices.[105] Similar to FACS, μFACS sorts cells online according to the intensity of their fluorescence,[106,107] although it still needs to be tested for separating neuronal cells.[105]

A device recently developed can separate cells according to their membrane capacitance ($C_{\text{specific membrane}}$) and cytoplasm conductivity ($\sigma_{\text{cytoplasm}}$) (Figure 2H) and has been used to monitor the changes of such electrophysiological properties during neuronal stem cell differentiation.[108] Microfluidic platforms can also be exploited to sort cells based on their functional response to a stimulus (Figure 2I). Combining this approach with postsorting analysis can provide multidimensional data of particular cell types. Tan et al., for instance, designed a microfluidic device to monitor the responses of single olfactory neuronal cells to a ligand, L-lysine, and then collected the population of responsive sensory neurons for subsequent transcriptional profiling.[109]

3.1.1. Perspectives on Microfluidic-Based Neuronal Cell Sorting. Given the abundance of techniques and tools available for sorting cells, selecting an appropriate method to separate specific neuronal cell types of interest might be challenging. Advantages and disadvantages of microfluidic-based cell sorting methods have been summarized in a review by Plouffe and Murthy.[110] Sorting methods that exploit cell size and shape like inertial microfluidics, hydrodynamic-based, and deformability-based approaches offer high throughput (>10^9 cells per hour). However, their efficiency is affected if physical differences between neuronal cell types are small.[88,91,111,112] To separate neuronal cell types with similar size and shape, dielectrophoresis and acoustophoresis may offer a better performance.[113,114] Nevertheless, different neuronal cell types can also have similar dielectric properties or compressibility that can affect the accuracy of these methods in separating different cell types. To sort neuronal cells with similar physical properties, size, and shape, label-based methods like FACS and MACS are suitable alternatives.

Cell viability after the sorting process is another crucial factor that needs to be considered. This is especially important if neurons will be used for further experiments or for engineering neuronal circuits and tissue.[115] Hydrostatic pressure and shear stress during the cell sorting process, as well as temperature and buffers, are all major factors that lead to sorter-induced cellular stress (SICS).[116,117] Cellular stress manifests in different ways including arrested growth, decreased viability, changes in cell morphology, and altered gene expression profiles.[116] Compared to other cell types, neurons and iPSC-derived cells are more fragile and prone to experience SICS.[116,117] For instance, dissociation of mature neurons with extended axons and dendrites and loss of these branches can induce stress signals.

https://doi.org/10.1021/acs.chemrev.2c00212
Chem. Rev. 2022, 122, 14842−14880

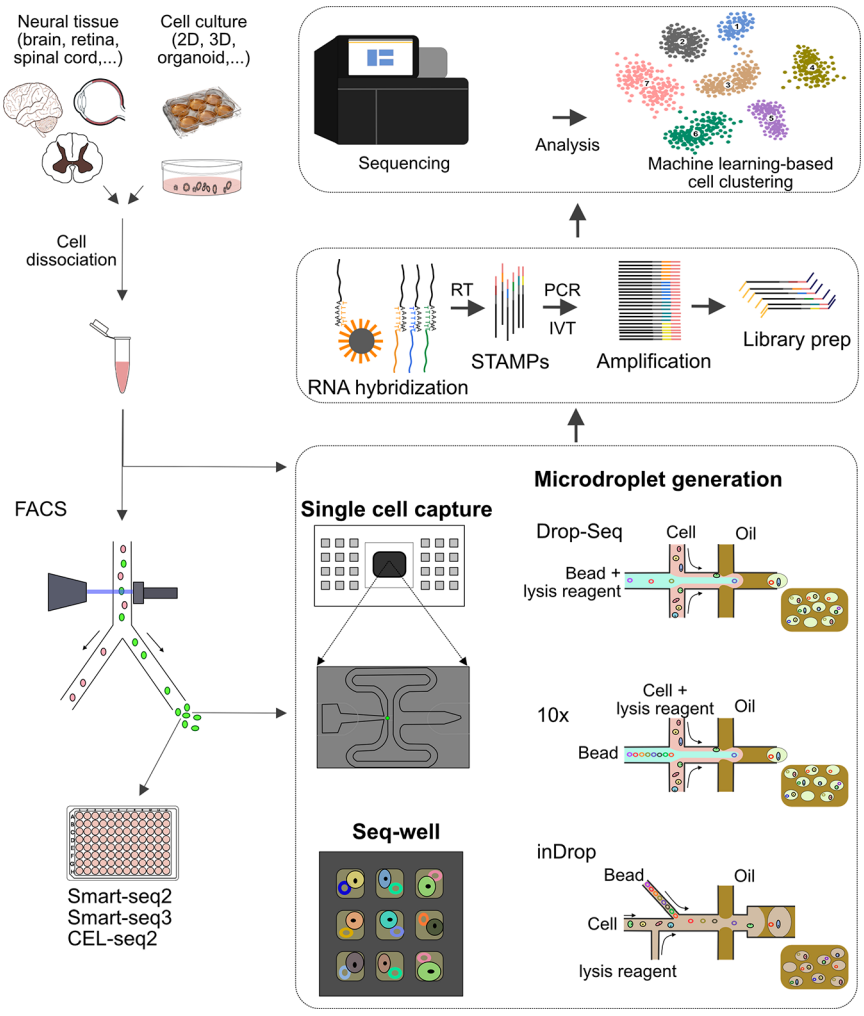

Figure 3. Contribution of microfluidics-based concepts to scRNA sequencing. Cells obtained either from primary neuronal tissues or from models engineered in vitro are dissociated and sorted by FACS. Purified cells are processed using either low-throughput RNA-Sequencing tools like Smart-Seq and CEL-Seq, or high-throughput microfluidic systems. In general, three main microfluidic approaches are used for single-cell analysis: valve-based (e.g., Fluidigm 1), droplet-based (Drop-Seq, inDrop, 10× Chromium, and Quartz-Seq), and microwell-based (Seq-well) systems. In all cases, trapped single cells are lysed, their RNA is hybridized and reverse transcribed (RT), and cDNA is then amplified either by PCR or linear isothermal amplification by T7-based in vitro transcription (IVT). Thereafter, the cDNA libraries generated in these steps are sequenced, and the data are demultiplexed, aligned to a reference transcriptome, and interpreted for classification of neuronal cell subpopulations. STAMP: single-cell transcriptomes attached to microparticles.

In a study by Bowles et al., MACS sorting of neuronal progenitor cells is shown to reduce SICS and increase viability compared to FACS.[115] On the other hand, MACS requires the use of metal nanoparticles, which can induce the generation of reactive oxygen species (ROS) that damage the cell membrane, DNA, and proteins.[110,118,119] A comprehensive and comparative investigation of different sorting methods, together with their potential advantages and disadvantages when used for sorting neuronal cells, could constitute a valuable reference resource and help improve sorting outcomes.

In contrast to other tissues, neuronal cells show a large functional diversity regardless of their structural similarity.[120−124] Thus, label-based methods and foremost FACS sorting perform better. In this sense, an optimal sorting device for neuronal cells would incorporate the possibility to perform functional evaluations in the sorting platform. Microfluidic tools that sort cells based on their membrane capacitance or response to stimuli are the preliminary models of such devices.[109,125] Yet, while these concepts may one day provide robust sorting platforms for neuronal cells, the feasibility of their integration with conventional cell sorting methods remains to be further investigated.

3.2. Classifying Brain Cells Based on Their Genomic and Transcriptomic Profile

Prior to the development of single-cell transcriptomics, neurons were classified based on their morphology, electrophysiological properties, and/or marker expression.[124] Advances in single-cell technologies offer the possibility to molecularly profile tens of thousands of single neurons in a single experiment. Single-cell RNA-Sequencing (scRNA-Seq), for example, allows dissection of the transcriptional profiles of individual brain cells.[33,120,128,129] Subsequent processing of such transcriptomic data using machine learning algorithms, i.e., Seurat,[130] permit clustering of neurons with similar gene expression profiles.[2] ScRNA-Seq is also useful to validate the identity of stem cell-derived neuronal cells by comparing their gene expression profiles with those of primary neurons.[34,131−133] Over the past decade, high-throughput scRNA-Seq data from different brain

https://doi.org/10.1021/acs.chemrev.2c00212
Chem. Rev. 2022, 122, 14842−14880

Table 1. Microfluidic-Based Approaches Applied to Single-Cell and Single-Nucleus Sequencing and Preparation of Cell Atlases from Different Brain Regions

cell source (brain region or organoid)	species (sample)	microfluidic platform	cells or nuclei (number)	sequencing depth (reads/cell)	results (types and number of detected cell clusters and subclusters)
whole brain	human healthy brain during surgery	Fluidigm	466 cells	2.83 million	Oligodendrocyte precursor cells (OPCs), oligodendrocytes, astrocytes, microglia, neurons (excitatory and inhibitory subclusters), endothelial cells, neuronal progenitors, and quiescent newly born neurons were identified.[165]
whole brain	post-mortem human	Fluidigm	3227 nuclei	8.34 million	Single-nucleus RNA sequencing showed 16 neuronal clusters with 16 neuronal subtypes annotated on the basis of cortical cytoarchitecture.[128]
telencephalon (cortex and MGE[a]): germinal zone, cortical plate, prefrontal cortex, and primary visual cortex	human developing brain	Fluidigm	4261 cells		11 classes including astrocytes, OPCs,[b] microglia, radial glia, intermediate progenitor cells, excitatory cortical neurons, ventral MGE progenitors, inhibitory cortical interneurons, choroid plexus cells, mural cells, and endothelial cells (plus temporal and spatial trajectories of radial glia maturation and neurogenesis).[138]
whole brain	23−25 dpf[c] zebrafish	Drop-Seq	58 492 cells	22 500	Simultaneous extraction of cell type and lineage information. More than 100 cell types and marker genes were identified, including 45 neuronal subtypes, 9 neuronal progenitor subtypes, and 3 oligodendrocyte subtypes.[80]
telencephalon, diencephalon, midbrain, hindbrain, and cerebellum	first trimester human	10× Chromium	289 000 cells		Nine progenitor populations were detected proximal to the telencephalon.[140]
cortex	P10 to P89[d] mouse	Fluidigm	50 cells	qPCR	Three subgroups of astrocytes were detected from P10 to P50.[178]
cortex	mouse	sNucDrop-Seq[e]	18 194 nuclei	15 471	40 clusters were identified, including 27 excitatory, 7 inhibitory, and 6 non-neuronal cells.[121]
cortex: germinal zone	16 wpc[f] human	Fluidigm	65 cells	5000	Four major groups of cells were identified including multiple progenitor and neuronal subtypes.[179]
cortex: VZ[g] and OSVZ[h]	16−18 wpc human	Fluidigm	393 cells	2.9 million	Transcriptional state associated with neuronal differentiation: radial glia, intermediate neuronal progenitor cells (INPCs), neuronal progenitor cells (NPCs), and excitatory and inhibitory neurons.[167]
cortex: primary motor cortex	mouse	10× Chromium and Smart-Seq4	175 000 and 6300 cells	1−2.1 million	59 GABAergic inhibitory neurons, 31 glutamatergic excitatory neurons, and 26 non-neurons were detected.[142]
cortex: primary motor cortex	mouse	SMART-Seq and 10× Chromium	280 327 and 94 162 cells	2.5 million 120 000	Linked the SMART-Seq resolved isoforms to the cell types defined by 10× Chromium. Spatially resolved isoform atlas of the mouse primary motor cortex was generated.[155]
cortex: primary motor cortex	post-mortem human monkey	SMART-Seq and 10× Chromium	>450 000 nuclei	17 576 and 77 816	Around 100 cell types were detected in each species, with distinct marker-gene expression and accessible chromatin sites.[180]
cortex: somatosensory S1 and hippocampus CA1	mouse	Fluidigm	3005 cells	500 000	47 molecularly distinct subclasses of cells: 7 S1 pyramidal neurons, 2 CA1 glutamatergic cells, 16 interneurons, 2 astrocytes, 2 immune cells, and 6 oligodendrocytes.[120]
cortex: primary visual cortex	mouse	Fluidigm	1679 cells	>5 million	49 transcriptomic cell types: 23 GABAergic, 19 glutamatergic, and 7 non-neuronal types.[181]
visual system	drosophila: multiple stages of neuronal development: over 100 h	10× Chromium	208 976 cells	176 636	Transcriptional atlas generated across multiple stages of visual system development (162 distinct neuronal populations were detected at 7 time points: prior to, during, and after synaptogenesis).[182]
olfactory epithelium	P4−P10 and P30−P90 mouse	Fluidigm	178 cells	1.06−4.52 million	Classified based on specific olfactory receptor expression in newborn and adult mouse.[183]
lateral ganglionic eminence (LGE)[i]	7−20 wpc human embryo	10× Chromium	96 789 cells	80 million	Fifteen different cell states were detected. A common progenitor generates medium spiny neurons with D1 or D2[j] receptors.[141]
striatum neurons	mouse	Fluidigm	1208 cells	1−5 million	Ten clusters of cells were detected, including neurons, astrocytes, oligodendrocytes, vascular, and 2 ependymal, 2 immune, and 2 stem cell types.[184]
striatum	P22−P28, P21−P26, and P55−P76 mouse	Fluidigm	1135 cells and 3417 cells	800−1500	529 cells identified as neurons. Seven interneuron classes (6 subclasses of GABAergic interneurons) were identified.[185]
substantia nigra (SN) and cortex	human	10× Chromium	2455 nuclei and 690 nuclei	46 598−59 513 and 18 377−44 710	SN[k] cell-type atlas together with a matching cortical atlas were extracted. Genetic risk in Parkinson's disease is associated with dopaminergic neurons and oligodendrocytes.[186]
thalamic reticular nucleus (TRN)[l]	mouse	Smart-Seq2 and 10× Chromium	1687 nuclei	1.3 million	Two neuronal populations expressing different genes were detected. Each population was connected to distinct thalamus nuclei and formed molecularly specific subnetworks.[187]
hypothalamus	mouse	Drop-Seq	3131 cells	>1500	Seven cell types were distinguished, including neurons. Neurons were further classified into 62 clusters of glutamatergic, dopaminergic, and GABAergic subclasses.[188]

https://doi.org/10.1021/acs.chemrev.2c00212
Chem. Rev. 2022, 122, 14842−14880

Table 1. continued

cell source (brain region or organoid)	species (sample)	microfluidic platform	cells or nuclei (number)	sequencing depth (reads/cell)	results (types and number of detected cell clusters and subclusters)
hypothalamus	mouse	Drop-Seq	14 437 cells	>800	45 cell clusters were identified, including 34 neuronal and 11 non-neuronal. Neuronal clusters further divided into 15 glutamatergic, 18 GABAergic, and 1 histamatergic subclasses.[35]
hypothalamus: preoptic region	mouse	10× Chromium	31 299 cells	101 771	23 excitatory neuron subclasses and 43 inhibitory neuron subclasses were identified.[189]
hypothalamus: ventral posterior hypothalamus (VPH)[m]	mouse	10× Chromium	16 000 cells	50 000	Twenty neuronal (excitatory and inhibitory) and 18 non-neuronal cell clusters were identified in VPH.[190]
hypothalamus: lateral hypothalamic neurons	P21−P23 mouse	Fluidigm	89 and 69 cells	qPCR	Both excitatory (glutamate) and inhibitory (GABA) neurons were identified.[191]
midbrain: dopaminergic neuron	mouse	Fluidigm	159 cells	qPCR	Simultaneous expression of 96 genes in single neuron. Six different subtypes of dopaminergic neurons were distinguished.[192]
midbrain: ventral midbrain	human embryos (6−11 week) E11.5−E18.5[n] mouse postnatal mouse	Fluidigm	1977 cells, 1907 cells, 245 cells	1200−24 000 2000−26 000 2000−30 000	25 human and 26 mouse clusters were identified. Human: 5 subtypes of radial glia-like cells and 4 of progenitors. Mouse embryo: 2 dopaminergic neuron subtypes. Mouse postnatal: 5 dopaminergic neuron subtypes. Clear differences in cell proliferation, developmental timing, and dopaminergic neuron development between species.[166]
midbrain: dopaminergic neurons	mouse	Fluidigm	111 cells	Single-cell qRT-PCR	Co-varying gene modules that link neurotransmitter identity and electrical phenotype.[193]
midbrain	*Drosophila*	Drop-Seq	10 286 cells	>800	Cell atlas of the fly brain provides a unique resource of gene expression across many cell types and regions of the visual neuropil. Twenty-nine cell clusters were identified.[194]
suprachiasmatic nucleus (SCN)	mouse	Fluidigm	352 cells	qRT-PCR	Five subtypes of mammalian SCN[o] neurons were distinguished.[195]
suprachiasmatic nucleus	mouse	10× Chromium and Drop-Seq	62 083 cells and 16 004 cells	1 million	Based on combinations of markers and their spatial distribution, circadian rhythmicity and light responsiveness, 5 SCN neuronal subtypes were identified.[196]
geniculate ganglion	mouse	Fluidigm	96 cells	1 million	Two main groups of gustatory and somatosensory neurons were detected. Gustatory neurons included 3 subclasses.[197]
trigeminal ganglion neurons	mouse	Drop-Seq	6998 cells		13 genetically defined classes of sensory neurons were identified.[198]
DRG sensory neurons	mouse	Fluidigm	334 cells	qRT-PCR	Six distinct subgroups of DRG[p] populations were identified.[199]
spinal cord	postnatal mouse	10× Chromium	19 353 nuclei	50 000	Unifying the previously published data sets[137,145,200−202] into a common reference framework.[203] Validated combinatory marker codes for 84 types of spinal-cord cells and mapped their spatial distributions.
retina	mouse	Drop-Seq	44 808 cells	>100 000	39 transcriptionally distinct clusters in 6 classes: photoreceptor, bipolar, horizontal, amacrine, and ganglion cells, and other cell types.[33]
retina	E18 chicken	droplet-based scRNA-Seq platform[160]	30 022 cells		Five neuronal classes (PRs,[q] HCs,[r] BCs,[s] ACs,[t] and RGCs[u]) as well as 2 glial types, Müller glia and oligodendrocytes were identified.[204]
retina: bipolar cells	mouse	Drop-Seq	27 499 cells	8200	26 cell classes identified: 14 bipolar, Müller glia, 11 rods and cones, and amacrine cells. These data were validated by in vivo matching of gene expression to bipolar cell morphology.[136]
retina: fovea and peripheral retina	human	10× Chromium	85 000 cells	4062−550 895	58 cell types were identified in following cell classes: photoreceptor, horizontal, bipolar, amacrine, retinal ganglion and non-neuronal cells.[205]
retina: amacrine cells (ACs)	P19 mouse	10× Chromium	32 000 cells		63 types of ACs were identified in mice retina.[206]
cerebral organoids vs fetal neocortex	hiPSC-derived organoids, 12−13 wpc human	Fluidigm	333 + 175 cells, 226 cells	2−5 million	Similar genetic features responsible for human cortical development between in vivo fetal brain and in vitro organoid culture were identified.[34]
cerebral organoids	hiPSC lines, chimpanzee iPSC lines, fetal human cortex	Fluidigm	52 cells, 344 cells, 220 cells		Transcriptomic similarities between human and chimpanzee neuronal stem and progenitor cells were highlighted.[132]
brain organoid	hiPSC lines, 3−6 month old organoids	Drop-Seq	82 291 cells		Beyond similarities between 3- and 6-month-old organoids, mature photoreceptors and mature astrocytes only presented in 6-month-old organoids.[168] Despite the differences in the profiling methods used (Drop-Seq and Fluidigm C1[v]), preferential correlation between corresponding cell types for radial glia, interneurons, projection neurons, and induced pluripotent stem cells were detected.

[a]Medial ganglionic eminence. [b]Oligodendrocyte precursor cells. [c]Days postfertilization. [d]Postnatal day. [e]Single-nucleus RNA-Seq approach. [f]Weeks post conception. [g]Ventricular zone. [h]Outer subventricular zone. [i]Lateral ganglionic eminence. [j]Dopamine receptor 1 and 2. [k]Substantia nigra. [l]Thalamic reticular nucleus. [m]Ventral posterior hypothalamus. [n]Embryonic day. [o]Suprachiasmatic nucleus. [p]Dorsal root ganglion. [q]Photoreceptors. [r]Horizontal cells. [s]Bipolar cells. [t]Amacrine cells. [u]Retinal ganglion cells. [v]C1TM single-cell auto prep integrated fluidic circuit (IFC).

https://doi.org/10.1021/acs.chemrev.2c00212
Chem. Rev. 2022, 122, 14842−14880

regions have been used to generate mouse and human neuronal cell atlases.[53,134−143] Similarly, genome, transcriptome, and epigenome sequencing assays at consecutive neuronal differentiation time points during embryonic or postnatal development have allowed to elucidate with unprecedented resolution the dynamic molecular changes that neuronal progenitor cells must undergo to differentiate.[52] Together, these data are central to deciphering the molecular mechanisms underlying neuronal diversity across species.[27,144,145]

For single-cell transcriptomic profiling (Figure 3), the first step is to isolate individual cells in micro- or nanoliter reaction volumes. The latter is mainly achieved by using FACS, valve- or droplet-based microfluidic systems, or microfluidic-controlled high-density microwell plates.[146,147] While cells are diverted into a well of a multiwell plate in low-throughput systems like Smart-Seq2 and CEL-Seq2,[148−152] in high-throughput bead-based systems, cells in suspension are distributed into droplets or nanowells.[153] Smart-Seq can generate full-length reads and enables individual gene isoforms to be identified.[154] However, the throughput for this system is limited, as it requires depositing cells in wells.[155] Two recently developed sequencing technologies, i.e., high-throughput high sensitivity Smart-Seq3[156] and low-cost portable Seq-Well,[157,158] have not yet been used to sequence neuronal cells.

In general, the major advantage of high-throughput bead-based systems is that they make it possible to run thousands of reactions simultaneously while reducing working volumes.[146] Common droplet-based microfluidic platforms, including Drop-Seq,[33] indexing droplets (inDrop),[159] 10× Genomics Chromium,[160] Quartz-Seq,[147,161] and Quartz-Seq2,[162] use oil to encapsulate cells together with barcoding beads in water droplets containing a cell lysis buffer (Figure 3). The design of barcoded beads includes a segment to attach the capturing oligonucleotide to the bead, a primer segment to amplify the captured transcript, a cell barcode that is the same for all oligonucleotides on one bead (to identify all transcripts originating from one particular cell), unique molecular identifiers (UMIs) for digitally counting RNA molecules and correcting amplification artifacts, and a polyd(T) segment to capture polyadenylated RNA.[147] InDrop performs reverse transcription in droplets, and then cDNA is collected for amplification, while Drop-Seq releases beads from droplets for reverse transcription and then cDNA is amplified by PCR.[52] Meanwhile, in the 10× Genomics platform, cell lysis, and cDNA library preparation occurs immediately after cells are encapsulated in gel bead-in-emulsions (GEMs).[52] cDNA libraries,[163] which are amplified after GEMs are broken, are then used for sequencing on a next-generation sequencing instrument (e.g., Illumina HiSeq).[129]

Single-cell transcriptomic data from these platforms have been used to identify the neuronal subtypes forming the CNS of humans and mice (Table 1). Studies using the Fluidigm C1-based scRNA-Seq platform have been reviewed by Tasic et al.[129] Table 1 summarizes the ways in which different microfluidic-based platforms have been used for trapping cells and generating cDNA in scRNA-Seq studies of primary neurons. Results suggest that the robustness of cell-type identification is higher when more cells are sequenced at a shallow depth (e.g., in droplet-based approaches like Drop-Seq) than when few cells are sequenced at high depth (microwell-based approaches like the Fluidigm C1 platform).[136,164] In addition to classifying in vivo-derived neurons from healthy or post-mortem adult human brains[128,165] and animals,[120] data obtained from developing human or mouse brains[166,167] and from cerebral organoids[34,166,168−170] has provided valuable information regarding the diversity of neuronal progenitor cells and mature neurons at different developmental stages[140,166,169,171] (Table 1). Comparing in vitro brain organoids with the developing fetal brain has also revealed a high degree of resemblance in transcriptional profiles, strongly supporting the idea that iPSC-derived organoids faithfully replicate the genetic features of in vivo systems.[53]

Currently, several comprehensive transcriptomic databases are being constructed from high-throughput scRNA-Seq studies (Table 1).[133,143,172] These atlases are optimal references for reverse-engineering neuronal cell subtypes and circuits. For instance, combinations of transcription factors (TFs) that potentially drive the differentiation of iPSCs into specific neuronal cell types have been extracted from databases and subsequently validated.[53,124,173,174] Transcriptomic data processed by machine learning techniques and computationally reconstructed differentiation trajectories have also predicted the path that stem cells take during their in vitro differentiation into a particular neuronal cell type.[27,175] In addition, the resemblance in transcriptional states between engineered neuronal cells and their corresponding in vivo counterparts has been ascertained by comparing scRNA-Seq data sets to reference atlases.[34,166,176] Thus, data obtained from in vivo and in vitro scRNA-Seq experiments serves as a powerful tool to determine the strengths and limitations of engineered neuronal models like brain organoids and to define the extent to which they resemble their in vivo counterparts.[34,53]

Going further, advanced multimodal microfluidic platforms are attempting to include an option to assess physiological heterogeneity in scRNA-Seq experiments: cells could be mapped based not only on their molecular features but also on their physiological properties.[177] Using a microfluidics-based platform that first measures changes in intracellular Ca^{2+} in response to different agonists and then conducts RNA sequencing, Mayer et al. showed a cell type-specific Ca^{2+} response that varied with lineage progression in the developing human neocortex.[177] The latter would enable the possibility to integrate biophysical and physiological cellular identities with molecular features and to thereby develop more powerful and accurate cell classification strategies.

Overall, microfluidics have had a major impact on the generation of genomic and transcriptomic data from native brain tissues and organoids (Table 1).[52] These data are of great value not only for classifying neuronal cell subtypes based on their transcriptomic profile but also for devising strategies to direct the differentiation of hiPSCs toward specific neuronal cell fates.[53] In this regard, integration of in vivo or in vitro electrophysiological recordings and morphological evaluations combined with scRNA-Seq data of the same cells provides information to precisely map neuronal subtypes and predict their functional contributions in brain networks.[121,207−211] Patch-Seq is an example of a low-throughput method capable of linking the transcriptomic profile of neuronal cells to their neurophysiological and morphological phenotypes and can also be used to investigate the cellular response to diverse chemical stimuli.[212−215] Notably, while high-throughput automated patch-clamp electrophysiology tools are available since the 1990s and early 2000s, they still need to be integrated with scRNA-Seq platforms.[216] However, major challenges remain: that dissociated neuronal cells commonly used in scRNA-Seq experiments are not compatible with patch-clamp recordings

https://doi.org/10.1021/acs.chemrev.2c00212
Chem. Rev. 2022, 122, 14842−14880

Table 2. Microfluidic Platforms for Neuronal Cell Reprogramming and Differentiation

application	cell type	microfluidic device	results
reprogramming	human somatic cells to hiPSCs	three-layer microfluidic platform:[36] (1) cell culture layer, (2) media distribution layer, (3) pneumatic layer	Fifty-fold increase in reprogramming efficiency. Direct differentiation into desired cell type.
differentiation	immortalized murine neuronal progenitor cells C17.2	microfluidic platform to deliver controlled amounts of culture media to cells[229]	Controlled differentiation to neurons using controlled delivery of culture media.
differentiation	mouse embryonic stem cells (mESCs)	gradient-generating microfluidic platform[230]	Parallel differentiation of neurons and Schwann cells; axonal myelination.
reprogramming	primary mouse embryonic fibroblasts to induced neuronal (iN) cells	microfluidic platform for 3D hydrogel culture; system based on decellularized brain extracellular matrix (BECM)[231]	3D BECM hydrogels replicated in vivo microenvironments and promoted neuronal conversion.
differentiation	human neuroepithelial stem cells (hNESCs) to dopaminergic neurons	phase-guided, 3D microfluidic cell-culture bioreactor with two perfusion lanes and one culture lane[82]	Efficient generation of iPSC-derived dopaminergic neurons.
differentiation	human neuronal stem cells (hNSCs) to astrocytes	gradient-generating microfluidic platform[232]	Graded differentiation and proliferation of astrocytes proportional to growth factor gradients.
differentiation	hNSC-derived neuronal progenitor cells to mature neurons	gradient-generating microfluidic platform[233]	Long-term neuronal culture from neuronal progenitor cells.
differentiation	fetal brain-derived neuronal stem cells	3D hydrogel[234]	Improved spontaneous differentiation to neurons and oligodendrocytes.

because they often lose their dendrites and axons in the dissociation process.[217,218] Therefore, a key point that needs to be considered in designing the next generation of microfluidic screening platforms is the feasibility of integrating molecular profiling with functional and morphological phenotyping approaches to achieve high-throughput multimodal single-cell profiling platforms. Another challenge lies on the difficulty to capture the dynamic transcriptional states of neurons as they differentiate from stem cells with full functional and morphological features, as current technologies are limited to capturing snapshots of these characteristics at specific time points.[219,220]

4. ENGINEERING CELL NICHES USING MICROFLUIDICS TO CONTROL STEM CELL DIFFERENTIATION AND NEURONAL CELL GROWTH

Physical and chemical cues in the developing brain have a deep modulatory effect on cell behavior, regulating processes such as proliferation, differentiation, and survival.[221,222] Similarly, NSC differentiation and survival capacities in vitro are highly dependent on the properties of their microenvironment.[61−63] Therefore, fine-tuning the physicochemical conditions of the culture media, and maintaining precise control over the cellular microenvironment, are crucial for driving differentiation processes efficiently and at high yields.[36,122,223] Microfluidics facilitate the design of complex cellular niches in which multiple parameters can be controlled simultaneously, including fluidic flows and the delivery of nutrients and biochemical agents. Moreover, microfluidic systems support diverse strategies for physical confinement and operate with small quantities of biological and chemical materials.[50,224,225]

Another notorious use of microfluidic devices is related to cellular reprogramming. In conventional cell-culture systems, somatic cell reprogramming occurs stochastically and with very low efficiency.[226] Reprogramming of human fibroblasts to iPSCs by ectopic expression of specific TFs, for example, often exhibits dramatically low yields in terms of iPSC production.[36] Reprogramming at the microliter scale in microfluidic chips, on the other hand, increases cellular autocrine and paracrine signaling, effectively creating a more suitable environment for pluripotency acquisition[223,227] (Table 2). Controlling the delivery of TFs in microfluidic devices has been shown to increase the yield of hiPSCs from human somatic cells up to 50-fold compared to the results obtained using cell-culture dishes.[36,228]

In a different context, the influence of fresh cell-culture media on the spontaneous differentiation of neuronal stem cells has been investigated using microfluidic devices with distinct microchannel dimensions capable of delivering defined volumes of fresh culture media.[229] These studies have revealed that shrinking the cellular environment by using microchannels with smaller dimensions increases the differentiation rate of neuronal stem cells,[223,229] suggesting that a continuous supply of fresh medium is crucial for neuronal stem cell maintenance.

4.1. Engineering Cell Niches to Differentiate and Guide NSC Fate

Beyond controlled media delivery, microfluidic channels can also be used to create growth and TF gradients[232] (Table 2). Two different cell types, neurons and Schwann cells, have been generated from a common population of mESCs in this way.[230] Co-differentiation was induced by generating long-term overlapping gradients of neurotrophic and Schwann cell-inducing factors in a microchannel.[230] Using one of these gradient-generator microfluidic platforms, Chung et al. differentiated human NSCs into astrocytes in a continuous gradient of epidermal growth factor (EGF), fibroblast growth factor 2 (FGF2), and platelet-derived growth factor (PDGF). In their study, human NSCs differentiated in a manner proportional to the gradient of factors sensed by the cells, with the highest percentage of NSC-derived astrocytes being found within the region of low growth factor concentration and proliferation occurring preferentially in the region of high growth factor concentration.[232] Such long-lasting gradients also support the maturation of long-term neuronal cultures, an essential process when modeling the chronic features of neurological disorders in vitro.[233] Moreover, the possibility to create chemical gradients in microchips can also be harnessed in large-scale studies, e.g., for investigating neural tube development in vitro. During neural tube development, temporal and spatial changes on the gradients of extracellular signaling molecules play a critical role on neuronal cell patterning and neural plate formation and folding.[235,236] To replicate this spatiotemporal distribution, a microfluidic device with orthogonally opposing chemical gradients has been devised.[237] Further, concentration gradients in microfluidic devices have also been used to differentiate

https://doi.org/10.1021/acs.chemrev.2c00212
Chem. Rev. 2022, 122, 14842−14880

Table 3. Microfluidic-Based Patterns and Gradients for Neuronal Cell Polarization and Axonal Guidance

method	microfluidic system	chemical cue	physical cue	cell types	axon	dendrite
Discontinuous Solid Patterns Method	microchannel device to pattern strips[249]	BDNF[a] and cAMP[b]		hippocampal neurons E18[c] rat	initiation and differentiation	
	microchannel device to pattern strips[250]	Sema3A[d]		hippocampal and cortical neurons E18 rat	Sema3A suppressed axon growth	Sema3A promoted dendrite growth
	microchannel device to pattern strips[253]	Sema3F and Sema3A		embryonic stem cell-derived motor neurons mouse	Sema3A and Sema3F strips repel axons	
Continuous Gradient of Soluble Cues Method	microjet arrays in multicompartment device[254]	Netrin-1		cortical neurons E14 mouse	axonal guidance toward Netrin-1 (73%)	
	collagen-loaded multicompartment device[238]	Netrin-1, brain pulp, and Slit-2		hippocampal neurons and DRG[e] E14.5−E16.5 mouse	Netrin-1 and brain pulp acted as axonal attractants. Slit-2 acted as an axonal repellent.	
	large-scale microfluidic gradient[255]	Netrin-1		hippocampal neurons E18 rat	Biphasic response: Netrin-1 150−200 ng mL^{-1} attracts and <50 ng mL^{-1} repels growth cone.	
	microfluidic channels with porous membrane[256]	Slit1 Netrin-1		rostral thalamic neurons E13.5 mouse and hippocampal neurons E18 rat	Lower concentrations of the repellent Slit-1 triggered an attractive response to Netrin-1.	
	microfluidic gradient generator capable of simulating shallow gradients[257]	Sonic Hedgehog (Shh) Netrin-1		commissural neurons from neuronal tubes E13 rat	Combined Shh + Netrin-1 gradients are effective for axonal guidance. Growth cone integrates Shh + Netrin-1 gradients.	
	Microfluidic device loaded with hydrogel to release Sema3C[258]	Sema3C[f]		dopaminergic neurons from E14 rats or derived from H9 human ES cells[g]	Hydrogel-released Sema3c attracts axons.	
	gradient generator with no shear stress[259]	forskolin		cortical neurons E18 rat	Axons grow in the direction of forskolin gradients.	
	microfluidic gradient generator with shallow or steep gradients[260]	EphrinA5		retinal ganglion cells E6−E7 chick	Shallow gradients of EphrinA5 attracted axons more than steep gradients.	
Combined Solid and Soluble Pattern Method	asymmetric microchannels gradient slop[251]	substrate-bound laminin and soluble netrin-1		hippocampal neurons E18 rat	Netrin-1 and laminin gradient attracted axonal growth.	
	microfluidics-based turning assay[252]	substrate-bound laminin and soluble BDNF gradients		spinal neurons E1 *Xenopus*	Laminin affected axonal growth cone response to BDNF gradients.	
Combined Chemical−Physical Cues Method	superimposed topographic and soluble cues[28]	Netrin-1 and Sema3A	hexagonal arrays with spatial frequencies (densities)	hippocampal neurons E16.5 mouse	Effects of netrin-1 (axonal attractant) and Sema3A (axonal repellent) were affected by physical cues.	

[a]Brain-derived neurotrophic factor. [b]Cyclic adenosine monophosphate. [c]Embryonic day. [d]Semaphorin 3A. [e]Dorsal root ganglion. [f]Semaphorin 3C. [g]Embryonic stem cells.

https://doi.org/10.1021/acs.chemrev.2c00212
Chem. Rev. 2022, 122, 14842−14880

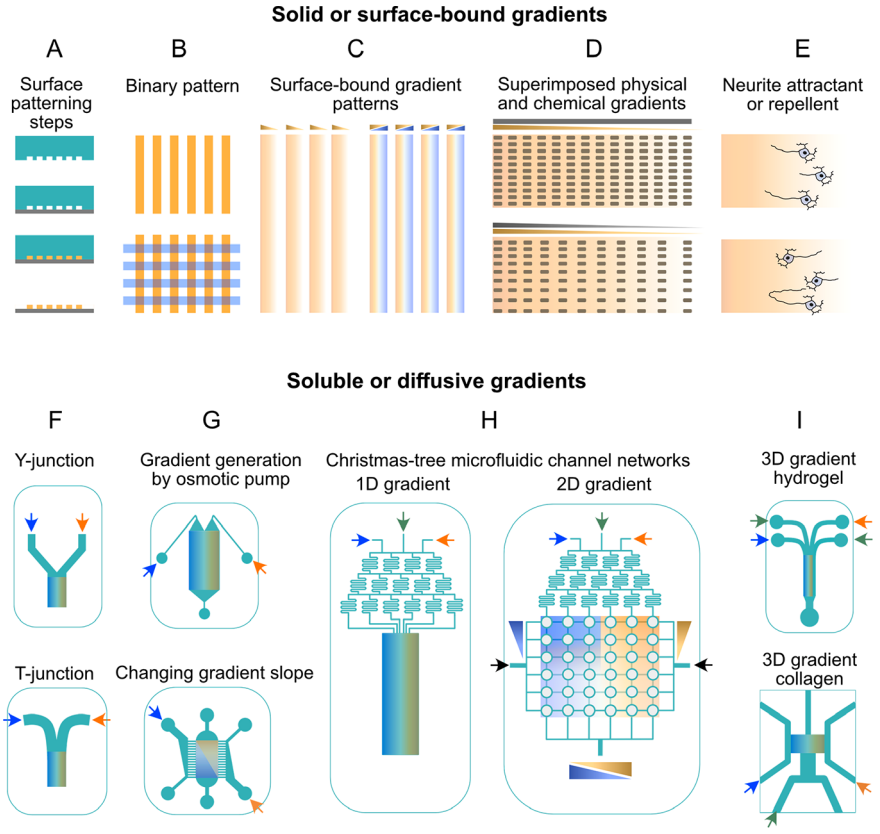

Figure 4. Engineering the neuronal cell niche using microfluidic gradient generators. (A) Microfluidic channels and microwells are used to deposit solid or surface-bound cues. (B,C) Surface-bound binary or gradient patterns have been generated by microchannel devices to probe neuronal cell polarization and axonal growth in response to attractant or repellent factors (also shown in E).[249,250,260,277,278] (D) Similarly, chemical gradients integrated with topographical gradients or cues have been deployed to guide neurites.[28] (E) Schematic axonal growth cone response to attractant (upper panel) and repellent (lower panel) cue gradients. (F) Two basic diffusive gradient generators are Y-junction and T-junction configurations. (G) Osmotic pump-derived ultraslow flow rate generates continuous and overlapping chemical gradients to induce a common stem cell population to differentiate into neurons and Schwann cells.[230] The lower panel shows a device with asymmetric peripheral channels whereby gradually changing gradients of soluble Netrin-1 are created. In such a device, the axon growth response can be subsequently measured.[251] (H) Christmas tree microfluidic channel networks have been used to create 1D or 2D gradients of neuronal growth factors to differentiate NSCs into neurons,[232] of Shh and Netrin-1 to guide axons,[257] and of Wnt to model neural tube development.[236] (I) 3D gradient of neurotrophic factors and axon guiding factors has also been generated in scaffold-based neuronal cultures embedded in microfluidic devices.[238,279,280]

neuronal cells in a specific orientation and to selectively induce axonal growth in particular directions inside a microchannel.[238]

Besides soluble chemical cues and gradients, microfluidic platforms also offer stable patterned cues for guiding or inducing differentiation. Research by Jin et al., for instance, has shown that the modification of either a 2D surface or a 3D microfluidic device with a decellularized brain ECM facilitates the transfection-based conversion of primary mouse embryonic fibroblasts into neurons while also promoting neuronal differentiation and maturation.[231] Microscale 3D environments in microfluidic chambers have also been reported to enhance differentiation of NSCs to neurons and glia.[82,234,239] In this context, Moreno et al. used a phase-guided 3D microfluidic cell-culture bioreactor system to differentiate hiPSC-derived neuroepithelial stem cells (hNESCs) into functional dopaminergic neurons. In the study, hNESCs were embedded in Matrigel in a microfluidic channel flanked by one or two channels supplying cell-culture media.[82] Phaseguides, i.e., geometric features that pattern fluid flow into the microchannel, were then used to partially separate pairs of 3D Matrigel cultures and to force them to follow their respective media lanes despite being in close contact with each other. This concept has been used in the development of commercially available two- or three-lane OrganoPlates consisting of 96 or 40 bioreactors, respectively.[82,240] Using such phaseguide OrganoPlates, ECM-embedded 3D cell-culture systems composed of neurons, microglia, astrocytes, and endothelial cells that mimic a functional blood–brain barrier (BBB), often known as BBB-on-a-chip, have been generated.[241] Together, these studies show that the 3D microenvironment can positively affect the differentiation and survival of hydrogel- or ECM-embedded neuronal cells in microfluidic chambers. Supporting this idea, Han et al. found that more neurons and oligodendrocytes are generated by using 3D ECM hydrogels inside microfluidic channels than using the same ECM hydrogels on culture plates.[234] Similarly, NSCs have been reported to exhibit increased self-renewal and differentiation capacities in low oxygen tension 3D ECM microfluidic culture systems.[239]

4.2. Engineering Cell Niches to Control Neuronal Cell Polarity

Asymmetric outgrowth of neurites, axons, and dendrites from neuronal cell bodies is commonly referred to as neuronal cell polarization and is a key step for neuronal network formation and CNS development.[242,243] Neuronal cell polarity and axonal growth direction are tightly connected by intrinsic and extrinsic

https://doi.org/10.1021/acs.chemrev.2c00212
Chem. Rev. 2022, 122, 14842−14880

chemical and mechanical cues.[244,245] In the absence of precise control over cell polarization and neurite growth direction, neuronal cells form redundant connectivity patterns with abnormal functionality, as often observed in neurological disorders.[246] Therefore, controlling cellular polarity and axonal and dendritic growth direction and connectivity patterns is crucial for the engineering of functional neuronal circuits. Several microfluidic platforms have been developed to study and control neuronal polarization and neurite growth (Table 3, Figure 4). Spatial patterns of chemical cues attracting or repelling neurites, for example, have been produced in microfluidic devices with different configurations (Figure 4), including solid and discontinuous biochemical patterns of neurite attractant/repellant materials on the surface of a substrate and continuous soluble gradients in microfluidic devices[247,248] (Table 3, Figure 4).

In a study by Shelly et al., microfluidic-based substrate patterning for neuronal cell polarization was realized by generating localized patterns of brain-derived neurotrophic factor (BDNF) or dibutyryl-cAMP (Figure 4A−C). Such patterns induced axonal initiation and differentiation through protein kinase A (PKA)-dependent LKB1 phosphorylation.[249] The same authors also showed that patterned strips of semaphorin 3A (sema3A) in microchannels prompted undifferentiated neurites to become dendrites while also repelling axonal differentiation and growth.[250] Therefore, intervals of axon-attractant/dendrite-repellent and dendrite-attractant/axon-repellent cues (Figure 4B,C) may be required to effectively separate axons and dendrites. In this sense, solid and discontinuous patterns of axon attractant and repellent cues can be integrated with topological cues to improve axonal guidance efficiency (Figure 4D,E).[28,251,252]

Microfluidic gradient generators have been used to test axon responsiveness to shallow and steep attractant gradients[230,257,260] (Figure 4F−H), as well as to generate parallel gradients of two chemical cues, like Slit1/Netrin-1 or Shh/Netrin-1, to mimic the overlapping gradients of chemical cues occurring in vivo.[256] Similarly, gradient-generating microfluidic platforms have been used to establish continuous gradients of Netrin-1, an axon attractant, to guide axonal cone growth (Figure 4H,I).[238,254]

Studies have also shown that combining axon-attracting chemical cues increases axonal differentiation and controls the direction of growth.[256,257] In contrast, embedding continuous gradients of axonal attractants in hydrogels before they are injected into microfluidic chambers allows for the slow and steady release of materials and thereby establishes a passive gradient (Figure 4I). Carballo-Molina et al., for instance, generated steady gradients of an axon-attracting cue, semaphorin 3C, by embedding it in a hydrogel. The authors showed that axonal growth and guidance was enhanced compared to similar studies using soluble semaphorin 3C.[258] Finally, microfluidic devices can be exploited to simultaneously provide continuous and discontinuous chemical gradients or to combine them with physical cues like surface patterns and structures, to provide more realistic models of the in vivo microenvironment[28,251,252] (Table 3).

4.3. Perspectives on Engineering Neuronal Cell Niches

Conventional microfluidic approaches for engineering neuronal cell niches are based on neurotrophic factors and axonal attractants and repellents. Microfluidic devices using this strategy are also compatible, after remodeling and optimization, with the use of TFs to control neuronal cell fate. Here, the comprehensive databases created from single-cell molecular profiling experiments of primary neurons and brain organoids contain invaluable information on the optimal combination of TFs to guide stem cells toward specific neuronal subtypes of interest. Considering the capability of microfluidic devices to precisely deliver chemical factors and to controllably mix nanoliter scale solutions, neuronal progenitor cells can be exposed to diverse combinations and concentrations of factors to determine the optimal molecular cocktail to dictate any neuronal fate.[63,174,228,261]

Besides TFs, small molecules are also able to manipulate cell fate choices.[262−266] Such molecules typically act by modulating cell signaling cascades, epigenetic mechanisms, and metabolic pathways.[263,264,267] In combination with TFs, certain small molecules can also improve reprogramming and forward programming efficiencies.[268−271] Overexpression of the Neurogenin-2 TF together with small molecules, for instance retinoic acid, enhances the yield of multiple subtypes of stem cell-derived motor neurons.[272] Additionally, combinations of small molecules can also induce reprogramming independent of TFs and thereby overcome the clinical and translational concerns associated with exogenous gene delivery.[263,267,273] Moreover, small molecules can easily cross the cell membrane, are generally inexpensive to synthetize and preserve, and their dosing can be tightly controlled in a straightforward manner.[263,267,274−276] These properties make small molecules attractive to be used in patterned and gradient-generating microfluidic platforms. In general, an optimal multimodal neuronal cell niche engineering platform should be able to incorporate the use of both TFs and small molecules for high yield and robust forward programming, while also supporting the utilization of neurotrophic and axonal attractant-repellent gradients to control neuronal cell polarity. Precise engineering of the chemical and physical attributes of the NSC niche at the nano- and microscales in 2D and 3D in microfluidic devices is expected to enable more efficient reprogramming and differentiation processes and to support a more accurate cell polarity control. Overall, by supporting the high-throughput generation of diverse neuronal cell types and the precise control of their connectivity patterns, microfluidic systems represent a valuable platform for developing a comprehensive toolbox of building blocks for neuronal circuit engineering.

5. ENGINEERING NEURONAL CIRCUITS USING MICROFLUIDICS

In vitro models of 2D and 3D neuronal circuits often aim to replicate the in vivo features of network formation in the developing brain.[281−283] When this is the aim, the ways and the extent to which the model recapitulates in vivo brain morphology, function, and microenvironment should all be considered prior to designing and assembling the circuits in vitro.[19,283−287] Thus, understanding the molecular and cellular mechanisms underlying the formation of in vivo brain circuits is a good starting point when engineering complicated circuits in vitro using a bottom-up approach,[288−291] paying particular attention to both morphological features and functional development.[13,290−292]

Important factors relevant to the establishment of organized brain networks include neuronal proliferation, migration, and differentiation rates, as well as the formation and elimination of functional synapses.[293−296] These steps of neuronal network organization can overlap or progress at a different pace in

https://doi.org/10.1021/acs.chemrev.2c00212
Chem. Rev. 2022, 122, 14842−14880

Table 4. Neuronal Cell Types Used for Engineering Neuronal Circuits in Microfluidic Devices

cell type	cell source	advantages	disadvantages
Primary Neurons[335]	embryonic or early postnatal brains	most closely express the markers and perform the functions of their tissue of origin	limited availability
			dissection and preparation require substantial skills
		well-established culturing protocols are available	heterogeneous neuronal cell types
		no genetic modifications	possible changes in cell types and numbers over time
Cell Lines[336,337]	mainly derived from tumors or genetically immortalized cells (e.g., PC12, NG 108, NIE)	offer an unlimited cell source	abnormal genotype of tumor-derived cells
		generate single cell types	
			might be functionally incomplete or different from in vivo and primary neurons
Fetal Neuronal Stem Cells[337]	aborted fetus brains	no genetic modifications	ethical issues associated with abortion
		naturally primed for neuronal fate	
Adult Neuronal Stem Cells[338]	subventricular zone (SVZ) of lateral ventricle and subgranular zone (SGZ) of hippocampal dentate gyrus	no genetic modifications	difficult to obtain
		ethical issues are avoided	limited source of cells
		naturally primed for neuronal fate	highly sensitive to chemical and mechanical manipulations
ESCs[337]	blastocysts inner cell mass (mainly obtained from embryos produced for in vitro fertilization)	extensively characterized biological features and differentiation paradigms	ethical issues due to destruction of embryos
			ESCs in differentiated NSCs may form teratomas
iPSCs[60]	reprogrammed adult human or rodent cells (e.g., skin fibroblasts)[42,43]	ethical issues are avoided	genomic instability may be induced by reprogramming
		can be differentiated to desired neuronal cell types	might be functionally incomplete or different from in vivo and primary neurons
		offer unlimited source of cells	

different brain areas and at different developmental stages.[293,294,297] In the human fetus, neuronal circuit formation starts with the proliferation of neuronal progenitor cells and radial glial cells, and the generation of immature neurons in the subgranular and subventicular zones of the dentate gyrus around gestational week 5.[293,298] Next, immature neurons undergo radial migration along radial glial cells and generate six cortical layers in an inside-out manner,[293,294,297,299] a process beginning around gestational week 7.[294,300,301] The innermost cortical layer is formed by the earliest-born neurons, while the outermost layer is formed by the latest born neurons and is completed around gestational week 18.[284,285,293,294,300,302,303] Around midgestation, neurites start to grow from immature neurons. This process is then followed by axonal elongation, dendritic arborization, and finally synaptogenesis. The latter continues to occur postnatally and all the way into early childhood.[294] Radial glial cells generate astrocytes and oligodendrocyte precursor cells also around midgestation.[304] Oligodendrocyte generation, migration, and maturation continues for the first two postnatal years. Axonal myelination by oligodendrocytes, on the other hand, continues for the first few decades of human life.[294,305] Notably, although synapses begin to form between individual neurons before the 27th week of gestation, most prenatal synapses are transient.[306] Starting from birth, and especially after the peak of synaptogenesis, a combination of intrinsic and extrinsic factors modulate the pruning of synaptic connections.[293,294,307,308] The latter means that neurons generally undergo an overconnectivity phase that is followed by dendrite pruning and synaptic elimination that then reduces and stabilizes the level of neuronal connectivity.[306,309,310]

Functional evaluation of the developing human brain is limited as methods for measuring electrophysiological activity in situ are invasive and pose a risk to a developing fetus.[311] In the developing rodent brain, however, studies have shown that widespread synchronized network activity arises from glutamatergic synapses.[309,312−316] This synchronized burst activity can be detected as early as embryonic day 18 and increases in frequency until birth.[309,313] In the human fetus, synchronized burst activity appears at gestational week 20 and is present until birth before it progressively disappears.[309,317−320] Notably, such features are recapitulated in hSC-derived in vitro neuronal networks.[31,321−324]

Engineering neuronal networks using microfluidic devices is a bottom-up approach that aims to extrapolate the function of small-world neuronal circuits to the complex high-level functions of in vivo neuronal systems. Such neuronal circuits serve a wide range of applications ranging from basic neuroscience to translational research, including: the deciphering of information processing in highly controlled and accessible experimental conditions, the understanding of the functional role of subcellular compartments like axons, dendrites, and synapses in processing neuronal signals, learning, and plasticity, the modeling of neurological diseases, and the undertaking of pharmacological screenings to identify potential therapeutic targets.

Different approaches used for engineering neuronal circuits have been expertly reviewed before.[325] Here, we focus on patterning strategies and microfluidic device configurations. In general, in vitro patterning of neuronal circuits is mainly achieved either by physically confining single neurons or neuron populations or by using neuro-adhesive materials. Both approaches have been widely tested in combination with microchannel devices to engineer modest 2D or 3D neuronal circuits in vitro.[326] By using compartmentalized microfluidic

https://doi.org/10.1021/acs.chemrev.2c00212
Chem. Rev. 2022, 122, 14842−14880

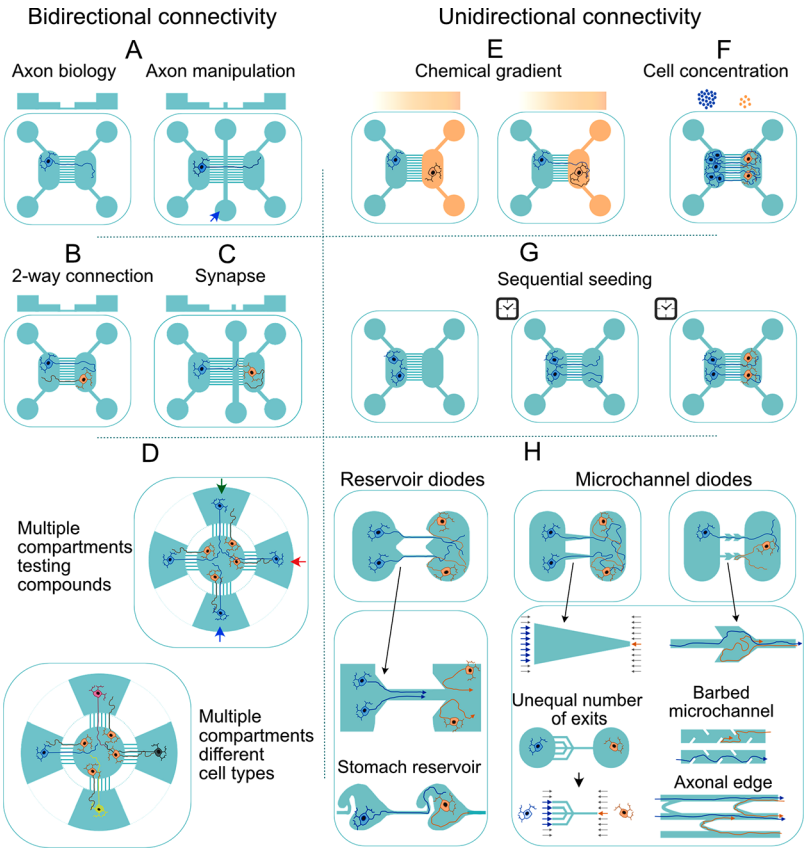

Figure 5. Main approaches for engineering neuronal circuits in microfluidic devices. (A) Two-compartment microfluidic devices can be used for axonal isolation.[351] In such devices, a third compartment is often added to manipulate isolated axonal branches.[354,359,399] (B) Seeding neurons in both compartments of such two-compartment devices allows for the generation of bidirectionally connected networks.[106,391,393,395,400,401] (C) Inserting a third compartment to two-compartment devices close to one neuronal population is a commonly used strategy to study synapses.[362,376] (D) Multicompartment devices connecting different neuronal populations bidirectionally enables the engineering of complex circuits and the testing of chemical compounds in specific populations.[343,394,402,403] (E−H) Unidirectional neuronal circuits are constructed in compartmentalized devices connected by straight microchannels or by diode-style configurations. In straight microchannels, the probability of axonal growth in one direction is manipulated by (E) the use of axonal attractant or repellent gradients,[255,404] (F) the seeding of different cell densities in the two connected compartments,[405,406] and/or (G) the sequential seeding of cells in each compartment.[327,385] (H) The axonal diode configuration of microfluidic devices is one of the most widely used approaches to direct axonal growth.[292,382] Diode structures can be embedded in reservoirs or, alternatively, entire reservoirs can be designed in a particular shape, e.g., stomach, to facilitate unidirectional axonal growth.[40,407] Microchannel diodes can also be designed by simply narrowing them on one side[382,383,404] to create arrow-like structures,[353,408] by including barbs that prompt axons to grow in one direction,[409] or by connecting adjacent channels with arches that allow growing axons to turn backward.[384] Overall, axonal diode layouts are designed to increase the probability of axons growing in a particular direction.

platforms, axons can be separated and guided toward specific neuronal populations, and synaptic connections can subsequently be visualized and manipulated to form either bidirectional or unidirectional connectivity patterns and construct 3D neuronal circuits with high precision. Feed-forward communication between two populations of the same or different neuronal cell types, for instance, has been achieved using two-compartment microfluidic devices.[327] Meanwhile, patterning neuronal networks in binodal configurations (i.e., grids) has been used in many studies to produce highly simplistic models of brain circuits.

An essential step to confirm that engineered circuits function as intended, i.e., that connectivity is taking place in the expected direction, is to capture neuronal activity at the network level for a prolonged time period. Neuronal network activity is recorded either optically, i.e., by calcium imaging or with voltage-sensitive indicators, or electrically using multielectrode arrays (MEAs).[328,329] MEAs offer high temporal resolution and are compatible with noninvasive long-term (several months) recordings.[31,330] In many cases, microfluidic circuit designs must be coupled with MEAs to make the functional data from the engineered circuits accessible. Such coupling enables to simultaneously record from neurons scattered throughout the circuit while also improving signal-to-noise ratios. The latter, in turn, makes it also feasible to record from tiny axonal branches in microfluidic-MEA sandwich devices.[29,30,331,332] Standard MEA chips fail to provide sufficient spatial resolution to effectively record from all network modules. To address this limitation, high-density MEAs based on complementary metal-oxide semiconductor (CMOS) technology scale down electrode sizes and the space between electrodes, thereby facilitating recording from almost all neurons in a circuit.[333] Using these devices, information flow can also be tracked along axons, making it possible to determine the direction and pattern of functional connectivity between individual neurons.[334] A summary of coupled microfluidic-MEA platforms designed to capture the activity of a neuronal network or to record the biophysical properties of axons as they grow in microtunnels is found in Tables 5−7.

https://doi.org/10.1021/acs.chemrev.2c00212
Chem. Rev. 2022, 122, 14842−14880

Table 5. Microfluidic Devices for Neurite Separation and Functional Evaluations

subcellular compartment	application	cell source	microfluidic device	functional studies
axon	axonal separation[351]	cortex and hippocampus E18[a] rat or E17 mouse	2-compartment device with microchannels	axonal biology and injury, axonal myelination
axon	axonal electrophysiology in chip[29,353,356,368]	cortex E19 rat	2-compartment device combined with MEAs	action potential propagation velocity
axon	axonal electrophysiology in chip[331]	cortex E18 rat	2-compartment device combined with MEAs	action potential recording
axon	axonal injury and electrophysiology[353]	cortex and hippocampus E18 rat	2-compartment device combined with MEAs	axonal pruning, long-term axonal electrophysiology
axon	axonal injury and regeneration[359]	hppocampus E17 rat	microchannels with valves	microscopy of axonal injury and regeneration
axon	long-term axonal electrophysiology[30]	cortex E18 rat	quasi-modular PDMS device combined with MEA	long-term axonal electrophysiology
axon	2-photon axonal stimulation[369]	hippocampus E18 rat	microchannel diodes combined with MEAs	optical stimulation of neuronal circuits
axon	axonal guidance using electrokinetic forces[370]	hippocampus E18 rat	neurite bridge chip with 4 compartments	neurite growth in collagen scaffolds
axon	axonal myelination[371]	DRG[b] E13 mice, OPCs[c] P1[d] mouse	2-compartment device with optogenetic stimulation	optically evoked axonal myelination by oligodendrocytes
axon	separating iPSC-derived neuronal axons[372,373]	H9 ESCs or NSCs differentiated into glutamatergic neurons	2-compartment device with microchannels	induction of presynaptic compartments in axonal compartment
axon	axonal branching[374]	brain cortex P1−P3 rat	bifurcating microchannels	branching neurites in bifurcated microchannel
axon	axonal transport[375]	DRG E15−E16 rat	2- and 3-compartment devices	retrograde axonal transport of quantum dots
axon−synapse	studying axonal transport and neurotransmitter release[354]	cortex and striatum E17.5 rat	3-compartment devices with a synaptic module	changes in axonal transport during maturation
synapse	visualization and manipulation of synapses[362]	hippocampus P0−P2 rat	3-compartment devices with a synaptic module	calcium imaging for studying synaptic transmission between two layers
synapse	recording from pre- and postsynaptic modules (UF-MEA chip)[365]	cortex E17.5 rat	3-compartment devices with synaptic module coupled with MEA electrophysiology	associating postsynaptic calcium oscillations with presynaptic axonal activity
synapse	modeling synaptic competition-on-a-chip (two-input pathway competition model)[376]	cortex E18-E19 rat	2-compartments on the sides connected to a target compartment in the middle	effect of inhibition of neuronal activity on synapse formation and axonal growth in the competing population
synapse	modeling peripheral pain synapse and signaling[367]	DRG neurons and DH[e] neurons from spinal cords E16 rat	3-compartment device	effect of distal axotomy on DRG-DH synaptic transmission
synapse	synaptogenesis assays[377]	hippocampus E18 rat	synapse microarray device with multiple wells	increased sensitivity and decreased duration for synaptogenesis assays
dendrite	studying dendrite-to-nucleus signaling[378]	cortex and hippocampus E18 rat	2-compartment device	probing molecular signals from the dendrite to the nucleus

[a]Embryonic day. [b]Dorsal root ganglion. [c]Oligodendrocyte progenitor cell. [d]Postnatal day. [e]Dorsal horn neurons.

5.1. Cell Types and Sources for Engineering Neuronal Circuits in Microfluidic Platforms

Neuronal circuits have been engineered using different cell sources, including primary neurons and stem cell-derived neurons (Table 4). In the case of primary cells, several established methods are available for dissociating cortical, hippocampal, sensory, and motor neurons, as well as astrocytes, from the neonatal or embryonic rodent brain.[335,339] Human primary neurons are mainly obtained either from post-mortem adult brains or from fetal tissue biopsies following an autopsy.[340] NSCs used in neuronal circuit engineering are either derived from stem cells or isolated from fetal or adult tissues.[16,58,341−344] Each of these cell sources has its own advantages and disadvantages (summarized in Table 4). NSCs differentiate into neurons within weeks and have recently been used as a new source of neuronal cells for circuit engineering.[17,343,345] While most neuronal circuits in microfluidic devices are created using primary murine neurons, such models possess neither the regulatory elements nor the cellular and network phenotypes required for results to be interpreted in terms of healthy and pathological human brain function.[17,346] Adult NSCs are found in the subventricular zone (SVZ) of the lateral ventricle and in the subgranular zone (SGZ) of the hippocampal dentate gyrus,[47,344] while ESCs are isolated from the inner cell mass of blastocysts.[347] Human iPSCs are commonly generated by exogenous expression of the TFs Oct4, Sox2, Klf4, and Myc in somatic cells.[43,344] Once established, human iPSC lines can differentiate into neurons or glial cells in response to the exogenous expression of specific genetic factors or in response to chemical agents in culture.[47,344] Circuits engineered with neurons derived from iPSCs which were produced from patients suffering specific neurological disorders caused by genomic abnormalities often replicate in vitro the disease phenotype and are thereby extremely valuable for drug screening and precision medicine.[348]

5.2. Microfluidic Devices for Axonal Guidance

Axonal growth and elongation occur after the establishment of neuronal polarity. Axonal pathfinding is a complex process in which a growth cone must elongate between many neuronal and non-neuronal structures to reach a target region in the brain, form complex branches, and finally make synaptic contact with specific neurons in this target region.[247] The growth cone is a motile structure at the tip of axons, which is highly sensitive to physicochemical cues present in its microenvironment.[248] Depending on their type and concentration, chemical cues can either exert attractant or repellent effects or induce axonal branching. Considering the numerous long-distance connections between neurons in the brain circuitry, the precise control

https://doi.org/10.1021/acs.chemrev.2c00212
Chem. Rev. 2022, 122, 14842−14880

of axon guidance processes is likely critical for the establishment of the complex in vivo neuronal network topology.[349,350] Axonal guidance in vitro is studied based on patterns and gradients of different attractant or repellent cues like laminin, neurotrophins, netrins, slits, semaphorins, and ephrins.[248] These patterns and gradients are generated by microtechnological methods like strip assays, microcontact printing (μCP), laser-assisted patterning, 3D-hydrogel patterning, and microfluidic platforms.[248]

Microfluidic devices with defined channel dimensions and configurations can physically prevent neuronal cell bodies from entering them while allowing axons to do so (Figure 5A,B).[351] Thus, such devices make it possible to study axonal biology in isolation within a chemically and physically controlled microenvironment.[26] Additionally, they can be used to study the axonal response to chemical cues or to guide them toward a particular population of neurons (Table 5, Figure 5). The latter can be exploited for manipulating connectivity orientation in neuronal circuits.[352] Furthermore, as microfluidic devices are primarily fabricated from transparent polymers, i.e., polydimethylsiloxane (PDMS), they constitute an optimal platform for monitoring the axonal growth process.[58,353] Thereby, axonal behavior as well as molecular and organelle transport along axons can be investigated simultaneously.[354,355] Additionally, these devices have been coupled with electrophysiology platforms like transparent MEA chips[29,30,356] to study the long-term function and biophysical properties of axons, with special interest in changes of the latter during elongation[30] and regeneration.[353,357−359]

5.3. Microfluidic Devices for Isolating Dendrites and Synapses

The establishment of synaptic connectivity between dendrites and axons and its modification or elimination lies at the center of neuronal network development in vivo.[360,361] Therefore, an optimal platform for neuronal circuit engineering should offer adequate control over synapse formation between axons of presynaptic neurons and dendrites or the cell body of postsynaptic neurons.[360] Indeed, microfluidic devices with interconnected compartments are used to control with high precision synapse formation between pairs of neurons or between neuronal populations and to manipulate the activity of such synapses using specific agonists and antagonists[26,362] (Figure 5, Table 5).

A typical microfluidic device for synapse formation between two neuronal populations includes three compartments, or reservoirs, connected through axon- and dendrite-guiding microchannels[363] (Figure 5C). As dendrites do not normally extend more than 400 μm, axons and dendrites can be kept separated by fine-tuning channel lengths.[15,351,362] In this case, pre- and postsynaptic cells are each seeded in one of two outer reservoirs so that axons from presynaptic neurons meet the dendrites of postsynaptic neurons in the middle compartment.[362] This so-called synaptic compartment has its own inlets and outlets to control the chemical environment of the synapses and to stimulate or inhibit synaptic communication.[362,364,365] Such devices have been used to model neurological diseases that affect synapses or that are related to their pathology.[366,367] For instance, Virlogeux et al. developed a Huntington's disease model in a three-compartment device incorporating presynaptic cortical neurons and postsynaptic striatal ones.[366] This unidirectional corticostriatal network-on-a-chip enabled the authors to investigate and precisely manipulate corticostriatal synaptic transmission. A similar three-compartment microfluidic device using spinal cord dorsal root ganglia (DRG) neurons and dorsal horn neurons has also been used for modeling the circuit involved in peripheral pain.[367] In this device, bipolar axons from DRG neurons in the middle compartment branched into side compartments and made synapses with dorsal horn neurons, with ablation of the DRG axonal branches inducing pain signaling.[367]

In certain microfluidic devices, synapse formation itself can also be experimentally controlled. A device incorporating synergistic gradients of nerve growth factor (NGF) and B27 supplement, for instance, exhibited enhanced synapse formation with increased concentration of such chemical agents in 3D hydrogel neuronal cultures.[279] This observation prompted the development of devices embedding neuronal cell layers in 3D hydrogels to achieve a heterogeneous spatial distribution of synapses. Remarkably, such systems closely resemble the heterogeneously distributed synapses found across the six layers of the cortex.[39,279] Three-compartment microfluidic devices with interconnected microchannels are also optimal for generating and modeling synaptic competition, a process in which the presence and activity of one synapse affects the formation, stabilization, or elimination of other synapses on the same postsynaptic neuron.[376,379] In synaptic competition, which occurs naturally, neuronal activity and sensory inputs play a major role in shaping neuronal connectivity patterns during development.[379] To model synaptic competition in vitro, Coquinco et al. utilized two populations of neurons seeded in the side compartments of a microfluidic device which then innervated each other in the central compartment. This model revealed that chemical blockade of neuronal activity in one compartment could promote the elongation of axons with capacity for synapse formation from neurons in the opposing compartment.[376]

5.4. Engineering 2D Neuronal Circuits with Controlled Connectivity Patterns

Two-layer neuronal circuits have their origin in the two-compartment microfluidic device designed for axonal separation[26,351,352] (Figure 5). A simple two-layer neuronal circuit inside a microfluidic device can be made by seeding neurons in two opposing reservoirs and letting axons grow from both neuronal populations toward the opposite compartment, which produces bidirectional connectivity[380,381] (Figure 5B). However, engineering layered neuronal networks with unidirectional connectivity is an essential step in modeling in vivo neuronal structures.[382−385] Microfluidic-engineered unidirectional and bidirectional neuronal circuit models are summarized in the following sections and in Tables 6 and 7.

Different strategies are available for seeding neuronal populations at specific locations in the microfluidic chambers. The NeuroArray device, for instance, uses a PDMS stencil with 20 μm pores to position populations of Purkinje neurons and NSCs at particular locations.[386] By decreasing pore diameters below 3 μm and using a sacrificial layer-protected PDMS molding method, Li et al. created a "cell sieve" to seed at single-cell resolution; functional connectivity was subsequently tracked by calcium imaging.[387] An alternative high-throughput method to seed neurons at single-cell resolution is block-cell printing. In this method, tiny protrusions on microchannel walls trap and restrain individual neuronal cells.[388]

5.4.1. Engineering 2D Neuronal Networks with Bidirectional Connectivity. Bidirectional connectivity between subpopulations of neurons was first achieved in

https://doi.org/10.1021/acs.chemrev.2c00212
Chem. Rev. 2022, 122, 14842−14880

Table 6. Microfluidic Devices for Engineering Layered Networks with Bidirectional Connectivity

circuit	cell types	microfluidic device	functional studies	results
cortical−thalamic cortical−cortical[390,391]	cortex E18[a] rat thalamus E18 rat	2-compartment device	MEA electrophysiology	bidirectional connectivity pattern between two populations
3-layer cortical circuits[376]	cortical neurons E18−E19 rat	3-compartment device	chemical inhibition time-lapse imaging	noninhibited populations win over inhibited populations in synaptic competition
2-layer cortical circuits[410]	cortical neurons P1[b] rat	2-compartment device	MEA electrophysiology and electrical stimulation	enhanced representation capacity of modular networks
4-layer cortical circuits (same or different size)[402]	cortical neurons P0−P1 mouse	4-compartment device	focalized optogenetic stimulation and patch clamp	propagation of evoked temporal and rate signals across different layers
hippocampal circuits: DG-CA3, CA3-CA3, or DG-DG[400]	hippocampal DG and CA3 cells P5 rat	2-compartment device	MEA electrophysiology of axons and soma and paired-pulse stimulation	CA3 neuron responses in engineered subnetworks decoded the stimulation site in the DG
hippocampal circuits: EC-DG, DG-CA3, CA3-CA1, or CA1-EC[393]	hippocampal EC, DG[c], CA3, CA1[d] cells P3 rat	2-compartment device	MEA electrophysiology of axons and soma	generating pairs of hippocampal subregional circuits
hippocampal circuit[411]	hippocampal neurons E18 rat	2-compartment device	optogenetic stimulation and whole-cell recording	detection of light-evoked excitatory postsynaptic responses confirmed synaptic communication between modules
hippocampal circuits: DG−CA3[395]	hESC-derived DG and CA3 neurons	2-compartment device		comparing DG−CA3 circuits of healthy subjects and schizophrenic patients
nultinodal DRG[e] networks[394]	DRGs rat	multiple compartments		construction of multinodal circuits in 2D and 3D
Simple nucleus model (one unit receiving inputs from several units)[343]	dopaminergic, glutamatergic, and GABAergic neurons derived from hiPSCs	multiple compartments	patch clamping electrophysiology, and optogenetic stimulation (ChR2[f])	defining synaptic connections and communication between several modules
retinal circuits[401]	immortalized R28 precursor cells P6 rat retina	2-compartment device		imaging synaptic communication between retinal cells

[a]Embryonic day. [b]Postnatal day. [c]Dentate gyrus. [d]CA1 and CA3: subregions of hippocampus. [e]Dorsal root ganglion. [f]Channelrhodopsin2.

https://doi.org/10.1021/acs.chemrev.2c00212
Chem. Rev. 2022, 122, 14842−14880

Table 7. Microfluidic Devices for Engineering Unidirectionally Connected Neuronal Circuits

applied method	circuit	cell source	microfluidic device	functional studies	results
sequential seeding[356]	cortico → cortical	cortex E18[a] rat	2-compartment device	MEA electrophysiology	unidirectional propagation of signals between two layers
sequential seeding[327]	cortico → cortical	cortex E18 rat	2-compartment device with different numbers of connecting microchannels	MEA electrophysiology	fidelity of feed-forward communication is dependent on the number of connecting microchannels
sequential seeding[327,356]	cortico → cortical	cortex E18 rat	2-compartment device with different numbers of connecting microchannels	MEA electrophysiology	strength of connectivity is dependent on the number of connecting microchannels
intrinsic connectivity[405]	hippocampal circuit: DG[b] → CA3[c]	hippocampus P3[d] rat	2-compartment device with different numbers of connecting microchannels	MEA electrophysiology	activity in CA3 networks driven by engineered inputs from DG networks
intrinsic connectivity[406]	hippocampal circuit: trisynaptic loop: DG → CA3	hippocampus P4 rat	2-compartment device	MEA electrophysiology	self-wired DG → CA3 circuits; marked enrichment of GAD67[e] and GABAergic neuron density in DG module.
cell concentration[363]	cortico → cortical	cortex E18 rat	3-compartment device (2 side compartments were seeded with higher cell densities)	calcium imaging and chemical treatment	axons from high-density populations connected to a low-density population in the middle
reservoir diode: asymmetric reservoir modules[407]	cortico → cortical	cortex E18 rat	multiple consecutive asymmetric compartments	MEA electrophysiology	75% of signals propagated in the predefined direction
reservoir diode: stomach-shaped reservoir[40]	hippocampal circuit: modular small-world networks	cortex E18 rat	multiple consecutive asymmetric compartments	MEA electrophysiology	92% of signals propagated in the predefined direction
microchannel diode[382]	cortico → striatal	cortex and striata E14 mouse	2-compartment device with diode-shaped microchannels	calcium imaging	97% unidirectionality of cortico−striatal synapses
microchannel diode[415]	hippocampal circuit: 2 populations	cortex E18 rat	2-compartment device with diode-shaped microchannels	optogenetic stimulation and calcium imaging	light-evoked excitatory postsynaptic responses confirmed synaptic communication
microchannel diode[404]	cortico → striatal	cortex and striata E7−E14 mouse	2-compartment device with diode-shaped microchannels	calcium imaging	functional cortico−striatal synapses with synchronous oscillation
microchannel diode: barbed microchannels[409]	cortico → cortical	cortex P19 rat	2-compartment device with barbed microchannels	MEA electrophysiology	unidirectional propagation of spontaneous and evoked activity
microchannel diode: axon edge device[384]	cortico → cortical	cortex E17 rat	2-compartment device with arch-shaped microchannels		unidirectionally connected cortico-cortical circuits
microchannel diode: different diode shapes[383]	hippocampal circuit: 2 populations	hippocampus E18 rat	2-compartment device and microchannels with diode motifs: spines, triangles, and zigzag	MEA electrophysiology	unidirectional propagation through the microchannels and activity triggered in the target compartment
microchannel diode: different diode shapes[408]	hippocampal circuit: 2 populations	hippocampus E15−E18 mouse	2-compartment device and microchannels with diode motifs: arch, pretzel, heart, and arrowhead		arrowhead- and pretzel-shaped diodes are more efficient at generating unidirectional connectivity
microchannel diode: tapered microchannels[292]	basal ganglia circuits-on-a-chip	SN,[f] GP,[g] and striatum E12−E16 rat Glutamatergic, GABAergic, dopaminergic neurons	5-compartment device with tapered microchannels. Each compartment is loaded with a specific cell type	calcium imaging and patch clamp	in vitro functional model to mimic complex neuronal circuit of the basal ganglia; axonal outgrowth was directed between modules

[a]Embryonic day. [b]Dentate gyrus. [c]CA3 subregion of hippocampus. [d]Postnatal day. [e]Glutamate decarboxylase; catalyzes the conversion of L-glutamic acid to γ-aminobutyric acid (GABA). [f]Substantia nigra. [g]Globus pallidus.

https://doi.org/10.1021/acs.chemrev.2c00212
Chem. Rev. 2022, 122, 14842−14880

microfluidic devices either by the use of microchannels or by printing lines of adhesion molecules using microchannel stamping.[373,381,389] Two-compartment microfluidic devices with straight microchannels connecting to each other,[351] however, offer no control over axonal growth direction (Figure 5B, Table 6): axons can grow in any direction and connect with any neuron. This leads to the formation of two-layer neuronal circuits with bidirectional connectivity.[390] Loading this kind of device with primary cortical neurons in one compartment and primary thalamic neurons in the other, for example, resulted in two neuronal populations connecting with each other through shallow microchannels (less than 3 μm in height); the reciprocal effects of the cortical and thalamic network activities were then investigated based on MEA recordings.[390,391]

A similar approach using microfluidic devices on MEA chips was used to engineer hippocampal circuits using cells extracted from the entorhinal cortex (EC), the dentate gyrus, and the CA1 and CA3 subfields.[392] Electrophysiology data recorded from axons of the presynaptic neurons and somata of the postsynaptic module confirmed connectivity between hippocampal regions.[393] Such connectivity was achieved by shrinking the width of the connecting microchannels to 2.5 μm, thereby effectively allowing only a few axonal branches into each of them. With this strategy, it was possible to record individual action potentials from specific axons, as well as the direction and kinetics of their propagation.[389]

Given that microfluidic device design is highly versatile, it is possible to adjust the number and type of communicating neuronal populations in circuits forming within them (Figure 5D) so as to mimic the structure of complex brain nuclei.[394] Fantuzzo et al., for instance, generated dopaminergic, glutamatergic, and GABAergic neuronal populations and loaded each of them into a separate compartment of a microfluidic device allowing for connections to be formed between populations through microchannels.[17,343] This kind of layout, in which each neuronal population receives inputs from the rest, is considered to mimic the in vivo circuitry of a single brain nucleus.[343] A similar approach was used by Sarkar et al. to examine the activity patterns of circuits formed by iPSC-derived neurons from healthy subjects or from individuals affected by schizophrenia, with particular focus on the hippocampal circuits formed by postsynaptic CA3 pyramidal neurons and presynaptic DG neurons.[395] Notably, bidirectional neuronal networks engineered in compartmentalized microfluidic devices have been adapted to a 96-well plate-based format and thereby constitute valuable resources for disease modeling and drug screening.[396]

5.4.2. Engineering 2D Neuronal Networks with Unidirectional Connectivity. While bidirectionally connected neuronal circuits in vitro have been developed to model mutually connected networks in the central nervous system (Table 6), many brain regions exhibit unidirectional connectivity patterns. In such regions, neurons receiving inputs from other parts of the brain do not communicate back to the neurons sending the signal. Unidirectional connections are common in most regions of the CNS and are the basic modules of complex hierarchically connected or layered networks.[6] Unidirectionally connected neuronal circuits decrease the complexity of the functional data within such systems, which in turn makes them easier to interpret.[397,398] Constructing oriented connectivity between neuronal populations can be achieved either by modifying culturing protocols or by altering the design of the microfluidic device being used (Table 7, Figure 5E−H).

5.4.2.1. Engineering Unidirectional Networks Based on Cell-Seeding Protocols. The capacity of two-compartment devices to intrinsically form feed-forward connections from hippocampal DG to CA3 populations has already been demonstrated.[405] By conducting MEA recordings on similar neuronal circuits, it has been shown that communication between DG−CA3 neurons is preferentially unidirectional (62%), while no directionality is observed in DG−DG and CA3−CA3 networks.[406] Whether polarized connections between DG−CA3 networks arise naturally or are caused by the DG:CA3 3:1 ratio used in these studies is not clear. In fact, seeding neuronal cells at different densities in two compartments constitutes in itself a strategy to produce directional connectivity between two modules: denser populations tend to occupy microchannels more promptly and with more axonal branches than low density ones (Figure 5F), thereby hindering the innervation of those channels by the low density population.[363]

Early in vitro models of layered neuronal networks were engineered by sequential seeding of neurons in two compartment devices[356,385] (Figure 5G). In a two-compartment microfluidic device, Pan et al. seeded rat cortical neurons in one compartment and allowed axons to reach the second compartment through connecting microtunnels. After 7−10 days, a new set of cortical neurons was added to the second compartment. This gave rise to a layered neuronal structure with pre- and postsynaptic modules.[356] Parallel electrophysiological recordings from each compartment proved unidirectional communication between the two modules.[385] Additionally, by increasing the number of connecting microtunnels, the authors showed that connectivity strength can also be manipulated.[327,385]

5.4.2.2. Engineering Unidirectional Networks Based on Microfluidic Device Design. The implementation of specific designs in microfluidic devices represents another commonly used approach to construct layered neuronal networks with directional connectivity (Figure 5H, Table 7). Asymmetric geometries have been proposed for this purpose by Feinerman et al., for example, who guided axonal branches of hippocampal neurons through triangular cell-adhesive patterns on a glass substrate.[412] Neuronal activity in such a device was measured using a calcium-sensitive fluorescent dye, which revealed signal propagation among all engineered modules.[412−414]

On this basis, Peyrin et al. designed diode microchannels which were wide at one end and very narrow at the other end[382] (Table 7) to guide axons from one compartment toward another. In this device, axonal growth occurred primarily in one direction (97% vs 3%). Additionally, the authors constructed an oriented corticostriatal circuit which triggered presynaptic clustering along striatal dendrites and increased striatal neuron maturation. Calcium imaging revealed that slow calcium oscillations in the cortical population were transferred to the striatal population, an effect not occurring in nonconnected striatal networks.[382] In a comparable device with an additional compartment to deliver chemical agents, Lassus et al. constructed corticostriatal networks with the same activity as that observed in corticostriatal circuits in situ.[404]

The axon-diode concept has been widely tested and optimized[40,383,384,408,409] (Table 7). Le Feber et al., for instance, inserted microchannels with barbs in all interconnecting channels (Figure 5H) to prevent axon growth in the unwanted

https://doi.org/10.1021/acs.chemrev.2c00212
Chem. Rev. 2022, 122, 14842−14880

Table 8. Microfluidic Concepts for Engineering Neuronal Circuits or Neural Tissues

3D model	cell source	scaffold material	microfluidic device	functional study	key findings
layered cortical circuits[39]	cortex E19[a] rat	agarose−alginate	device with four inlets converging on a single channel	microscopic imaging	3D multilayered cortical networks were formed in two cell-hydrogel layers separated by cell-free hydrogel layers in a single channel.
neuronal cell blocks[424]	hippocampus E18 rat hiPSC-derived neurons	collagen	multiple microwells for loading cell-matrix mixtures; gelling to form cell blocks	MEA electrophysiology, calcium imaging	Aligned collagen fibers guided axons between 3D neuronal cell blocks. Bidirectional functional connectivity was confirmed by MEA electrophysiology.
aligned cortical circuits[425]	cortex E17 rat	Matrigel	device with pre- and postsynaptic compartments, and a gel-alignment compartment	calcium imaging	Matrigel aligned by applying hydrostatic pressure from presynaptic side. 3D cortical circuits with functional connectivity between pre- and postsynaptic modules.
anisotropically organized hippocampal circuits[426]	hippocampus CA3 and CA1[b] neurons E18.5 mouse	collagen	device with 3 inlets merging on a single channel	patch-clamp electrophysiology, calcium imaging	Collagen was aligned by stretch and release to guide axons between CA3 and CA1 populations. Synaptic contact between CA3 and CA1 neurons confirmed by microscopy and patch clamp.
neurospheroid blocks, cortical−hippocampal circuit[423]	cortex and hippocampus E17−E18 rat	scaffold-free	PDMS-based neuronal blocks used to mold neuronal spheroids	calcium imaging, microscopy	Synaptic contact between cortical and hippocampal spheroid networks confirmed by oscillations in calcium signals detected by microscopy.
neurospheroid-on-a-chip[449]	cortex E16 rat	scaffold-free self-assembly	multiple microwells and low interstitial level fluidic flow		High-throughput spheroid platform for modeling β-amyloid-induced Alzheimer's disease.
brain organoid-on-a-chip[450]	hiPSCs	Matrigel	parallel organoid chambers and media perfusion channels	microscopy of organoid growth on chip	Perfusion of brain organoids improved cortical development compared to static organoid cultures.
motor unit-on-a-chip[452]	myoblast and mESC[c]-derived motor neurons (MNs)	collagen−Matrigel hydrogel	parallel gel channels flanked by medium channels assembled on top of a PDMS membrane with two sets of capped pillars	patch clamp, optogenetic stimulation of MNs[d], measurement of contraction forces	Functional 3D neuromuscular junction. Capped pillars in myoblast compartment measured their contraction force. Optical stimulation of MNs induced myoblast contraction.
ALS[e] motor unit-on-a-chip[453]	MNs from ALS patient iPSC-derived skeletal muscle cells	collagen−Matrigel hydrogel	device with multiple compartments for MN, muscle cells, and neurite elongation; pillars on muscle cell compartment	electrical and optical stimulation of MNs, measurement of contraction forces in the muscle cells	Functional 3D motor unit derived from ALS patient compared with a motor unit from a healthy subject. Optically or electrically induced contraction forces were measured.
neurovascular unit[458]	cortex E18 rat astrocytes P0−P2[f] rat HUVECs[g]	collagen type I	parallel compartments for medium, neuron-hydrogel, astrocyte-hydrogel, and an endothelial cell monolayer separated by trapezoidal structures	calcium imaging, permeability assay	Functional 3D-engineered neuronal network with vascular unit. Compound selectivity of the endothelial monolayer was used to analyze the effect of different compounds and factors on neuronal growth and maturation.
BBB-on-a-chip[459]	cortex E17−E18 rat motor neurons, E12 mouse Schwann cells P4, mouse HBMECs[h]	collagen type I	A 96-well plate-format device with hydrogel injection ports, media reservoirs, hydrogel channels, and micropost arrays.	calcium imaging, permeability testing, quantification of protein expression levels	High-throughput 3D-engineered cortical circuits, BBB[i] and myelinated MNs.
brain organoid-on-a-chip[450]	hiPSCs	Matrigel	parallel organoid chambers and supporting media channels with interconnecting apertures	immunolabeling of cortical markers	Brain organoids benefited from an improved nutrient exchange. Enhanced expression of cortical markers compared to static cultures.
brain organoid-on-a-chip[451]	hiPSCs	brain ECM[j] mixed with Matrigel	multicompartment device with 3D assembled microchannels and rocker-system driven flow	immunostaining, calcium imaging, patch-clamp electrophysiology	Improved and reproducible corticogenesis, complex structural organization, diverse and mature neuronal identities, and enhanced electrophysiological properties.
retinal organoid-on-a-chip[463]	hiPSCs	HyStem-C[k]	2-layer structure: top layer (organoids) and lower layer (vasculature system) with a porous membrane in between	immunostaining, drug testing, calcium imaging	Replicated the interaction of mature photoreceptors and RPE[l]. Enhanced retinal outer segment formation. Modeling key processes of the visual cycle.

[a]Embryonic day. [b]CA1 and CA3 subregions of hippocampus. [c]Mouse embryonic stem cell. [d]Motor neurons. [e]Amyotrophic lateral sclerosis. [f]Postnatal day. [g]Human umbilical vein endothelial cells. [h]Human brain microvascular endothelial cells. [i]Blood−brain barrier. [j]Extracellular matrix. [k]A hyaluronic acid-based hydrogel. [l]Retinal pigment epithelium.

direction.[409] By using MEA electrophysiology on this device, it was possible to confirm the unidirectional propagation of spontaneous or evoked signals along axons and between the two compartments.[409] Meanwhile, in an axonal edge guidance device (Figure 5H), axons were hindered from growing in one of the directions and instead guided to the source reservoir by the use of curved or arched microchannels connecting back to the main microchannels.[384]

The use of multiple sequential axon-diode modules along microchannels increases the likelihood of achieving unidirectional axonal growth.[40,383,408] In a recent study, Gladkov et al. designed miniaturized diodes in "spine", "triangular", and "zigzag" configurations and incorporated them over the length of

https://doi.org/10.1021/acs.chemrev.2c00212
Chem. Rev. 2022, 122, 14842−14880

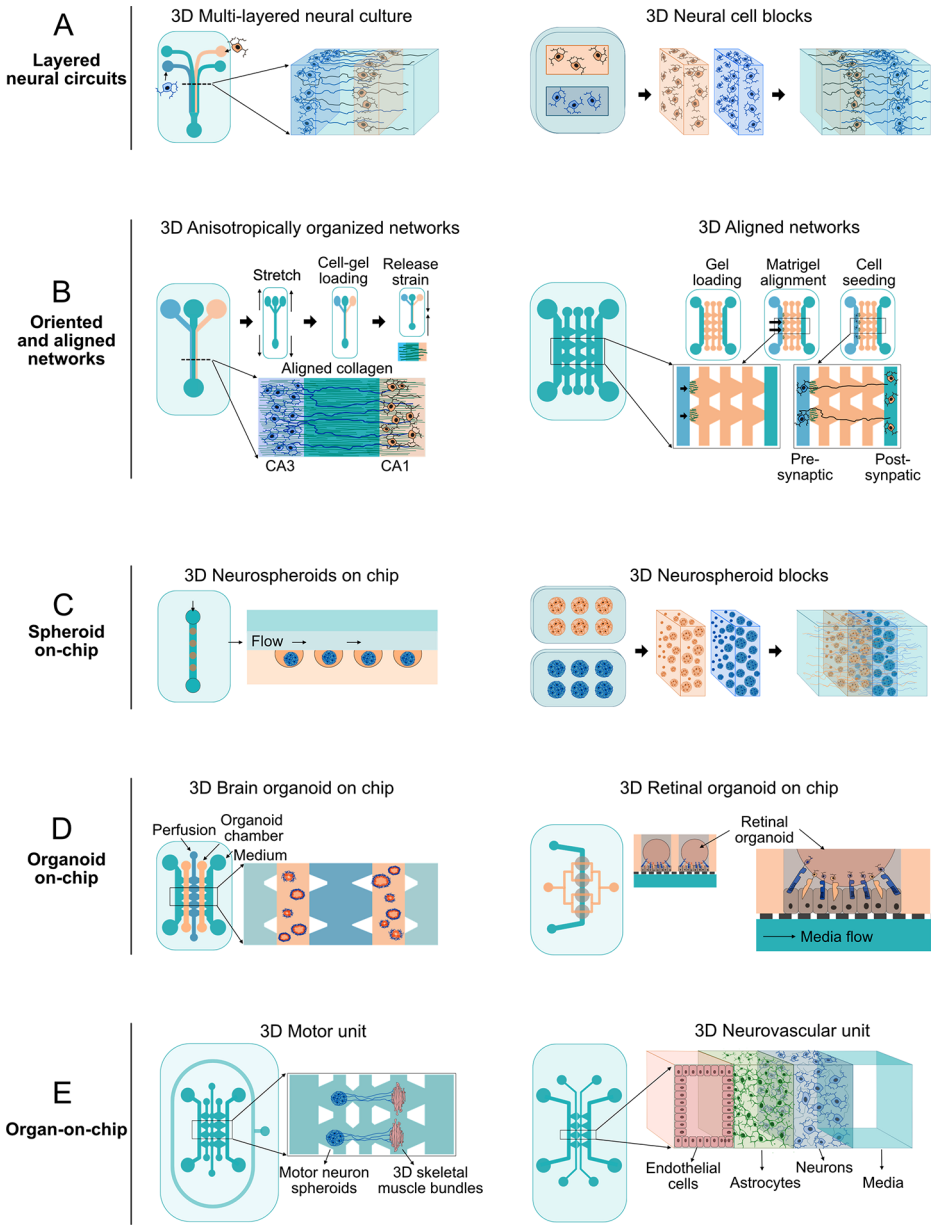

Figure 6. Construction of 3D neuronal circuits in microfluidic devices. (A) Layered neuronal circuits: Different neuronal types are embedded in hydrogel and pushed through microchannels in microfluidic devices to engineer 3D layers. Hydrogel-embedded neuronal cell blocks can be generated using PDMS devices and placed next to each other afterward. (B) Oriented and aligned networks: 3D hydrogel scaffolds supporting neuronal cells are aligned either by stretching the microfluidic device during the polymerization process or by applying hydrostatic pressure. Aligning collagen or Matrigel fibers enables the axons to be better guided from presynaptic to postsynaptic compartments and to thereby form unidirectional networks. (C) Spheroid-on-a-chip: High-throughput scaffold-free neurospheroid cultures are generated in perfused microwell microfluidic systems. Spheroid blocks from different neuronal cell types can be engineered and subsequently placed next to each other. (D) Organoid-on-a-chip: Growing brain and retinal organoids in microfluidic devices with improved diffusion extends their lifespan. (E) Organ-on-a-chip: By integrating additional cell types such as myocytes or endothelial cells, functional units like the motor unit or the blood–brain barrier (BBB) can be replicated in microfluidic platforms.

entire microchannels. MEA recordings showed that spontaneous burst activity in the source compartment propagated directionally through the microchannels, triggering activity in the target compartment.[383] In a different study, axonal pathfinding in microchannels with several types of diode motifs, such as arch, pretzel, heart, and arrowhead, was investigated (Figure 5H).[408] The authors reported that axon-diodes with acute corners (e.g., arrowhead) or complex paths (e.g., pretzel) were more effective in forcing axons to grow toward a target reservoir and could be applied to more effectively achieve unidirectional connectivity between compartments.[408]

Asymmetric microchannel designs have been extensively used to engineer complex brain circuits with particular connectivity patterns. Kamudzandu et al., for instance, seeded five cell types extracted from rat basal ganglia (BG) into an interconnected five-compartment microfluidic device in an attempt to reconstruct the BG neuronal circuitry.[292] Directional connectivity between glutamatergic cortical neurons, GABAergic and dopaminergic neurons of the substantia nigra, and GABAergic neurons of the globus pallidus and striatum was established using tapered microchannels and functionally confirmed by calcium imaging and patch-clamp electro-

https://doi.org/10.1021/acs.chemrev.2c00212
Chem. Rev. 2022, 122, 14842−14880

physiology.[292] Such complex models that replicate circuits within specific brain nuclei can be exploited for modeling neurological disorders like Huntington's and Parkinson's disease.

To guide axonal branches in predefined directions, reservoirs instead of microchannels can also be designed with a diode configuration (Figure 5H). In a device developed by Isomura et al., unidirectional bias was achieved by designing compartments with arrow-shaped structures that forced axons to grow preferentially toward the peak of the arrow.[407] Probing the activity propagation between networks in such a device using electrodes embedded in the substrate confirmed 75% unidirectionality.[407] Similarly, Forró et al. constructed asymmetric reservoir modules with several geometries.[40] Among the different configurations, the authors showed that a stomach-shaped reservoir with one sharp and one round side can guide axons in the desired direction with 92% fidelity. Long-term evaluation of the spontaneous and evoked activities demonstrated more information flow between layers than in a randomly connected network.[40]

Although there is a strong trend toward the 3D engineering of neuronal tissues in vitro, simplistic models of 2D-engineered neuronal circuits are better suited for their use with conventional functional recording technologies such as MEA electrophysiology. Likewise, there are well-established methods for imaging the development and formation of 2D-engineered neuronal circuits in microfluidic platforms. Furthermore, the activity of 2D-engineered neuronal circuits can be controlled using chemical factors or optical and electrical tools without the need for extremely sophisticated instruments.

5.5. Engineering 3D Neuronal Networks in Microfluidic Devices

Neuronal circuits in microfluidic platforms have so far been constructed primarily in two dimensions. However, 2D neuronal circuits fail to fully replicate the in vivo neuronal architecture. Therefore, despite the difficulties engineering and experimenting with them, there is widespread interest in the development of 3D neuronal tissue models for basic research and disease modeling.[416,417] Several methods have been developed to fabricate 3D scaffolds for neuronal tissue engineering. Here we focus solely on microfluidic-based 3D neuronal tissue engineering to model brain circuits (Table 8).

One of the first steps in designing neuronal tissues in 3D is finding an optimal biomaterial to support the neuronal structure in three dimensions.[418] Therefore, the 3D engineering of neuronal circuits in microfluidic platforms relies heavily on biomaterial research.[419] The major categories of biomaterials for the construction of 3D neuronal tissue include natural polymers, synthetic polymers, composite polymers, and decellularized ECM; the use and properties of these materials have been previously reviewed by others.[417,420,421] As in 2D microfluidic devices, compartments and microchannels are used in biocompatible 3D scaffolds to position and connect neurons.[422]

An early 3D neuronal circuit was engineered in a microfluidic device[39] by embedding primary cortical neurons in an agarose-alginate-based mixture which was subsequently injected through two inlets (Figure 6A). Simultaneous injection of a cell-free alginate−agarose mixture through an additional pair of inlets produced four laminar opposing flows of cell-containing and cell-free mixtures through four separate lines which, as the temperature dropped, solidified to form two layers of 3D cortical circuits inside a single microfluidic channel (Figure 6A). After a few weeks, neurites from each layer elongated and crossed the cell-free layer to connect with cells in the other layer.[39] Alternatively, such circuits can also be created by first molding an individual 3D neuronal network in a PDMS-based template and then assembling these "neuronal blocks" (Figure 6A) to produce layered neuronal networks (e.g., cortical and hippocampal).[423] Using this method, parallel layers of different neuronal populations that remain in close contact with each other can be fabricated with no mechanical barrier between them (Figure 6A).

Layered 3D neuronal circuits have also been constructed by loading a cell−collagen mixture into parallelly aligned open compartments in a microfluidic device. After gel formation, PDMS was removed, and the space between layers was filled with a mixture of collagen fibers which solidified after incubating the device at 37 °C. Using this method, three-layer networks containing hippocampal- and hiPSC-derived neurons were assembled. MEA recordings of these devices confirmed bidirectional communication between the distinct layers.[424] Bang et al. applied a microfluidic device with diode-shaped pillars to separate pre- and postsynaptic compartments.[425] They aligned Matrigel between the two compartments by applying hydrostatic pressure through the first (presynaptic) compartment (Figure 6B). Synaptic communication between the two populations of 3D neuronal layers was confirmed by calcium imaging.[425] Further, Kim et al. exploited the elastic properties of PDMS and the fibrillogenesis kinetics of collagen to form aligned fibrous structures between populations of CA3 and CA1 hippocampal networks.[426] The 3D collagen fibrous structures were aligned by stretching or compressing the microfluidic devices during the gelation process (Figure 6B). Collagen fibrous structures guided the axons of the CA3 population toward CA1 neurons, effectively recreating an oriented 3D CA3−CA1 circuit.

Other common approaches for 3D neuronal tissue engineering like neuronal spheroids and organoids can also be adapted to microfluidic platforms for microenvironment control, diffusion improvement, or disease modeling and drug screening[427] (Table 8). Spheroids and organoids are 3D structures grown from stem cells, either embryonic, adult, or induced pluripotent, that exhibit organ-specific cell types and that self-organize through spatially restricted lineage commitment.[12,428,429] Brain and cortical organoids are normally formed by diverse cell types, including neuronal and glial progenitor cells.[430−432] Different to other 3D models, brain organoids exhibit structures characteristic of the developing brain[34,131,133,169,171,428,433] as they are created largely based on intrinsic hiPSC differentiation mechanisms.[12,34,168,434,435] Notably, brain region-specific organoids can also be created but require the use of extrinsic modulatory factors like small molecules or growth factors.[432,436,437] Indeed, some research groups have tried to fuse brain region-specific organoids together into what are now known as assembloids to control inter-regional interactions.[438−443] In a cortical−thalamic assembloid, Xiang et al. showed that axons of neurons from the thalamic organoid extended and innervated the superficial layers of the cortical organoid.[283,443] Such directionality in connection patterns between the two organoids recapitulated the process of neuronal circuit assembly occurring during human brain development. Thus, brain organoids and assembloids can be exploited for studying a variety of developmental features like neuronal migration, axonal elongation, synaptogenesis, and synapse pruning in vitro.[283]

https://doi.org/10.1021/acs.chemrev.2c00212
Chem. Rev. 2022, 122, 14842−14880

Although the organoid field has grown exponentially in recent years, brain organoid technology is still in its infancy and multiple challenges remain to be overcome. For instance, different types of cells may need months to develop within a brain organoid. Moreover, the molecular gradients governing cell organization and axonal guidance are absent. Importantly, large organoids tend to develop a necrotic core due to the lack of vasculature within them, and the occurrence of randomly positioned neural tubes in brain organoids interferes with their proper organization.[283,429,444,445] Luckily, microfluidic concepts to improve perfusion, control and establish molecular gradients, and provide geometric constraints, have all already been implemented to different extents to simplify and optimize organoid generation procedures.[445−448] Park et al., for example, developed a microfluidic-based 3D system in which neuronal spheroids are trapped in microwells with continuous exposure to slow interstitial fluid flows (Figure 6C) to simulate the brain microenvironment.[449] Wang et al. embedded hiPSC-derived embryoid bodies in Matrigel and injected them into parallel microfluidic channels (Figure 6D) connected through diagonal microchannels.[450] Remarkably, the brain organoids produced by the authors under perfused culture conditions showed regionalization and cortical organization.[450] In a different study, Cho et al. embedded brain organoids into brain extracellular matrix in a pump-free microfluidic device that used a rocker system to flow media through the ECM to show that periodic flow of media and 3D ECM matrix improves organoid survival and reproducibly enhances the formation of a cortical layer and its electrophysiological function.[451] Recently developed intelligent microfluidic minibioreactors continuously modulate the media flow to brain organoids and use a reinforcement learning-based controller to regulate mode, direction, and speed of rotation in organoid microwells.[445]

3D neuronal circuits engineered in microfluidic devices have also been coupled with cells of a target tissue (e.g., muscle cells; Figure 6E) to provide a model of an organ, often referred as organ-on-a-chip platforms.[452] Uzel and colleagues, for example, embedded either myoblasts or Channelrhodopsin-2-expressing motor neurons into collagen-Matrigel matrices and loaded them into two separate compartments of a microfluidic device connected through microchannels (Figure 6E). While Channelrhodopsin-2 allowed for the motor neurons to be optically stimulated to fire action potentials, the compartment onto which myoblasts were loaded contained PDMS pillars whose tilting could be used as a measure of muscle contraction. With this system in place, the authors could confirm that optical stimulation of motor neurons could effectively induce the contraction of innervated muscle cells.[452] Such a system is an elegant example of 3D neuromuscular junction (NMJ) models, which have been also used to study amyotrophic lateral sclerosis (ALS) by incorporating hiPSC-derived motor neurons of individuals affected by the disease.[453,454]

The neurovascular unit can also be formed in microfluidic devices by seeding neuronal spheroids and endothelial cells embedded in hydrogel into a single channel supported by adjacent media delivery channels.[455] Meanwhile, multilayer assembly is also useful to mimic the neurovascular unit and the BBB in other organ-in-a-chip platforms (Figure 6E). Although in most instances these devices do not offer control over neuronal polarity or network organization, they offer great potential for drug screening and disease modeling applications.[49,456] For the neurovascular unit, neurons and endothelial cells are commonly cultured in 2D but separated by a thin porous membrane, which makes it possible to control the media in the neuronal and endothelial chambers separately,[456,457] while for the BBB, four-compartment devices with parallel microchannel structures are used to culture hydrogel-embedded astrocytes and neurons. Such microchannels are then put in contact with an endothelial cell monolayer in the outer compartment that mimics the BBB and enables to investigate size-selective permeability.[458,459]

In conclusion, microfluidics-based 3D neuronal circuit engineering techniques are flexible and support the culture of brain organoids and the development of brain-on-a-chip models.[447,460,461] Unlike brain-on-a-chip models, brain organoids faithfully replicate fetal neocortex development while also exhibiting segregated brain regions, cell type heterogeneity, and brain-endogenous gene expression programs.[34,131] On the other hand, while brain organoid platforms often fail to provide tools for controlling the cellular microenvironment, brain-on-a-chip models are compatible with microenvironmental control as they incorporate diverse microfluidic concepts.[462,463] Low throughput and lack of reproducibility, however, remain as major challenges in the organoid field.[464] Initial attempts at adapting droplet-based microfluidic concepts, which have been exploited extensively for single-cell sorting and sequencing, are being undertaken as to generate uniform organoids at scale.[447] Such a robust platform could enhance the translational capacity of human-derived brain organoids and upgrade their physiological relevance.[460,461] In turn, brain region-specific organoids[465−467] can also be adapted to multicompartment microfluidic devices to engineer on-chip assembloids. Similar to two-layered 2D and 3D network structures in compartmentalized microfluidic devices, 3D brain region-specific organoids could also be studied in physically and chemically isolated environments while synaptically interacting with each other. Thus, combining these two technologies, brain-on-a-chip and brain organoids, could allow the scientific community to more closely recapitulate brain development. Achberger et al. showed that integrating retinal organoids into a microfluidic system with vasculature-like perfusion (Figure 6D), for instance, improved the formation of an outer retinal segment and photoreceptor development.[463] In a different study, it was also shown that perfusing brain organoids in microfluidic systems (Figure 6D) resulted in the organoids exhibiting a higher expression of cortical layer markers than their counterparts cultured under static nonperfusing conditions.[450] Hence, microfluidic-based approaches represent an excellent platform to replicate the long-term features of the developing human cortex and retina in vitro. In addition, optimized perfusion systems and cell culture media can be integrated with advanced microscopy and electrophysiology tools to enable the uninterrupted collection of data from developing 2D or 3D neuronal networks and organoids.[468−472] Together with advances in strategies for the derivation of neuronal cells from hiPSCs, which partially circumvent the need for animals as primary cell sources, microfluidic-based approaches represent an excellent platform to advance our understanding of CNS development and disease.

6. LIMITATIONS OF MICROFLUIDICS FOR ENGINEERING NEURONS AND NEURONAL CIRCUITS

In spite of the numerous technological advantages that microfluidic platforms offer for engineering neuronal circuits, there are still limitations in the physical and chemical effects of the microfluidic environment on the cell, as well as challenges in coupling microfluidic devices with other platforms, especially

https://doi.org/10.1021/acs.chemrev.2c00212
Chem. Rev. 2022, 122, 14842−14880

those for imaging and for electrophysiological recordings.[247] Subtle changes in the concentration of cell-culture media components and supplements, whose quality sometimes varies between production batches, can dramatically influence cell fate and behavior. Thus, the implementation of stringent and frequent quality checks is of the utmost importance for the generation of robust, reliable, and reproducible results.

Experiments in microfluidic devices can be significantly complex. High-throughput microfluidic platforms for highly parallelized experiments, for instance, require meticulous evaluation and precise control of intricate microchannel systems before their use. Moreover, although the shallow channels of shrunken cellular microenvironments impose no limitation on nutrient and gas diffusion, the effects of synthetic physical and chemical environments on neuronal cells must be thoroughly assessed.[13] For instance, elevated shear forces arising from high-speed flows along microchannels, the absorption and adsorption of soluble materials in cell-culture media, and the desorption of materials from the microfluidic device need to be taken into account not only when actually conducting experiments but already at the design and manufacturing stages.[13,16]

At the circuit level, microfluidic platforms usually provide conditions that support the survival of low-density networks. However, a sealed cellular environment is often problematic for certain experimental measurements, such as patch-clamp electrophysiology, which requires access from the top of the device. Although microfluidic platforms have been successfully integrated with planar MEA electrodes, the use of recently developed 3D MEAs to investigate 3D-engineered neuronal circuits in microfluidic platforms remains challenging and still requires optimization.[473] In addition, the use of optical tools to record from and to stimulate 3D neuronal networks in microfluidic devices is not always straightforward, as substances from diverse fluids can be absorbed by PDMS and affect the optical properties of the device.[474]

7. CONCLUSION AND OUTLOOK

Progress in hiPSC technology has facilitated the engineering of a multitude of cell types, including multiple neuronal cells. In parallel, diverse advances in microfluidics have laid the foundations for the development of strategies to isolate and transcriptionally profile individual cells from virtually any tissue, including those of the CNS. Together, these technological advances have enabled us to deepen our understanding of the organization and function of cells and tissues, ultimately providing crucial information for tissue engineering, for more accurately modeling neurodegenerative and developmental disorders in vitro and for developing advanced cell-replacement therapies.[475]

The creation of more sophisticated microfluidic tools has accelerated the sorting and classification of the cells forming the CNS. Microfluidic-based systems have delivered substantial progress in single-cell sequencing and high-throughput screening platforms that have made it possible to categorize a myriad of neuronal cells based on their molecular profiles. The latter is crucial for engineering neuronal cells, which are essential for the in vitro development of neuronal circuits.[86] Additionally, microfluidic systems offer the possibility to closely recreate many cellular microenvironments through the fine-tuning of their physical and chemical properties. Thereby, microfluidic devices offer the possibility to efficiently and controllably drive the differentiation and maturation of multiple cell types, including neurons.[476]

The electrophysiological and molecular properties of neuronal cells can be studied at the axonal and synaptic levels in compartmentalized microfluidic systems. Within them, neuronal cell wiring can be finely controlled by adjusting various design parameters. Although microfluidic-based neuronal circuit engineering is still in its infancy, it has already been successfully applied to the construction of 2D and 3D neuronal networks made up of multiple neuronal (and in some cases non-neuronal) cell types.[17,425] These engineered models can be used to recreate specific brain circuits in vitro and to study both their function and dysfunction in health and disease.

By integrating additional cell types, such as astrocytes, muscle cells, microglia and endothelial cells, into neuronal circuits, it is also possible to study the features of a variety of physiologically relevant functional units and to investigate their response to a variety of stimuli, as in the frame of drug screenings and disease modeling.[450,463,477] Similarly, microfluidic platforms offer an optimal experimental environment for the long-term culture of stem cell-derived brain and retinal organoids, which closely replicate the main developmental features of these tissues in vivo.

In general, the possibility of coupling microfluidic devices with a wide range of technologies, and to use them both with classical 2D cultures as well as with sophisticated 3D systems, makes them highly valuable tools for investigating the inner workings of CNS components and modules in health and disease. Therefore, taking into account the advantages of microfluidic platforms for classifying, sorting, and engineering neuronal cells, as well as either simple or complicated neuronal circuits and tissues, it is difficult to understate their value as an experimental platform for studying a wide variety of central nervous system processes.

ASSOCIATED CONTENT

Special Issue Paper

This paper is an additional review for *Chem. Rev.* **2022**, volume *122*, issue 7, "Microfluidics".

AUTHOR INFORMATION

Corresponding Author

Volker Busskamp − *Department of Ophthalmology, Universitäts-Augenklinik Bonn, University of Bonn, D-53127 Bonn, Germany;* orcid.org/0000-0001-7517-8944; Email: volker.busskamp@ukbonn.de

Authors

Rouhollah Habibey − *Department of Ophthalmology, Universitäts-Augenklinik Bonn, University of Bonn, D-53127 Bonn, Germany*

Jesús Eduardo Rojo Arias − *Wellcome—MRC Cambridge Stem Cell Institute, Jeffrey Cheah Biomedical Centre, Cambridge Biomedical Campus, University of Cambridge, Cambridge CB2 0AW, United Kingdom*

Johannes Striebel − *Department of Ophthalmology, Universitäts-Augenklinik Bonn, University of Bonn, D-53127 Bonn, Germany*

Complete contact information is available at: https://pubs.acs.org/10.1021/acs.chemrev.2c00212

Author Contributions

§R.H. and J.E.R.A. contributed equally to the work. CRediT: **Rouhollah Habibey** conceptualization, visualization, writing-

https://doi.org/10.1021/acs.chemrev.2c00212
Chem. Rev. 2022, 122, 14842−14880

original draft, writing-review & editing; **Jesús Eduardo Rojo Arias** writing-original draft, writing-review & editing; **Johannes Striebel** writing-review & editing; **Volker Busskamp** funding acquisition, supervision, writing-review & editing.

Notes

The authors declare no competing financial interest.

Biographies

Rouhollah Habibey is a Postdoctoral researcher at the University of Bonn (Germany). As a Postdoctoral researcher, he worked at the Italian Institute of Technology (Italy, 2017) and at the Center for Regenerative Therapies Dresden (CTRD) at TU Dresden (Germany, until 2021). He obtained his degree in Human Physiology from Tehran University of Medical Sciences (Iran), in 2006, and completed his Ph.D. in Neuroscience and Brain Technologies in a joint Ph.D. program between the Italian Institute of Technology (IIT) and and University of Genova (Italy) in 2015. His research is focused on bottom-up engineering of brain-mimetic human derived neuronal circuits by combining bioengineering tools (microfluidics, microscopy, electrophysiology, and optogenetics) with advances in cellular and network neuroscience.

Jesús Eduardo Rojo Arias is a Guest Scientist at the Wellcome-MRC Cambridge Stem Cell Institute of the University of Cambridge and a Senior Scientist at Xap Therapeutics Ltd (United Kingdom). A Biotechnology Engineer by training (Monterrey Institute of Technology and Higher Education, Mexico), Eduardo holds an Erasmus Mundus M.Sc. degree in Nanoscience and Nanotechnology, jointly awarded by the Katholieke Universiteit Leuven (Belgium) and the TU Dresden (Germany), and a Ph.D. in Experimental Biology and Regenerative Medicine awarded by the TU Dresden. Dr. Rojo's work spans the fields of retinal angiogenesis, gastrointestinal cancer, stem cell forward programming, genome engineering, and transcriptomics.

Johannes Striebel received a B.Sc. in Physics from Karlsruhe Institute of Technology (Germany), a PSM in Nanotechnology from Arizona State University (USA) and a M.Sc. in Physics from WWU Münster (Germany). Currently, he is a Ph.D. candidate in Neuroscience at the University of Bonn (Germany), where he is investigating the dynamics of human neural circuits, their reproducible formation, and their computational capabilities.

Volker Busskamp is a trained biotechnologist (TU Braunschweig, Germany, 2006) and performed his Ph.D. in Neuroscience (University of Geneva and University of Basel, Switzerland, 2010) and his postdoctoral training in Systems Biology and Stem Cell Technology (Harvard Medical School, Boston, 2011−2014). In 2014, he started his independent research group as a Volkswagen Foundation Freigeist Fellow and a ERC Starting Investigator at TU Dresden, Germany. In 2019, Volker Busskamp was appointed Professor for Degenerative Retinal Diseases at the Eye Clinic of the University of Bonn, Germany.

ACKNOWLEDGMENTS

V.B. acknowledges funding from the Deutsche Forschungsgemeinschaft (BU 2974/4-1, BU 2974/3-2, and EXC-2151-390873048−Cluster of Excellence−ImmunoSensation^2 at the University of Bonn), the Pro Retina Foundation, the Paul Ehrlich Foundation, and the Volkswagen Foundation (Freigeist-A110720). J.S. acknowledges support by the Joachim Herz Foundation.

ABBREVIATIONS

AC = alternating current
ALS = amyotrophic lateral sclerosis
BBB = blood−brain barrier
BDNF = brain-derived neurotrophic factor
BG = basal ganglia
C1TM = single-cell auto prep integrated fluidic circuit (IFC)
CA1 and CA3 = subregions of hippocampus
cAMP = cyclic adenosine monophosphate
ChR2 = channel rhodopsin 2
cMOS = complementary metal-oxide semiconductor
CNS = central nervous system
$C_{\text{specific membrane}}$ = specific membrane capacitance
DEP = dielectrophoresis
DG = dentate gyrus
dpf = days postfertilization
DRG = dorsal root ganglion
E = embryonic day
EC = entorhinal cortex
ECM = extracellular matrix
EGF = epidermal growth factor
ESCs = embryonic stem cells
FACS = fluorescence-activated cell sorting
FGF2 = fibroblast growth factor 2
GAD = glutamate decarboxylase; catalyzes the conversion of L-glutamic acid to γ-aminobutyric acid (GABA)
GEM = gel bead in emulsion
GP = globus pallidus
HD = Huntington's disease
hiPSCs = human induced pluripotent stem cells
hNESCs = hiPSC-derived neuroepithelial stem cells
inDrop = indexing droplets
iPSCs = induced pluripotent stem cells
MEAs = multielectrode arrays
mESCs = mouse embryonic stem cells
MGE = medial ganglionic eminence
NGF = nerve growth factor
NSCs = neural stem cells
OPCs = oligodendrocyte precursor cells
OSVZ = outer subventricular zone
P = postnatal day
PD = Parkinson's disease
PDGF = platelet-derived growth factor
PDMS = polydimethylsiloxane
PKA = protein kinase A
PNS = peripheral nervous system
qRT-PCR = quantitative reverse transcription polymerase chain reaction
RGC = retinal ganglion cell
scRNA-Seq = single-cell RNA sequencing
SGZ = subgranular zone
SN = substantia nigra
sNucDrop-Seq = single-nucleus RNA-Seq
SVZ = subventricular zone
TF = transcription factor
UMI = unique molecular identifiers
VZ = ventricular zone
wpc = weeks post conception
μFACS = microfluidic FACS platform
$\sigma_{\text{cytoplasm}}$ = cytoplasm conductivity
μCP = microcontact printing

REFERENCES

(1) Huang, Z. J.; Paul, A. The Diversity of GABAergic Neurons and Neural Communication Elements. *Nat. Rev. Neurosci.* **2019**, *20*, 563−572.

https://doi.org/10.1021/acs.chemrev.2c00212
Chem. Rev. 2022, 122, 14842−14880

(2) Poulin, J. F.; Tasic, B.; Hjerling-Leffler, J.; Trimarchi, J. M.; Awatramani, R. Disentangling Neural Cell Diversity Using Single-Cell Transcriptomics. *Nat. Neurosci.* **2016**, *19*, 1131−1141.
(3) Mu, Q.; Chen, Y.; Wang, J. Deciphering Brain Complexity Using Single-Cell Sequencing. *Genomics, Proteomics Bioinforma.* **2019**, *17*, 344−366.
(4) Bassett, D. S.; Gazzaniga, M. S. Understanding Complexity in the Human Brain. *Trends Cogn. Sci.* **2011**, *15*, 200−209.
(5) Pastrana, E. Focus on Mapping the Brain. *Nat. Methods* **2013**, *10*, 481−481.
(6) Suárez, L. E.; Markello, R. D.; Betzel, R. F.; Misic, B. Linking Structure and Function in Macroscale Brain Networks. *Trends Cogn. Sci.* **2020**, *24*, 302−315.
(7) Latifi, S.; Tamayol, A.; Habibey, R.; Sabzevari, R.; Kahn, C.; Geny, D.; Eftekharpour, E.; Annabi, N.; Blau, A.; Linder, M. Natural Lecithin Promotes Neural Network Complexity and Activity. *Sci. Rep.* **2016**, *6*, 23777.
(8) Azzarelli, R.; Oleari, R.; Lettieri, A.; Andre', V.; Cariboni, A. In Vitro, Ex Vivo and in Vivo Techniques to Study Neuronal Migration in the Developing Cerebral Cortex. *Brain Sci.* **2017**, *7*, 48−68.
(9) Croft, C. L.; Futch, H. S.; Moore, B. D.; Golde, T. E. Organotypic Brain Slice Cultures to Model Neurodegenerative Proteinopathies. *Mol. Neurodegener.* **2019**, *14*, 45−56.
(10) Cromwell, H. C. Translating Striatal Activity from Brain Slice to Whole Animal Neurophysiology: A Guide for Neuroscience Research Integrating Diverse Levels of Analysis. *J. Neurosci. Res.* **2019**, *97*, 1528−1545.
(11) Paşca, S. P. The Rise of Three-Dimensional Human Brain Cultures. *Nature* **2018**, *553*, 437−445.
(12) Hattori, N. Cerebral Organoids Model Human Brain Development and Microcephaly. *Mov. Disord.* **2014**, *29*, 185−185.
(13) Ndyabawe, K.; Kisaalita, W. S. Engineering Microsystems to Recapitulate Brain Physiology on a Chip. *Drug Discovery Today* **2019**, *24*, 1725−1730.
(14) Latifi, S.; Mitchell, S.; Habibey, R.; Hosseini, F.; Donzis, E.; Estrada-Sanchez, A. M.; Rezaei Nejad, H.; Levine, M.; Golshani, P.; Carmichael, S. T. Neuronal Network Topology Indicates Distinct Recovery Processes after Stroke. *Cereb. Cortex* **2020**, *30*, 6363−6375.
(15) Taylor, A. M.; Jeon, N. L. Micro-Scale and Microfluidic Devices for Neurobiology. *Curr. Opin. Neurobiol.* **2010**, *20*, 640−647.
(16) Karimi, M.; Bahrami, S.; Mirshekari, H.; Basri, S. M. M.; Nik, A. B.; Aref, A. R.; Akbari, M.; Hamblin, M. R. Microfluidic Systems for Stem Cell-Based Neural Tissue Engineering. *Lab Chip* **2016**, *16*, 2551−2571.
(17) Fantuzzo, J. A.; Hart, R. P.; Zahn, J. D.; Pang, Z. P. Compartmentalized Devices as Tools for Investigation of Human Brain Network Dynamics. *Dev. Dyn.* **2019**, *248*, 65−77.
(18) Wan, J.; Zhou, S.; Mea, H. J.; Guo, Y.; Ku, H.; Urbina, B. M. Emerging Roles of Microfluidics in Brain Research: From Cerebral Fluids Manipulation to Brain-on-A-Chip and Neuroelectronic Devices Engineering. *Chem. Rev.* **2022**, *122*, 7142−7181.
(19) Vázquez-Guardado, A.; Yang, Y.; Bandodkar, A. J.; Rogers, J. A. Recent Advances in Neurotechnologies with Broad Potential for Neuroscience Research. *Nat. Neurosci.* **2020**, *23*, 1522−1536.
(20) Chen, X.; Liu, C.; Muok, L.; Zeng, C.; Li, Y. Dynamic 3d On-Chip Bbb Model Design, Development, and Applications in Neurological Diseases. *Cells* **2021**, *10*, 3183−3206.
(21) Nikolakopoulou, P.; Rauti, R.; Voulgaris, D.; Shlomy, I.; Maoz, B. M.; Herland, A. Recent Progress in Translational Engineered in Vitro Models of the Central Nervous System. *Brain* **2020**, *143*, 3181−3213.
(22) Shang, L.; Cheng, Y.; Zhao, Y. Emerging Droplet Microfluidics. *Chem. Rev.* **2017**, *117*, 7964−8040.
(23) Liu, Y.; Sun, L.; Zhang, H.; Shang, L.; Zhao, Y. Microfluidics for Drug Development: From Synthesis to Evaluation. *Chem. Rev.* **2021**, *121*, 7468−7529.
(24) Huber, D.; Oskooei, A.; Casadevall Solvas, X.; Demello, A.; Kaigala, G. V. Hydrodynamics in Cell Studies. *Chem. Rev.* **2018**, *118*, 2042−2079.
(25) Thorsen, T.; Maerkl, S. J.; Quake, S. R. Microfluidic Large-Scale Integration. *Science* **2002**, *298*, 580−584.
(26) Park, J. W.; Vahidi, B.; Taylor, A. M.; Rhee, S. W.; Jeon, N. L. Microfluidic Culture Platform for Neuroscience Research. *Nat. Protoc.* **2006**, *1*, 2128−2136.
(27) Treutlein, B.; Lee, Q. Y.; Camp, J. G.; Mall, M.; Koh, W.; Shariati, S. A. M.; Sim, S.; Neff, N. F.; Skotheim, J. M.; Wernig, M.; et al. Dissecting Direct Reprogramming from Fibroblast to Neuron Using Single-Cell RNA-Seq. *Nature* **2016**, *534*, 391−395.
(28) Kundu, A.; Micholt, L.; Friedrich, S.; Rand, D. R.; Bartic, C.; Braeken, D.; Levchenko, A. Superimposed Topographic and Chemical Cues Synergistically Guide Neurite Outgrowth. *Lab Chip* **2013**, *13*, 3070−3081.
(29) Habibey, R.; Golabchi, A.; Blau, A. *Microchannel Scaffolds for Neural Signal Acquisition and Analysis BT - Neurotechnology, Electronics, and Informatics*; Londral, A. R., Encarnação, P., Rovira, J. L. P., Eds.; Springer International Publishing: Cham, 2015; pp 47−64.
(30) Habibey, R.; Latifi, S.; Mousavi, H.; Pesce, M.; Arab-Tehrany, E.; Blau, A. A Multielectrode Array Microchannel Platform Reveals Both Transient and Slow Changes in Axonal Conduction Velocity. *Sci. Rep.* **2017**, *7*, 8558.
(31) Schmieder, F.; Habibey, R.; Striebel, J.; Büttner, L.; Czarske, J.; Busskamp, V. Tracking Connectivity Maps in Human Stem Cell-Derived Neuronal Networks by Holographic Optogenetics. *Life Sci. Alliance* **2022**, *5*, No. e202101268.
(32) Schmieder, F.; Klapper, S. D.; Koukourakis, N.; Busskamp, V.; Czarske, J. W. Optogenetic Stimulation of Human Neural Networks Using Fast Ferroelectric Spatial Light Modulator-Based Holographic Illumination. *Appl. Sci.* **2018**, *8*, 1180−1194.
(33) Macosko, E. Z.; Basu, A.; Satija, R.; Nemesh, J.; Shekhar, K.; Goldman, M.; Tirosh, I.; Bialas, A. R.; Kamitaki, N.; Martersteck, E. M.; et al. Highly Parallel Genome-Wide Expression Profiling of Individual Cells Using Nanoliter Droplets. *Cell* **2015**, *161*, 1202−1214.
(34) Camp, J. G.; Badsha, F.; Florio, M.; Kanton, S.; Gerber, T.; Wilsch-Bräuninger, M.; Lewitus, E.; Sykes, A.; Hevers, W.; Lancaster, M.; et al. Human Cerebral Organoids Recapitulate Gene Expression Programs of Fetal Neocortex Development. *Proc. Natl. Acad. Sci. U. S. A.* **2015**, *112*, 15672−15677.
(35) Chen, R.; Wu, X.; Jiang, L.; Zhang, Y. Single-Cell RNA-Seq Reveals Hypothalamic Cell Diversity. *Cell Rep.* **2017**, *18*, 3227−3241.
(36) Luni, C.; Giulitti, S.; Serena, E.; Ferrari, L.; Zambon, A.; Gagliano, O.; Giobbe, G. G.; Michielin, F.; Knöbel, S.; Bosio, A.; et al. High-Efficiency Cellular Reprogramming with Microfluidics. *Nat. Methods* **2016**, *13*, 446−452.
(37) Cunningham, M.; Cho, J. H.; Leung, A.; Savvidis, G.; Ahn, S.; Moon, M.; Lee, P. K. J.; Han, J. J.; Azimi, N.; Kim, K. S.; et al. HPSC-Derived Maturing GABAergic Interneurons Ameliorate Seizures and Abnormal Behavior in Epileptic Mice. *Cell Stem Cell* **2014**, *15*, 559−573.
(38) Jung, Y. H.; Phillips, M. J.; Lee, J.; Xie, R.; Ludwig, A. L.; Chen, G.; Zheng, Q.; Kim, T. J.; Zhang, H.; Barney, P.; et al. 3D Microstructured Scaffolds to Support Photoreceptor Polarization and Maturation. *Adv. Mater.* **2018**, *30*, 1803550.
(39) Kunze, A.; Giugliano, M.; Valero, A.; Renaud, P. Micropatterning Neural Cell Cultures in 3D with a Multi-Layered Scaffold. *Biomaterials* **2011**, *32*, 2088−2098.
(40) Forró, C.; Thompson-Steckel, G.; Weaver, S.; Weydert, S.; Ihle, S.; Dermutz, H.; Aebersold, M. J.; Pilz, R.; Demkó, L.; Vörös, J. Modular Microstructure Design to Build Neuronal Networks of Defined Functional Connectivity. *Biosens. Bioelectron.* **2018**, *122*, 75−87.
(41) Molina-Martínez, B.; Jentsch, L. V.; Ersoy, F.; Van Der Moolen, M.; Donato, S.; Ness, T. V.; Heutink, P.; Jones, P. D.; Cesare, P. A Multimodal 3D Neuro-Microphysiological System with Neurite-Trapping Microelectrodes. *Biofabrication* **2022**, *14*, 025004.
(42) Takahashi, K.; Yamanaka, S. Induction of Pluripotent Stem Cells from Mouse Embryonic and Adult Fibroblast Cultures by Defined Factors. *Cell* **2006**, *126*, 663−676.

https://doi.org/10.1021/acs.chemrev.2c00212
Chem. Rev. 2022, 122, 14842−14880

(43) Takahashi, K.; Tanabe, K.; Ohnuki, M.; Narita, M.; Ichisaka, T.; Tomoda, K.; Yamanaka, S. Induction of Pluripotent Stem Cells from Adult Human Fibroblasts by Defined Factors. *Cell* **2007**, *131*, 861−872.
(44) Yamanaka, S. Pluripotent Stem Cell-Based Cell Therapy—Promise and Challenges. *Cell Stem Cell* **2020**, *27*, 523−531.
(45) Weatherbee, B. A. T.; Cui, T.; Zernicka-Goetz, M. Modeling Human Embryo Development with Embryonic and Extra-Embryonic Stem Cells. *Dev. Biol.* **2021**, *474*, 91−99.
(46) Song, C. G.; Zhang, Y. Z.; Wu, H. N.; Cao, X. L.; Guo, C. J.; Li, Y. Q.; Zheng, M. H.; Han, H. Stem Cells: A Promising Candidate to Treat Neurological Disorders. *Neural Regen. Res.* **2018**, *13*, 1294−1304.
(47) Wang, Y.; Pan, J.; Wang, D.; Liu, J. The Use of Stem Cells in Neural Regeneration: A Review of Current Opinion. *Curr. Stem Cell Res. Ther.* **2018**, *13*, 608−617.
(48) Engle, S. J.; Blaha, L.; Kleiman, R. J. Best Practices for Translational Disease Modeling Using Human IPSC-Derived Neurons. *Neuron* **2018**, *100*, 783−797.
(49) van der Helm, M. W.; van der Meer, A. D.; Eijkel, J. C. T.; van den Berg, A.; Segerink, L. I. Microfluidic Organ-on-Chip Technology for Blood-Brain Barrier Research. *Tissue Barriers* **2016**, *4*, e1142493−e1142493.
(50) Millet, L. J.; Gillette, M. U. Over a Century of Neuron Culture: From the Hanging Drop to Microfluidic Devices. *Yale J. Biol. Med.* **2012**, *85*, 501−521.
(51) Allazetta, S.; Lutolf, M. P. Stem Cell Niche Engineering through Droplet Microfluidics. *Curr. Opin. Biotechnol.* **2015**, *35*, 86−93.
(52) Zhou, W.; Yan, Y.; Guo, Q.; Ji, H.; Wang, H.; Xu, T.; Makabel, B.; Pilarsky, C.; He, G.; Yu, X.; et al. Microfluidics Applications for High-Throughput Single Cell Sequencing. *J. Nanobiotechnol.* **2021**, *19*, 312−333.
(53) Camp, J. G.; Wollny, D.; Treutlein, B. Single-Cell Genomics to Guide Human Stem Cell and Tissue Engineering. *Nat. Methods* **2018**, *15*, 661−667.
(54) Muotri, A. R.; Gage, F. H. Generation of Neuronal Variability and Complexity. *Nature* **2006**, *441*, 1087−1093.
(55) Gordon, J.; Amini, S.; White, M. K. General Overview of Neuronal Cell Culture. *Methods Mol. Biol.* **2013**, *1078*, 1−8.
(56) Martínez-Morales, P. L.; Revilla, A.; Ocaña, I.; González, C.; Sainz, P.; McGuire, D.; Liste, I. Progress in Stem Cell Therapy for Major Human Neurological Disorders. *Stem Cell Rev. Reports* **2013**, *9*, 685−699.
(57) Gögel, S.; Gubernator, M.; Minger, S. L. Progress and Prospects: Stem Cells and Neurological Diseases. *Gene Ther.* **2011**, *18*, 1−6.
(58) Lee, N.; Park, J. W.; Kim, H. J.; Yeon, J. H.; Kwon, J.; Ko, J. J.; Oh, S. H.; Kim, H. S.; Kim, A.; Han, B. S.; et al. Monitoring the Differentiation and Migration Patterns of Neural Cells Derived from Human Embryonic Stem Cells Using a Microfluidic Culture System. *Mol. Cells* **2014**, *37*, 497−502.
(59) Rowe, R. G.; Daley, G. Q. Induced Pluripotent Stem Cells in Disease Modelling and Drug Discovery. *Nat. Rev. Genet.* **2019**, *20*, 377−388.
(60) Farkhondeh, A.; Li, R.; Gorshkov, K.; Chen, K. G.; Might, M.; Rodems, S.; Lo, D. C.; Zheng, W. Induced Pluripotent Stem Cells for Neural Drug Discovery. *Drug Discovery Today* **2019**, *24*, 992−999.
(61) Tabata, Y.; Lutolf, M. P. Multiscale Microenvironmental Perturbation of Pluripotent Stem Cell Fate and Self-Organization. *Sci. Rep.* **2017**, *7*, 44711.
(62) Wang, Y.; Ma, J.; Li, N.; Wang, L.; Shen, L.; Sun, Y.; Wang, Y.; Zhao, J.; Wei, W.; Ren, Y.; et al. Microfluidic Engineering of Neural Stem Cell Niches for Fate Determination. *Biomicrofluidics* **2017**, *11*, 014106.
(63) Riemens, R. J. M.; van den Hove, D. L. A.; Esteller, M.; Delgado-Morales, R. Directing Neuronal Cell Fate in Vitro: Achievements and Challenges. *Prog. Neurobiol.* **2018**, *168*, 42−68.
(64) Kikuchi, T.; Morizane, A.; Doi, D.; Magotani, H.; Onoe, H.; Hayashi, T.; Mizuma, H.; Takara, S.; Takahashi, R.; Inoue, H.; et al. Human IPS Cell-Derived Dopaminergic Neurons Function in a Primate Parkinson's Disease Model. *Nature* **2017**, *548*, 592−596.
(65) Tofoli, F. A.; Semeano, A. T. S.; Oliveira-Giacomelli, Á.; Gonçalves, M. C. B.; Ferrari, M. F. R.; Veiga Pereira, L.; Ulrich, H. Midbrain Dopaminergic Neurons Differentiated from Human-Induced Pluripotent Stem Cells. *Methods Mol. Biol.* **2019**, *1919*, 97−118.
(66) Daadi, M. M. Differentiation of Neural Stem Cells Derived from Induced Pluripotent Stem Cells into Dopaminergic Neurons. *Methods Mol. Biol.* **2019**, *1919*, 89−96.
(67) Cao, S. Y.; Hu, Y.; Chen, C.; Yuan, F.; Xu, M.; Li, Q.; Fang, K. H.; Chen, Y.; Liu, Y. Enhanced Derivation of Human Pluripotent Stem Cell-Derived Cortical Glutamatergic Neurons by a Small Molecule. *Sci. Rep.* **2017**, *7*, 3282.
(68) Vazin, T.; Ball, K. A.; Lu, H.; Park, H.; Ataeijannati, Y.; Head-Gordon, T.; Poo, M.; Schaffer, D. V. Efficient Derivation of Cortical Glutamatergic Neurons from Human Pluripotent Stem Cells: A Model System to Study Neurotoxicity in Alzheimer's Disease. *Neurobiol. Dis.* **2014**, *62*, 62−72.
(69) Yang, N.; Chanda, S.; Marro, S.; Ng, Y. H.; Janas, J. A.; Haag, D.; Ang, C. E.; Tang, Y.; Flores, Q.; Mall, M.; et al. Generation of Pure GABAergic Neurons by Transcription Factor Programming. *Nat. Methods* **2017**, *14*, 621−628.
(70) Sun, A. X.; Yuan, Q.; Tan, S.; Xiao, Y.; Wang, D.; Khoo, A. T. T.; Sani, L.; Tran, H. D.; Kim, P.; Chiew, Y. S.; et al. Direct Induction and Functional Maturation of Forebrain GABAergic Neurons from Human Pluripotent Stem Cells. *Cell Rep.* **2016**, *16*, 1942−1953.
(71) Vadodaria, K. C.; Marchetto, M. C.; Mertens, J.; Gage, F. H. Generating Human Serotonergic Neurons in Vitro: Methodological Advances. *BioEssays* **2016**, *38*, 1123−1129.
(72) Ochalek, A.; Szczesna, K.; Petazzi, P.; Kobolak, J.; Dinnyes, A. Generation of Cholinergic and Dopaminergic Interneurons from Human Pluripotent Stem Cells as a Relevant Tool for in Vitro Modeling of Neurological Disorders Pathology and Therapy. *Stem Cells Int.* **2016**, *2016*, 5838934.
(73) Kim, H. S.; Lee, J.; Lee, D. Y.; Kim, Y. D.; Kim, J. Y.; Lim, H. J.; Lim, S.; Cho, Y. S. Schwann Cell Precursors from Human Pluripotent Stem Cells as a Potential Therapeutic Target for Myelin Repair. *Stem Cell Reports* **2017**, *8*, 1714−1726.
(74) García-León, J. A.; Kumar, M.; Boon, R.; Chau, D.; One, J.; Wolfs, E.; Eggermont, K.; Berckmans, P.; Gunhanlar, N.; de Vrij, F.; et al. SOX10 Single Transcription Factor-Based Fast and Efficient Generation of Oligodendrocytes from Human Pluripotent Stem Cells. *Stem Cell Reports* **2018**, *10*, 655−672.
(75) TCW, J.; Wang, M.; Pimenova, A. A.; Bowles, K. R.; Hartley, B. J.; Lacin, E.; Machlovi, S. I.; Abdelaal, R.; Karch, C. M.; Phatnani, H.; et al. An Efficient Platform for Astrocyte Differentiation from Human Induced Pluripotent Stem Cells. *Stem Cell Reports* **2017**, *9*, 600−614.
(76) Canals, I.; Ginisty, A.; Quist, E.; Timmerman, R.; Fritze, J.; Miskinyte, G.; Monni, E.; Hansen, M. G.; Hidalgo, I.; Bryder, D.; et al. Rapid and Efficient Induction of Functional Astrocytes from Human Pluripotent Stem Cells. *Nat. Methods* **2018**, *15*, 693−696.
(77) Shembekar, N.; Chaipan, C.; Utharala, R.; Merten, C. A. Droplet-Based Microfluidics in Drug Discovery, Transcriptomics and High-Throughput Molecular Genetics. *Lab Chip* **2016**, *16*, 1314−1331.
(78) Zilionis, R.; Nainys, J.; Veres, A.; Savova, V.; Zemmour, D.; Klein, A. M.; Mazutis, L. Single-Cell Barcoding and Sequencing Using Droplet Microfluidics. *Nat. Protoc.* **2017**, *12*, 44−73.
(79) Bhagat, A. A. S.; Bow, H.; Hou, H. W.; Tan, S. J.; Han, J.; Lim, C. T. Microfluidics for Cell Separation. *Med. Biol. Eng. Comput.* **2010**, *48*, 999−1014.
(80) Raj, B.; Wagner, D. E.; McKenna, A.; Pandey, S.; Klein, A. M.; Shendure, J.; Gagnon, J. A.; Schier, A. F. Simultaneous Single-Cell Profiling of Lineages and Cell Types in the Vertebrate Brain. *Nat. Biotechnol.* **2018**, *36*, 442−450.
(81) Wu, Z.; Wicher, G.; Svenningsen, A. F.; Hjort, K. Microfluidic High Viability Separation of Neural Cells. In *4th IEEE International Conference on Nano/Micro Engineered and Molecular Systems, NEMS 2009*, 2009; pp 1079−1083, DOI: DOI: 10.1109/NEMS.2009.5068760.
(82) Moreno, E. L.; Hachi, S.; Hemmer, K.; Trietsch, S. J.; Baumuratov, A. S.; Hankemeier, T.; Vulto, P.; Schwamborn, J. C.;

Fleming, R. M. T. Differentiation of Neuroepithelial Stem Cells into Functional Dopaminergic Neurons in 3D Microfluidic Cell Culture. *Lab Chip* **2015**, *15*, 2419−2428.
(83) Nathamgari, S. S. P.; Dong, B.; Zhou, F.; Kang, W.; Giraldo-Vela, J. P.; McGuire, T.; McNaughton, R. L.; Sun, C.; Kessler, J. A.; Espinosa, H. D. Isolating Single Cells in a Neurosphere Assay Using Inertial Microfluidics. *Lab Chip* **2015**, *15*, 4591−4597.
(84) Dalili, A.; Samiei, E.; Hoorfar, M. A Review of Sorting, Separation and Isolation of Cells and Microbeads for Biomedical Applications: Microfluidic Approaches. *Analyst* **2019**, *144*, 87−113.
(85) Martin, D.; Xu, J.; Porretta, C.; Nichols, C. D. Neurocytometry: Flow Cytometric Sorting of Specific Neuronal Populations from Human and Rodent Brain. *ACS Chem. Neurosci.* **2017**, *8*, 356−367.
(86) Shen, Y.; Yalikun, Y.; Tanaka, Y. Recent Advances in Microfluidic Cell Sorting Systems. *Sens. Actuators B Chem.* **2019**, *282*, 268−281.
(87) Jackson, E. L.; Lu, H. Advances in Microfluidic Cell Separation and Manipulation. *Curr. Opin. Chem. Eng.* **2013**, *2*, 398−404.
(88) Shields, C. W., IV; Reyes, C. D.; López, G. P. Microfluidic Cell Sorting: A Review of the Advances in the Separation of Cells from Debulking to Rare Cell Isolation. *Lab Chip* **2015**, *15*, 1230−1249.
(89) Herbig, M.; Tessmer, K.; Nötzel, M.; Nawaz, A. A.; Santos-Ferreira, T.; Borsch, O.; Gasparini, S. J.; Guck, J.; Ader, M. Label-Free Imaging Flow Cytometry for Analysis and Sorting of Enzymatically Dissociated Tissues. *Sci. Rep.* **2022**, *12*, 963.
(90) Luo, T.; Fan, L.; Zhu, R.; Sun, D. Microfluidic Single-Cell Manipulation and Analysis: Methods and Applications. *Micromachines (Basel)* **2019**, *10*, 104−145.
(91) Di Carlo, D. Inertial Microfluidics. *Lab Chip* **2009**, *9*, 3038−3046.
(92) Huebner, A.; Sharma, S.; Srisa-Art, M.; Hollfelder, F.; Edel, J. B.; DeMello, A. J. Microdroplets: A Sea of Applications? *Lab Chip* **2008**, *8*, 1244−1254.
(93) Santos-Ferreira, T.; Herbig, M.; Otto, O.; Carido, M.; Karl, M. O.; Michalakis, S.; Guck, J.; Ader, M. Morpho-Rheological Fingerprinting of Rod Photoreceptors Using Real-Time Deformability Cytometry. *Cytom. Part A* **2019**, *95*, 1145−1157.
(94) Wu, Z.; Hjort, K.; Wicher, G.; Fex Svenningsen, Å. Microfluidic High Viability Neural Cell Separation Using Viscoelastically Tuned Hydrodynamic Spreading. *Biomed. Microdevices* **2008**, *10*, 631−638.
(95) Jin, T.; Yan, S.; Zhang, J.; Yuan, D.; Huang, X. F.; Li, W. A Label-Free and High-Throughput Separation of Neuron and Glial Cells Using an Inertial Microfluidic Platform. *Biomicrofluidics* **2016**, *10*, 034104.
(96) Jiang, A. Y. L.; Yale, A. R.; Aghaamoo, M.; Lee, D. H.; Lee, A. P.; Adams, T. N. G.; Flanagan, L. A. High-Throughput Continuous Dielectrophoretic Separation of Neural Stem Cells. *Biomicrofluidics* **2019**, *13*, 064111.
(97) Zalis, M. C.; Reyes, J. F.; Augustsson, P.; Holmqvist, S.; Roybon, L.; Laurell, T.; Deierborg, T. Label-Free Concentration of Viable Neurons, HESCs and Cancer Cells by Means of Acoustophoresis. *Integr. Biol. (United Kingdom)* **2016**, *8*, 332−340.
(98) Çetin, B.; Li, D. Dielectrophoresis in Microfluidics Technology. *Electrophoresis* **2011**, *32*, 2410−2427.
(99) Zhang, H.; Chang, H.; Neuzil, P. DEP-on-a-Chip: Dielectrophoresis Applied to Microfluidic Platforms. *Micromachines* **2019**, *10*, 423−445.
(100) Adams, T. N. G.; Jiang, A. Y. L.; Vyas, P. D.; Flanagan, L. A. Separation of Neural Stem Cells by Whole Cell Membrane Capacitance Using Dielectrophoresis. *Methods* **2018**, *133*, 91−103.
(101) Olm, F.; Urbansky, A.; Dykes, J. H.; Laurell, T.; Scheding, S. Label-Free Neuroblastoma Cell Separation from Hematopoietic Progenitor Cell Products Using Acoustophoresis - towards Cell Processing of Complex Biological Samples. *Sci. Rep.* **2019**, *9*, 8777.
(102) Otto, O.; Rosendahl, P.; Mietke, A.; Golfier, S.; Herold, C.; Klaue, D.; Girardo, S.; Pagliara, S.; Ekpenyong, A.; Jacobi, A.; et al. Real-Time Deformability Cytometry: On-the-Fly Cell Mechanical Phenotyping. *Nat. Methods* **2015**, *12*, 199−202.
(103) Liu, C. Microfluidic FACS Becoming Real. *Cytom. Part A* **2018**, *93*, 589−591.
(104) Gong, Y.; Fan, N.; Yang, X.; Peng, B.; Jiang, H. New Advances in Microfluidic Flow Cytometry. *Electrophoresis* **2019**, *40*, 1212−1229.
(105) Yang, R. J.; Fu, L. M.; Hou, H. H. Review and Perspectives on Microfluidic Flow Cytometers. *Sens. Actuators B Chem.* **2018**, *266*, 26−45.
(106) Sugino, H.; Ozaki, K.; Shirasaki, Y.; Arakawa, T.; Shoji, S.; Funatsu, T. On-Chip Microfluidic Sorting with Fluorescence Spectrum Detection and Multiway Separation. *Lab Chip* **2009**, *9*, 1254−1260.
(107) Cheng, Z.; Wu, X.; Cheng, J.; Liu, P. Microfluidic Fluorescence-Activated Cell Sorting (MFACS) Chip with Integrated Piezoelectric Actuators for Low-Cost Mammalian Cell Enrichment. *Microfluid. Nanofluidics* **2017**, *21*, 9−20.
(108) Zhao, Y.; Liu, Q.; Sun, H.; Chen, D.; Li, Z.; Fan, B.; George, J.; Xue, C.; Cui, Z.; Wang, J.; et al. Electrical Property Characterization of Neural Stem Cells in Differentiation. *PLoS One* **2016**, *11*, No. e0158044.
(109) Tan, S. J.; Kee, M. Z. L.; Mathuru, A. S.; Burkholder, W. F.; Jesuthasan, S. J. A Microfluidic Device to Sort Cells Based on Dynamic Response to a Stimulus. *PLoS One* **2013**, *8*, No. e78261.
(110) Plouffe, B. D.; Murthy, S. K. Perspective on Microfluidic Cell Separation: A Solved Problem? *Anal. Chem.* **2014**, *86*, 11481−11488.
(111) Wu, Z.; Chen, Y.; Wang, M.; Chung, A. J. Continuous Inertial Microparticle and Blood Cell Separation in Straight Channels with Local Microstructures. *Lab Chip* **2016**, *16*, 532−542.
(112) Shields, C. W.; Ohiri, K. A.; Szott, L. M.; López, G. P. Translating Microfluidics: Cell Separation Technologies and Their Barriers to Commercialization. *Cytom. Part B - Clin. Cytom.* **2017**, *92*, 115−125.
(113) Karthick, S.; Pradeep, P. N.; Kanchana, P.; Sen, A. K. Acoustic Impedance-Based Size-Independent Isolation of Circulating Tumour Cells from Blood Using Acoustophoresis. *Lab Chip* **2018**, *18*, 3802−3813.
(114) Waheed, W.; Alazzam, A.; Mathew, B.; Christoforou, N.; Abu-Nada, E. Lateral Fluid Flow Fractionation Using Dielectrophoresis (LFFF-DEP) for Size-Independent, Label-Free Isolation of Circulating Tumor Cells. *J. Chromatogr. B* **2018**, *1087-1088*, 133−137.
(115) Bowles, K. R.; TCW, J.; Qian, L.; Jadow, B. M.; Goate, A. M. Reduced Variability of Neural Progenitor Cells and Improved Purity of Neuronal Cultures Using Magnetic Activated Cell Sorting. *PLoS One* **2019**, *14*, No. e0213374.
(116) Ryan, K.; Rose, R. E.; Jones, D. R.; Lopez, P. A. Sheath Fluid Impacts the Depletion of Cellular Metabolites in Cells Afflicted by Sorting Induced Cellular Stress (SICS). *Cytom. Part A* **2021**, *99*, 921−929.
(117) Pfister, G.; Toor, S. M.; Sasidharan Nair, V.; Elkord, E. An Evaluation of Sorter Induced Cell Stress (SICS) on Peripheral Blood Mononuclear Cells (PBMCs) after Different Sort Conditions - Are Your Sorted Cells Getting SICS? *J. Immunol. Methods* **2020**, *487*, 112902.
(118) Sharifi, S.; Behzadi, S.; Laurent, S.; Forrest, M. L.; Stroeve, P.; Mahmoudi, M. Toxicity of Nanomaterials. *Chem. Soc. Rev.* **2012**, *41*, 2323−2343.
(119) Woelfle, U.; Breit, E.; Pantel, K. Influence of Immunomagnetic Enrichment on Gene Expression of Tumor Cells. *J. Transl. Med.* **2005**, *3*, 12.
(120) Zeisel, A.; Muñoz-Manchado, A. B.; Codeluppi, S.; Lönnerberg, P.; La Manno, G.; Juréus, A.; Marques, S.; Munguba, H.; He, L.; Betsholtz, C.; et al. Cell Types in the Mouse Cortex and Hippocampus Revealed by Single-Cell RNA-Seq. *Science* **2015**, *347*, 1138−1142.
(121) Hu, P.; Fabyanic, E.; Kwon, D. Y.; Tang, S.; Zhou, Z.; Wu, H. Dissecting Cell-Type Composition and Activity-Dependent Transcriptional State in Mammalian Brains by Massively Parallel Single-Nucleus RNA-Seq. *Mol. Cell* **2017**, *68*, 1006−1015.
(122) Tsunemoto, R.; Lee, S.; Szucs, A.; Chubukov, P.; Sokolova, I.; Blanchard, J. W.; Eade, K. T.; Bruggemann, J.; Wu, C.; Torkamani, A.; et al. Diverse Reprogramming Codes for Neuronal Identity. *Nature* **2018**, *557*, 375−380.
(123) Gouwens, N. W.; Sorensen, S. A.; Berg, J.; Lee, C.; Jarsky, T.; Ting, J.; Sunkin, S. M.; Feng, D.; Anastassiou, C. A.; Barkan, E.; et al.

https://doi.org/10.1021/acs.chemrev.2c00212
Chem. Rev. 2022, 122, 14842−14880

Classification of Electrophysiological and Morphological Neuron Types in the Mouse Visual Cortex. *Nat. Neurosci.* **2019**, *22*, 1182−1195.
(124) Zeng, H.; Sanes, J. R. Neuronal Cell-Type Classification: Challenges, Opportunities and the Path Forward. *Nat. Rev. Neurosci.* **2017**, *18*, 530−546.
(125) Zhao, Y.; Chen, D.; Luo, Y.; Li, H.; Deng, B.; Huang, S. B.; Chiu, T. K.; Wu, M. H.; Long, R.; Hu, H.; et al. A Microfluidic System for Cell Type Classification Based on Cellular Size-Independent Electrical Properties. *Lab Chip* **2013**, *13*, 2272−2277.
(126) Zhao, Y.; Abdelfattah, A. S.; Zhao, Y.; Ruangkittisakul, A.; Ballanyi, K.; Campbell, R. E.; Harrison, D. J. Microfluidic Cell Sorter-Aided Directed Evolution of a Protein-Based Calcium Ion Indicator with an Inverted Fluorescent Response. *Integr. Biol. (United Kingdom)* **2014**, *6*, 714−725.
(127) Zhao, Y.; Chen, D.; Li, H.; Luo, Y.; Deng, B.; Huang, S. B.; Chiu, T. K.; Wu, M. H.; Long, R.; Hu, H.; et al. A Microfluidic System Enabling Continuous Characterization of Specific Membrane Capacitance and Cytoplasm Conductivity of Single Cells in Suspension. *Biosens. Bioelectron.* **2013**, *43*, 304−307.
(128) Lake, B. B.; Ai, R.; Kaeser, G. E.; Salathia, N. S.; Yung, Y. C.; Liu, R.; Wildberg, A.; Gao, D.; Fung, H. L.; Chen, S.; et al. Neuronal Subtypes and Diversity Revealed by Single-Nucleus RNA Sequencing of the Human Brain. *Science* **2016**, *352*, 1586−1590.
(129) Tasic, B.; Levi, B. P.; Menon, V. Single-Cell Transcriptomic Characterization of Vertebrate Brain Composition, Development, and Function. In *Decoding Neural Circuit Structure and Function: Cellular Dissection Using Genetic Model Organisms*; Çelik, A., Wernet, M. F., Eds.; Springer International Publishing: Cham, 2017; pp 437−468, DOI: DOI: 10.1007/978-3-319-57363-2_18.
(130) Satija, R.; Farrell, J. A.; Gennert, D.; Schier, A. F.; Regev, A. Spatial Reconstruction of Single-Cell Gene Expression Data. *Nat. Biotechnol.* **2015**, *33*, 495−502.
(131) Luo, C.; Lancaster, M. A.; Castanon, R.; Nery, J. R.; Knoblich, J. A.; Ecker, J. R. Cerebral Organoids Recapitulate Epigenomic Signatures of the Human Fetal Brain. *Cell Rep.* **2016**, *17*, 3369−3384.
(132) Mora-Bermúdez, F.; Badsha, F.; Kanton, S.; Camp, J. G.; Vernot, B.; Köhler, K.; Voigt, B.; Okita, K.; Maricic, T.; He, Z.; et al. Differences and Similarities between Human and Chimpanzee Neural Progenitors during Cerebral Cortex Development. *Elife* **2016**, *5*, No. e18683.
(133) Kiaee, K.; Jodat, Y. A.; Bassous, N. J.; Matharu, N.; Shin, S. R. Transcriptomic Mapping of Neural Diversity, Differentiation and Functional Trajectory in Ipsc-Derived 3d Brain Organoid Models. *Cells* **2021**, *10*, 3422.
(134) Habib, N.; Li, Y.; Heidenreich, M.; Swiech, L.; Avraham-Davidi, I.; Trombetta, J. J.; Hession, C.; Zhang, F.; Regev, A. Div-Seq: Single-Nucleus RNA-Seq Reveals Dynamics of Rare Adult Newborn Neurons. *Science* **2016**, *353*, 925−928.
(135) Bhaduri, A.; Sandoval-Espinosa, C.; Otero-Garcia, M.; Oh, I.; Yin, R.; Eze, U. C.; Nowakowski, T. J.; Kriegstein, A. R. An Atlas of Cortical Arealization Identifies Dynamic Molecular Signatures. *Nature* **2021**, *598*, 200−204.
(136) Shekhar, K.; Lapan, S. W.; Whitney, I. E.; Tran, N. M.; Macosko, E. Z.; Kowalczyk, M.; Adiconis, X.; Levin, J. Z.; Nemesh, J.; Goldman, M.; et al. Comprehensive Classification of Retinal Bipolar Neurons by Single-Cell Transcriptomics. *Cell* **2016**, *166*, 1308.
(137) Rosenberg, A. B.; Roco, C. M.; Muscat, R. A.; Kuchina, A.; Sample, P.; Yao, Z.; Graybuck, L. T.; Peeler, D. J.; Mukherjee, S.; Chen, W.; et al. Single-Cell Profiling of the Developing Mouse Brain and Spinal Cord with Split-Pool Barcoding. *Science* **2018**, *360*, 176−182.
(138) Nowakowski, T. J.; Bhaduri, A.; Pollen, A. A.; Alvarado, B.; Mostajo-Radji, M. A.; Di Lullo, E.; Haeussler, M.; Sandoval-Espinosa, C.; Liu, S. J.; Velmeshev, D.; et al. Spatiotemporal Gene Expression Trajectories Reveal Developmental Hierarchies of the Human Cortex. *Science* **2017**, *358*, 1318−1323.
(139) Trevino, A. E.; Müller, F.; Andersen, J.; Sundaram, L.; Kathiria, A.; Shcherbina, A.; Farh, K.; Chang, H. Y.; Paşca, A. M.; Kundaje, A.; et al. Chromatin and Gene-Regulatory Dynamics of the Developing Human Cerebral Cortex at Single-Cell Resolution. *Cell* **2021**, *184*, 5053.
(140) Eze, U. C.; Bhaduri, A.; Haeussler, M.; Nowakowski, T. J.; Kriegstein, A. R. Single-Cell Atlas of Early Human Brain Development Highlights Heterogeneity of Human Neuroepithelial Cells and Early Radial Glia. *Nat. Neurosci.* **2021**, *24*, 584−594.
(141) Bocchi, V. D.; Conforti, P.; Vezzoli, E.; Besusso, D.; Cappadona, C.; Lischetti, T.; Galimberti, M.; Ranzani, V.; Bonnal, R. J. P.; De Simone, M.; et al. The Coding and Long Noncoding Single-Cell Atlas of the Developing Human Fetal Striatum. *Science* **2021**, *372*, No. eabf5759.
(142) Yao, Z.; Liu, H.; Xie, F.; Fischer, S.; Adkins, R. S.; Aldridge, A. I.; Ament, S. A.; Bartlett, A.; Behrens, M. M.; Van den Berge, K.; et al. A Transcriptomic and Epigenomic Cell Atlas of the Mouse Primary Motor Cortex. *Nature* **2021**, *598*, 103−110.
(143) Song, L.; Pan, S.; Zhang, Z.; Jia, L.; Chen, W. H.; Zhao, X. M. STAB: A Spatio-Temporal Cell Atlas of the Human Brain. *Nucleic Acids Res.* **2021**, *49*, D1029−D1037.
(144) Shang, Z.; Chen, D.; Wang, Q.; Wang, S.; Deng, Q.; Wu, L.; Liu, C.; Ding, X.; Wang, S.; Zhong, J.; et al. Single-Cell RNA-Seq Reveals Dynamic Transcriptome Profiling in Human Early Neural Differentiation. *Gigascience* **2018**, *7*, 1−19.
(145) Delile, J.; Rayon, T.; Melchionda, M.; Edwards, A.; Briscoe, J.; Sagner, A. Single Cell Transcriptomics Reveals Spatial and Temporal Dynamics of Gene Expression in the Developing Mouse Spinal Cord. *Dev.* **2019**, *146*, dev173807.
(146) Lafzi, A.; Moutinho, C.; Picelli, S.; Heyn, H. Tutorial: Guidelines for the Experimental Design of Single-Cell RNA Sequencing Studies. *Nat. Protoc.* **2018**, *13*, 2742−2757.
(147) Salomon, R.; Kaczorowski, D.; Valdes-Mora, F.; Nordon, R. E.; Neild, A.; Farbehi, N.; Bartonicek, N.; Gallego-Ortega, D. Droplet-Based Single Cell RNAseq Tools: A Practical Guide. *Lab Chip* **2019**, *19*, 1706−1727.
(148) Mereu, E.; Lafzi, A.; Moutinho, C.; Ziegenhain, C.; McCarthy, D. J.; Álvarez-Varela, A.; Batlle, E.; Sagar; Grün, D.; Lau, J. K.; et al. Benchmarking Single-Cell RNA-Sequencing Protocols for Cell Atlas Projects. *Nat. Biotechnol.* **2020**, *38*, 747−755.
(149) Picelli, S.; Björklund, Å. K.; Faridani, O. R.; Sagasser, S.; Winberg, G.; Sandberg, R. Smart-Seq2 for Sensitive Full-Length Transcriptome Profiling in Single Cells. *Nat. Methods* **2013**, *10*, 1096−1100.
(150) Hashimshony, T.; Senderovich, N.; Avital, G.; Klochendler, A.; de Leeuw, Y.; Anavy, L.; Gennert, D.; Li, S.; Livak, K. J.; Rozenblatt-Rosen, O.; et al. CEL-Seq2: Sensitive Highly-Multiplexed Single-Cell RNA-Seq. *Genome Biol.* **2016**, *17*, 77.
(151) Yanai, I.; Hashimshony, T. CEL-Seq2-Single-Cell RNA Sequencing by Multiplexed Linear Amplification. *Methods Mol. Biol.* **2019**, *1979*, 45−56.
(152) Wang, X.; He, Y.; Zhang, Q.; Ren, X.; Zhang, Z. Direct Comparative Analyses of 10X Genomics Chromium and Smart-Seq2. *Genomics, Proteomics Bioinforma.* **2021**, *19*, 253−266.
(153) Ding, J.; Adiconis, X.; Simmons, S. K.; Kowalczyk, M. S.; Hession, C. C.; Marjanovic, N. D.; Hughes, T. K.; Wadsworth, M. H.; Burks, T.; Nguyen, L. T.; et al. Systematic Comparison of Single-Cell and Single-Nucleus RNA-Sequencing Methods. *Nat. Biotechnol.* **2020**, *38*, 737−746.
(154) Ramsköld, D.; Luo, S.; Wang, Y. C.; Li, R.; Deng, Q.; Faridani, O. R.; Daniels, G. A.; Khrebtukova, I.; Loring, J. F.; Laurent, L. C.; et al. Full-Length MRNA-Seq from Single-Cell Levels of RNA and Individual Circulating Tumor Cells. *Nat. Biotechnol.* **2012**, *30*, 777−782.
(155) Booeshaghi, A. S.; Yao, Z.; van Velthoven, C.; Smith, K.; Tasic, B.; Zeng, H.; Pachter, L. Isoform Cell-Type Specificity in the Mouse Primary Motor Cortex. *Nature* **2021**, *598*, 195−199.
(156) Hagemann-Jensen, M.; Ziegenhain, C.; Chen, P.; Ramsköld, D.; Hendriks, G. J.; Larsson, A. J. M.; Faridani, O. R.; Sandberg, R. Single-Cell RNA Counting at Allele and Isoform Resolution Using Smart-Seq3. *Nat. Biotechnol.* **2020**, *38*, 708−714.
(157) Kumar, V.; Seq-Well, S. Seeking A Simpler Way to Profile RNA from Single Cells. *Clin. Chem.* **2021**, *67*, 454−456.

https://doi.org/10.1021/acs.chemrev.2c00212
Chem. Rev. 2022, 122, 14842−14880

(158) Gierahn, T. M.; Wadsworth, M. H.; Hughes, T. K.; Bryson, B. D.; Butler, A.; Satija, R.; Fortune, S.; Love, J. C.; Shalek, A. K. Seq-Well: Portable, Low-Cost Rna Sequencing of Single Cells at High Throughput. *Nat. Methods* **2017**, *14*, 395−398.
(159) Klein, A. M.; Mazutis, L.; Akartuna, I.; Tallapragada, N.; Veres, A.; Li, V.; Peshkin, L.; Weitz, D. A.; Kirschner, M. W. Droplet Barcoding for Single-Cell Transcriptomics Applied to Embryonic Stem Cells. *Cell* **2015**, *161*, 1187−1201.
(160) Zheng, G. X. Y.; Terry, J. M.; Belgrader, P.; Ryvkin, P.; Bent, Z. W.; Wilson, R.; Ziraldo, S. B.; Wheeler, T. D.; McDermott, G. P.; Zhu, J.; et al. Massively Parallel Digital Transcriptional Profiling of Single Cells. *Nat. Commun.* **2017**, *8*, 14049.
(161) Sasagawa, Y.; Nikaido, I.; Hayashi, T.; Danno, H.; Uno, K. D.; Imai, T.; Ueda, H. R. Quartz-Seq: A Highly Reproducible and Sensitive Single-Cell RNA Sequencing Method, Reveals Nongenetic Gene-Expression Heterogeneity. *Genome Biol.* **2013**, *14*, 3097.
(162) Sasagawa, Y.; Danno, H.; Takada, H.; Ebisawa, M.; Tanaka, K.; Hayashi, T.; Kurisaki, A.; Nikaido, I. Quartz-Seq2: A High-Throughput Single-Cell RNA-Sequencing Method That Effectively Uses Limited Sequence Reads. *Genome Biol.* **2018**, *19*, 29.
(163) Gong, H.; Do, D.; Ramakrishnan, R. Single-Cell MRNA-Seq Using the Fluidigm C1 System and Integrated Fluidics Circuits. In *Methods in Molecular Biology*; Raghavachari, N., Garcia-Reyero, N., Eds.; Springer: New York, 2018; Vol. *1783*, pp 193−207, DOI: DOI: 10.1007/978-1-4939-7834-2_10.
(164) Pandey, S.; Shekhar, K.; Regev, A.; Schier, A. F. Comprehensive Identification and Spatial Mapping of Habenular Neuronal Types Using Single-Cell RNA-Seq. *Curr. Biol.* **2018**, *28*, 1052.
(165) Darmanis, S.; Sloan, S. A.; Zhang, Y.; Enge, M.; Caneda, C.; Shuer, L. M.; Hayden Gephart, M. G.; Barres, B. A.; Quake, S. R. A Survey of Human Brain Transcriptome Diversity at the Single Cell Level. *Proc. Natl. Acad. Sci. U. S. A.* **2015**, *112*, 7285−7290.
(166) La Manno, G.; Gyllborg, D.; Codeluppi, S.; Nishimura, K.; Salto, C.; Zeisel, A.; Borm, L. E.; Stott, S. R. W.; Toledo, E. M.; Villaescusa, J. C.; et al. Molecular Diversity of Midbrain Development in Mouse, Human, and Stem Cells. *Cell* **2016**, *167*, 566.
(167) Pollen, A. A.; Nowakowski, T. J.; Chen, J.; Retallack, H.; Sandoval-Espinosa, C.; Nicholas, C. R.; Shuga, J.; Liu, S. J.; Oldham, M. C.; Diaz, A.; et al. Molecular Identity of Human Outer Radial Glia during Cortical Development. *Cell* **2015**, *163*, 55−67.
(168) Quadrato, G.; Nguyen, T.; Macosko, E. Z.; Sherwood, J. L.; Yang, S. M.; Berger, D. R.; Maria, N.; Scholvin, J.; Goldman, M.; Kinney, J. P.; et al. Cell Diversity and Network Dynamics in Photosensitive Human Brain Organoids. *Nature* **2017**, *545*, 48−53.
(169) Fleck, J. S.; Sanchís-Calleja, F.; He, Z.; Santel, M.; Boyle, M. J.; Camp, J. G.; Treutlein, B. Erratum: Resolving Organoid Brain Region Identities by Mapping Single-Cell Genomic Data to Reference Atlases. *Cell Stem Cell* **2021**, *28*, 1177−1180.
(170) Miura, Y.; Paşca, S. P. Mapping Human Brain Organoids on a Spatial Atlas. *Cell Stem Cell* **2021**, *28*, 983−984.
(171) Kanton, S.; Boyle, M. J.; He, Z.; Santel, M.; Weigert, A.; Sanchís-Calleja, F.; Guijarro, P.; Sidow, L.; Fleck, J. S.; Han, D.; et al. Organoid Single-Cell Genomic Atlas Uncovers Human-Specific Features of Brain Development. *Nature* **2019**, *574*, 418−422.
(172) Keil, J. M.; Qalieh, A.; Kwan, K. Y. Brain Transcriptome Databases: A User's Guide. *J. Neurosci.* **2018**, *38*, 2399−2412.
(173) Rackham, O. J. L.; Firas, J.; Fang, H.; Oates, M. E.; Holmes, M. L.; Knaupp, A. S.; Suzuki, H.; Nefzger, C. M.; Daub, C. O.; Shin, J. W.; et al. A Predictive Computational Framework for Direct Reprogramming between Human Cell Types. *Nat. Genet.* **2016**, *48*, 331−335.
(174) Ng, A. H. M.; Khoshakhlagh, P.; Rojo Arias, J. E.; Pasquini, G.; Wang, K.; Swiersy, A.; Shipman, S. L.; Appleton, E.; Kiaee, K.; Kohman, R. E.; et al. A Comprehensive Library of Human Transcription Factors for Cell Fate Engineering. *Nat. Biotechnol.* **2021**, *39*, 510−519.
(175) Trapnell, C.; Cacchiarelli, D.; Grimsby, J.; Pokharel, P.; Li, S.; Morse, M.; Lennon, N. J.; Livak, K. J.; Mikkelsen, T. S.; Rinn, J. L. The Dynamics and Regulators of Cell Fate Decisions Are Revealed by Pseudotemporal Ordering of Single Cells. *Nat. Biotechnol.* **2014**, *32*, 381−386.
(176) Quadrato, G.; Arlotta, P. Present and Future of Modeling Human Brain Development in 3D Organoids. *Curr. Opin. Cell Biol.* **2017**, *49*, 47−52.
(177) Mayer, S.; Chen, J.; Velmeshev, D.; Mayer, A.; Eze, U. C.; Bhaduri, A.; Cunha, C. E.; Jung, D.; Arjun, A.; Li, E.; et al. Multimodal Single-Cell Analysis Reveals Physiological Maturation in the Developing Human Neocortex. *Neuron* **2019**, *102*, 143.
(178) Rusnakova, V.; Honsa, P.; Dzamba, D.; Ståhlberg, A.; Kubista, M.; Anderova, M. Heterogeneity of Astrocytes: From Development to Injury - Single Cell Gene Expression. *PLoS One* **2013**, *8*, No. e69734.
(179) Pollen, A. A.; Nowakowski, T. J.; Shuga, J.; Wang, X.; Leyrat, A. A.; Lui, J. H.; Li, N.; Szpankowski, L.; Fowler, B.; Chen, P.; et al. Low-Coverage Single-Cell MRNA Sequencing Reveals Cellular Heterogeneity and Activated Signaling Pathways in Developing Cerebral Cortex. *Nat. Biotechnol.* **2014**, *32*, 1053−1058.
(180) Bakken, T. E.; Jorstad, N. L.; Hu, Q.; Lake, B. B.; Tian, W.; Kalmbach, B. E.; Crow, M.; Hodge, R. D.; Krienen, F. M.; Sorensen, S. A.; et al. Comparative Cellular Analysis of Motor Cortex in Human, Marmoset and Mouse. *Nature* **2021**, *598*, 111−119.
(181) Tasic, B.; Menon, V.; Nguyen, T. N.; Kim, T. K.; Jarsky, T.; Yao, Z.; Levi, B.; Gray, L. T.; Sorensen, S. A.; Dolbeare, T.; et al. Adult Mouse Cortical Cell Taxonomy Revealed by Single Cell Transcriptomics. *Nat. Neurosci.* **2016**, *19*, 335−346.
(182) Kurmangaliyev, Y. Z.; Yoo, J.; Valdes-Aleman, J.; Sanfilippo, P.; Zipursky, S. L. Transcriptional Programs of Circuit Assembly in the Drosophila Visual System. *Neuron* **2020**, *108*, 1045.
(183) Tan, L.; Li, Q.; Xie, X. S. Olfactory Sensory Neurons Transiently Express Multiple Olfactory Receptors during Development. *Mol. Syst. Biol.* **2015**, *11*, 844.
(184) Gokce, O.; Stanley, G. M.; Treutlein, B.; Neff, N. F.; Camp, J. G.; Malenka, R. C.; Rothwell, P. E.; Fuccillo, M. V.; Südhof, T. C.; Quake, S. R. Cellular Taxonomy of the Mouse Striatum as Revealed by Single-Cell RNA-Seq. *Cell Rep.* **2016**, *16*, 1126−1137.
(185) Muñoz-Manchado, A. B.; Bengtsson Gonzales, C.; Zeisel, A.; Munguba, H.; Bekkouche, B.; Skene, N. G.; Lönnerberg, P.; Ryge, J.; Harris, K. D.; Linnarsson, S.; et al. Diversity of Interneurons in the Dorsal Striatum Revealed by Single-Cell RNA Sequencing and PatchSeq. *Cell Rep.* **2018**, *24*, 2179.
(186) Agarwal, D.; Sandor, C.; Volpato, V.; Caffrey, T. M.; Monzón-Sandoval, J.; Bowden, R.; Alegre-Abarrategui, J.; Wade-Martins, R.; Webber, C. A Single-Cell Atlas of the Human Substantia Nigra Reveals Cell-Specific Pathways Associated with Neurological Disorders. *Nat. Commun.* **2020**, *11*, 4183.
(187) Li, Y.; Lopez-Huerta, V. G.; Adiconis, X.; Levandowski, K.; Choi, S.; Simmons, S. K.; Arias-Garcia, M. A.; Guo, B.; Yao, A. Y.; Blosser, T. R.; et al. Distinct Subnetworks of the Thalamic Reticular Nucleus. *Nature* **2020**, *583*, 819−824.
(188) Romanov, R. A.; Zeisel, A.; Bakker, J.; Girach, F.; Hellysaz, A.; Tomer, R.; Alpár, A.; Mulder, J.; Clotman, F.; Keimpema, E.; et al. Molecular Interrogation of Hypothalamic Organization Reveals Distinct Dopamine Neuronal Subtypes. *Nat. Neurosci.* **2017**, *20*, 176−188.
(189) Moffitt, J. R.; Bambah-Mukku, D.; Eichhorn, S. W.; Vaughn, E.; Shekhar, K.; Perez, J. D.; Rubinstein, N. D.; Hao, J.; Regev, A.; Dulac, C.; et al. Molecular, Spatial, and Functional Single-Cell Profiling of the Hypothalamic Preoptic Region. *Science* **2018**, *362*, No. eaau5324.
(190) Mickelsen, L. E.; Flynn, W. F.; Springer, K.; Wilson, L.; Beltrami, E. J.; Bolisetty, M.; Robson, P.; Jackson, A. C. Cellular Taxonomy and Spatial Organization of the Murine Ventral Posterior Hypothalamus. *Elife* **2020**, *9*, 1−34.
(191) Mickelsen, L. E.; Kolling, F. W.; Chimileski, B. R.; Fujita, A.; Norris, C.; Chen, K.; Nelson, C. E.; Jackson, A. C. Neurochemical Heterogeneity among Lateral Hypothalamic Hypocretin/Orexin and Melanin-Concentrating Hormone Neurons Identified through Single-Cell Gene Expression Analysis. *eNeuro* **2017**, *4*, 0013-17.2017.
(192) Poulin, J. F.; Zou, J.; Drouin-Ouellet, J.; Kim, K. Y. A.; Cicchetti, F.; Awatramani, R. B. Defining Midbrain Dopaminergic Neuron Diversity by Single-Cell Gene Expression Profiling. *Cell Rep.* **2014**, *9*, 930−943.

(193) Tapia, M.; Baudot, P.; Formisano-Tréziny, C.; Dufour, M. A.; Temporal, S.; Lasserre, M.; Marquèze-Pouey, B.; Gabert, J.; Kobayashi, K.; Goaillard, J. M. Neurotransmitter Identity and Electrophysiological Phenotype Are Genetically Coupled in Midbrain Dopaminergic Neurons. *Sci. Rep.* **2018**, *8*, 13637.
(194) Croset, V.; Treiber, C. D.; Waddell, S. Cellular Diversity in the Drosophila Midbrain Revealed by Single-Cell Transcriptomics. *Elife* **2018**, *7*, No. e34550.
(195) Park, J.; Zhu, H.; O'Sullivan, S.; Ogunnaike, B. A.; Weaver, D. R.; Schwaber, J. S.; Vadigepalli, R. Single-Cell Transcriptional Analysis Reveals Novel Neuronal Phenotypes and Interaction Networks Involved in the Central Circadian Clock. *Front. Neurosci.* **2016**, *10*, 481.
(196) Wen, S.; Ma, D.; Zhao, M.; Xie, L.; Wu, Q.; Gou, L.; Zhu, C.; Fan, Y.; Wang, H.; Yan, J. Spatiotemporal Single-Cell Analysis of Gene Expression in the Mouse Suprachiasmatic Nucleus. *Nat. Neurosci.* **2020**, *23*, 456−467.
(197) Dvoryanchikov, G.; Hernandez, D.; Roebber, J. K.; Hill, D. L.; Roper, S. D.; Chaudhari, N. Transcriptomes and Neurotransmitter Profiles of Classes of Gustatory and Somatosensory Neurons in the Geniculate Ganglion. *Nat. Commun.* **2017**, *8*, 760.
(198) Nguyen, M. Q.; Wu, Y.; Bonilla, L. S.; von Buchholtz, L. J.; Ryba, N. J. P. Diversity amongst Trigeminal Neurons Revealed by High Throughput Single Cell Sequencing. *PLoS One* **2017**, *12*, No. e0185543.
(199) Chiu, I. M.; Barrett, L. B.; Williams, E. K.; Strochlic, D. E.; Lee, S.; Weyer, A. D.; Lou, S.; Bryman, G. S.; Roberson, D. P.; Ghasemlou, N. Transcriptional Profiling at Whole Population and Single Cell Levels Reveals Somatosensory Neuron Molecular Diversity. *Elife* **2014**, *3*, e04660.
(200) Häring, M.; Zeisel, A.; Hochgerner, H.; Rinwa, P.; Jakobsson, J. E. T.; Lönnerberg, P.; La Manno, G.; Sharma, N.; Borgius, L.; Kiehn, O.; et al. Neuronal Atlas of the Dorsal Horn Defines Its Architecture and Links Sensory Input to Transcriptional Cell Types. *Nat. Neurosci.* **2018**, *21*, 869−880.
(201) Blum, J. A.; Klemm, S.; Shadrach, J. L.; Guttenplan, K. A.; Nakayama, L.; Kathiria, A.; Hoang, P. T.; Gautier, O.; Kaltschmidt, J. A.; Greenleaf, W. J.; et al. Single-Cell Transcriptomic Analysis of the Adult Mouse Spinal Cord Reveals Molecular Diversity of Autonomic and Skeletal Motor Neurons. *Nat. Neurosci.* **2021**, *24*, 572−583.
(202) Alkaslasi, M. R.; Piccus, Z. E.; Hareendran, S.; Silberberg, H.; Chen, L.; Zhang, Y.; Petros, T. J.; Le Pichon, C. E. Single Nucleus RNA-Sequencing Defines Unexpected Diversity of Cholinergic Neuron Types in the Adult Mouse Spinal Cord. *Nat. Commun.* **2021**, *12*, 2471.
(203) Russ, D. E.; Cross, R. B. P.; Li, L.; Koch, S. C.; Matson, K. J. E.; Yadav, A.; Alkaslasi, M. R.; Lee, D. I.; Le Pichon, C. E.; Menon, V.; et al. A Harmonized Atlas of Mouse Spinal Cord Cell Types and Their Spatial Organization. *Nat. Commun.* **2021**, *12*, 5722.
(204) Yamagata, M.; Yan, W.; Sanes, J. R. A Cell Atlas of the Chick Retina Based on Single-Cell Transcriptomics. *Elife* **2021**, *10*, 1−39.
(205) Yan, W.; Peng, Y. R.; van Zyl, T.; Regev, A.; Shekhar, K.; Juric, D.; Sanes, J. R. Cell Atlas of The Human Fovea and Peripheral Retina. *Sci. Rep.* **2020**, *10*, 9802.
(206) Yan, W.; Laboulaye, M. A.; Tran, N. M.; Whitney, I. E.; Benhar, I.; Sanes, J. R. Mouse Retinal Cell Atlas: Molecular Identification of over Sixty Amacrine Cell Types. *J. Neurosci.* **2020**, *40*, 5177−5195.
(207) Fuzik, J.; Zeisel, A.; Mate, Z.; Calvigioni, D.; Yanagawa, Y.; Szabo, G.; Linnarsson, S.; Harkany, T. Integration of Electrophysiological Recordings with Single-Cell RNA-Seq Data Identifies Neuronal Subtypes. *Nat. Biotechnol.* **2016**, *34*, 175−183.
(208) Cadwell, C. R.; Scala, F.; Li, S.; Livrizzi, G.; Shen, S.; Sandberg, R.; Jiang, X.; Tolias, A. S. Multimodal Profiling of Single-Cell Morphology, Electrophysiology, and Gene Expression Using Patch-Seq. *Nat. Protoc.* **2017**, *12*, 2531−2553.
(209) Cadwell, C. R.; Palasantza, A.; Jiang, X.; Berens, P.; Deng, Q.; Yilmaz, M.; Reimer, J.; Shen, S.; Bethge, M.; Tolias, K. F.; et al. Electrophysiological, Transcriptomic and Morphologic Profiling of Single Neurons Using Patch-Seq. *Nat. Biotechnol.* **2016**, *34*, 199−203.
(210) Scala, F.; Kobak, D.; Bernabucci, M.; Bernaerts, Y.; Cadwell, C. R.; Castro, J. R.; Hartmanis, L.; Jiang, X.; Laturnus, S.; Miranda, E.; et al. Phenotypic Variation of Transcriptomic Cell Types in Mouse Motor Cortex. *Nature* **2021**, *598*, 144−150.
(211) Peng, H.; Xie, P.; Liu, L.; Kuang, X.; Wang, Y.; Qu, L.; Gong, H.; Jiang, S.; Li, A.; Ruan, Z.; et al. Morphological Diversity of Single Neurons in Molecularly Defined Cell Types. *Nature* **2021**, *598*, 174−181.
(212) van den Hurk, M.; Erwin, J. A.; Yeo, G. W.; Gage, F. H.; Bardy, C. Corrigendum: Patch-Seq Protocol to Analyze the Electrophysiology, Morphology and Transcriptome of Whole Single Neurons Derived from Human Pluripotent Stem Cells. *Front. Mol. Neurosci.* **2019**, *12*, 150.
(213) Földy, C.; Darmanis, S.; Aoto, J.; Malenka, R. C.; Quake, S. R.; Südhof, T. C. Single-Cell RNAseq Reveals Cell Adhesion Molecule Profiles in Electrophysiologically Defined Neurons. *Proc. Natl. Acad. Sci. U. S. A.* **2016**, *113*, E5222−E5231.
(214) Bardy, C.; Van Den Hurk, M.; Kakaradov, B.; Erwin, J. A.; Jaeger, B. N.; Hernandez, R. V.; Eames, T.; Paucar, A. A.; Gorris, M.; Marchand, C.; et al. Predicting the Functional States of Human IPSC-Derived Neurons with Single-Cell RNA-Seq and Electrophysiology. *Mol. Psychiatry* **2016**, *21*, 1573−1588.
(215) Pfeffer, C. K.; Beltramo, R. Correlating Anatomy and Function with Gene Expression in Individual Neurons by Combining in Vivo Labeling, Patch Clamp, and Single Cell RNA-Seq. *Front. Cell. Neurosci.* **2017**, *11*, 376.
(216) Obergrussberger, A.; Rinke-Weiß, I.; Goetze, T. A.; Rapedius, M.; Brinkwirth, N.; Becker, N.; Rotordam, M. G.; Hutchison, L.; Madau, P.; Pau, D.; et al. The Suitability of High Throughput Automated Patch Clamp for Physiological Applications. *J. Physiol.* **2022**, *600*, 277−297.
(217) Mattei, D.; Ivanov, A.; van Oostrum, M.; Pantelyushin, S.; Richetto, J.; Mueller, F.; Beffinger, M.; Schellhammer, L.; von Berg, J.; Wollscheid, B.; et al. Enzymatic Dissociation Induces Transcriptional and Proteotype Bias in Brain Cell Populations. *Int. J. Mol. Sci.* **2020**, *21*, 7944.
(218) Golan, N.; Cafferty, W. B. Dissociation of Intact Adult Mouse Cortical Projection Neurons for Single-Cell RNA-Seq. *STAR Protoc.* **2021**, *2*, 100941.
(219) Sun, C.; Wang, H.; Ma, Q.; Chen, C.; Yue, J.; Li, B.; Zhang, X. Time-Course Single-Cell RNA Sequencing Reveals Transcriptional Dynamics and Heterogeneity of Limbal Stem Cells Derived from Human Pluripotent Stem Cells. *Cell Biosci.* **2021**, *11*, 24.
(220) Weinreb, C.; Wolock, S.; Tusi, B. K.; Socolovsky, M.; Klein, A. M. Fundamental Limits on Dynamic Inference from Single-Cell Snapshots. *Proc. Natl. Acad. Sci. U. S. A.* **2018**, *115*, E2467−E2476.
(221) Goodhill, G. J. Can Molecular Gradients Wire the Brain? *Trends Neurosci.* **2016**, *39*, 202−211.
(222) Nóbrega-Pereira, S.; Marín, O. Transcriptional Control of Neuronal Migration in the Developing Mouse Brain. *Cereb. Cortex* **2009**, *19*, i107−13.
(223) Wong, S. Y.; Soto, J.; Li, S. Biophysical Regulation of Cell Reprogramming. *Curr. Opin. Chem. Eng.* **2017**, *15*, 95−101.
(224) Zhang, Q.; Austin, R. H. Applications of Microfluidics in Stem Cell Biology. *Bionanoscience* **2012**, *2*, 277−286.
(225) Wu, H. W.; Lin, C. C.; Lee, G. B. Stem Cells in Microfluidics. *Biomicrofluidics* **2011**, *5*, 013401.
(226) Schlaeger, T. M.; Daheron, L.; Brickler, T. R.; Entwisle, S.; Chan, K.; Cianci, A.; DeVine, A.; Ettenger, A.; Fitzgerald, K.; Godfrey, M.; et al. A Comparison of Non-Integrating Reprogramming Methods. *Nat. Biotechnol.* **2015**, *33*, 58−63.
(227) Giobbe, G. G.; Michielin, F.; Luni, C.; Giulitti, S.; Martewicz, S.; Dupont, S.; Floreani, A.; Elvassore, N. Functional Differentiation of Human Pluripotent Stem Cells on a Chip. *Nat. Methods* **2015**, *12*, 637−640.
(228) Tolomeo, A. M.; Laterza, C.; Grespan, E.; Michielin, F.; Canals, I.; Kokaia, Z.; Muraca, M.; Gagliano, O.; Elvassore, N. NGN2MmRNA-Based Transcriptional Programming in Microfluidic Guides HiPSCs Toward Neural Fate With Multiple Identities. *Front. Cell. Neurosci.* **2021**, *15*, 602888.

https://doi.org/10.1021/acs.chemrev.2c00212
Chem. Rev. 2022, 122, 14842−14880

(229) Wang, B.; Jedlicka, S.; Cheng, X. Maintenance and Neuronal Cell Differentiation of Neural Stem Cells C17.2 Correlated to Medium Availability Sets Design Criteria in Microfluidic Systems. *PLoS One* **2014**, *9*, No. e109815.
(230) Ramamurthy, P.; White, J. B.; Yull Park, J.; Hume, R. I.; Ebisu, F.; Mendez, F.; Takayama, S.; Barald, K. F. Concomitant Differentiation of a Population of Mouse Embryonic Stem Cells into Neuron-like Cells and Schwann Cell−like Cells in a Slow-Flow Microfluidic Device. *Dev. Dyn.* **2017**, *246*, 7−27.
(231) Jin, Y.; Lee, J. S.; Kim, J.; Min, S.; Wi, S.; Yu, J. H.; Chang, G. E.; Cho, A. N.; Choi, Y.; Ahn, D. H.; et al. Three-Dimensional Brain-like Microenvironments Facilitate the Direct Reprogramming of Fibroblasts into Therapeutic Neurons. *Nat. Biomed. Eng.* **2018**, *2*, 522−539.
(232) Chung, B. G.; Flanagan, L. A.; Rhee, S. W.; Schwartz, P. H.; Lee, A. P.; Monuki, E. S.; Jeon, N. L. Human Neural Stem Cell Growth and Differentiation in a Gradient-Generating Microfluidic Device. *Lab Chip* **2005**, *5*, 401−406.
(233) Park, J. Y.; Kim, S. K.; Woo, D. H.; Lee, E. J.; Kim, J. H.; Lee, S. H. Differentiation of Neural Progenitor Cells in a Microfluidic Chip-Generated Cytokine Gradient. *Stem Cells* **2009**, *27*, 2646−2654.
(234) Han, S.; Yang, K.; Shin, Y.; Lee, J. S.; Kamm, R. D.; Chung, S.; Cho, S. W. Three-Dimensional Extracellular Matrix-Mediated Neural Stem Cell Differentiation in a Microfluidic Device. *Lab Chip* **2012**, *12*, 2305−2308.
(235) Gurdon, J. B.; Bourillot, P. Y. Morphogen Gradient Interpretation. *Nature* **2001**, *413*, 797−803.
(236) Rifes, P.; Isaksson, M.; Rathore, G. S.; Aldrin-Kirk, P.; Møller, O. K.; Barzaghi, G.; Lee, J.; Egerod, K. L.; Rausch, D. M.; Parmar, M.; et al. Modeling Neural Tube Development by Differentiation of Human Embryonic Stem Cells in a Microfluidic WNT Gradient. *Nat. Biotechnol.* **2020**, *38*, 1265−1273.
(237) Demers, C. J.; Soundararajan, P.; Chennampally, P.; Cox, G. A.; Briscoe, J.; Collins, S. D.; Smith, R. L. Development-on-Chip: In Vitro Neural Tube Patterning with a Microfluidic Device. *Dev.* **2016**, *143*, 1884−1892.
(238) Kothapalli, C. R.; Van Veen, E.; De Valence, S.; Chung, S.; Zervantonakis, I. K.; Gertler, F. B.; Kamm, R. D. A High-Throughput Microfluidic Assay to Study Neurite Response to Growth Factor Gradients. *Lab Chip* **2011**, *11*, 497−507.
(239) Yang, K.; Han, S.; Shin, Y.; Ko, E.; Kim, J.; Park, K. I.; Chung, S.; Cho, S. W. A Microfluidic Array for Quantitative Analysis of Human Neural Stem Cell Self-Renewal and Differentiation in Three-Dimensional Hypoxic Microenvironment. *Biomaterials* **2013**, *34*, 6607−6614.
(240) Vulto, P.; Podszun, S.; Meyer, P.; Hermann, C.; Manz, A.; Urban, G. A. Phaseguides: A Paradigm Shift in Microfluidic Priming and Emptying. *Lab Chip* **2011**, *11*, 1596−1602.
(241) Koo, Y.; Hawkins, B. T.; Yun, Y. Three-Dimensional (3D) Tetra-Culture Brain on Chip Platform for Organophosphate Toxicity Screening. *Sci. Rep.* **2018**, *8*, 2841.
(242) Takano, T.; Funahashi, Y.; Kaibuchi, K. Neuronal Polarity: Positive and Negative Feedback Signals. *Front. Cell Dev. Biol.* **2019**, *7*, 69.
(243) Barnes, A. P.; Polleux, F. Establishment of Axon-Dendrite Polarity in Developing Neurons. *Annu. Rev. Neurosci.* **2009**, *32*, 347−381.
(244) Takano, T.; Xu, C.; Funahashi, Y.; Namba, T.; Kaibuchi, K. Neuronal Polarization. *Dev.* **2015**, *142*, 2088−2093.
(245) Yogev, S.; Shen, K. Establishing Neuronal Polarity with Environmental and Intrinsic Mechanisms. *Neuron* **2017**, *96*, 638−650.
(246) Hakanen, J.; Ruiz-Reig, N.; Tissir, F. Linking Cell Polarity to Cortical Development and Malformations. *Front. Cell Neurosci.* **2019**, *13*, 244.
(247) Millet, L. J.; Gillette, M. U. New Perspectives on Neuronal Development via Microfluidic Environments. *Trends Neurosci.* **2012**, *35*, 752−761.
(248) Roy, J.; Kennedy, T. E.; Costantino, S. Engineered Cell Culture Substrates for Axon Guidance Studies: Moving beyond Proof of Concept. *Lab Chip* **2013**, *13*, 498−508.
(249) Shelly, M.; Cancedda, L.; Heilshorn, S.; Sumbre, G.; Poo, M.-M. LKB1/STRAD Promotes Axon Initiation During Neuronal Polarization. *Cell* **2007**, *129*, 565−577.
(250) Shelly, M.; Cancedda, L.; Lim, B. K.; Popescu, A. T.; Cheng, P.; Gao, H.; Poo, M. Semaphorin3A Regulates Neuronal Polarization by Suppressing Axon Formation and Promoting Dendrite Growth. *Neuron* **2011**, *71*, 433.
(251) Xiao, R. R.; Zeng, W. J.; Li, Y. T.; Zou, W.; Wang, L.; Pei, X. F.; Xie, M.; Huang, W. H. Simultaneous Generation of Gradients with Gradually Changed Slope in a Microfluidic Device for Quantifying Axon Response. *Anal. Chem.* **2013**, *85*, 7842−7850.
(252) Joanne Wang, C.; Li, X.; Lin, B.; Shim, S.; Ming, G. L.; Levchenko, A. A Microfluidics-Based Turning Assay Reveals Complex Growth Cone Responses to Integrated Gradients of Substrate-Bound ECM Molecules and Diffusible Guidance Cues. *Lab Chip* **2008**, *8*, 227−237.
(253) Nédelec, S.; Peljto, M.; Shi, P.; Amoroso, M. W.; Kam, L. C.; Wichterle, H. Concentration-Dependent Requirement for Local Protein Synthesis in Motor Neuron Subtype-Specific Response to Axon Guidance Cues. *J. Neurosci.* **2012**, *32*, 1496−1506.
(254) Bhattacharjee, N.; Li, N.; Keenan, T. M.; Folch, A. A Neuron-Benign Microfluidic Gradient Generator for Studying the Response of Mammalian Neurons towards Axon Guidance Factors. *Integr. Biol.* **2010**, *2*, 669−679.
(255) Bhattacharjee, N.; Folch, A. Large-Scale Microfluidic Gradient Arrays Reveal Axon Guidance Behaviors in Hippocampal Neurons. *Microsystems Nanoeng.* **2017**, *3*, 17003.
(256) Dupin, I.; Lokmane, L.; Dahan, M.; Garel, S.; Studer, V. Subrepellent Doses of Slit1 Promote Netrin-1 Chemotactic Responses in Subsets of Axons. *Neural Dev.* **2015**, *10*, 5.
(257) Sloan, T. F. W.; Qasaimeh, M. A.; Juncker, D.; Yam, P. T.; Charron, F. Integration of Shallow Gradients of Shh and Netrin-1 Guides Commissural Axons. *PLoS Biol.* **2015**, *13*, e1002119−e1002119.
(258) Carballo-Molina, O. A.; Sánchez-Navarro, A.; López-Ornelas, A.; Lara-Rodarte, R.; Salazar, P.; Campos-Romo, A.; Ramos-Mejía, V.; Velasco, I. Semaphorin 3C Released from a Biocompatible Hydrogel Guides and Promotes Axonal Growth of Rodent and Human Dopaminergic Neurons. *Tissue Eng. - Part A* **2016**, *22*, 850−861.
(259) Xu, H.; Ferreira, M. M.; Heilshorn, S. C. Small-Molecule Axon-Polarization Studies Enabled by a Shear-Free Microfluidic Gradient Generator. *Lab Chip* **2014**, *14*, 2047−2056.
(260) Lang, S.; Von Philipsborn, A. C.; Bernard, A.; Bonhoeffer, F.; Bastmeyer, M. Growth Cone Response to Ephrin Gradients Produced by Microfluidic Networks. *Anal. Bioanal. Chem.* **2008**, *390*, 809−816.
(261) Pang, Z. P.; Yang, N.; Vierbuchen, T.; Ostermeier, A.; Fuentes, D. R.; Yang, T. Q.; Citri, A.; Sebastiano, V.; Marro, S.; Südhof, T. C.; et al. Induction of Human Neuronal Cells by Defined Transcription Factors. *Nature* **2011**, *476*, 220−223.
(262) Lin, T.; Wu, S. Reprogramming with Small Molecules Instead of Exogenous Transcription Factors. *Stem Cells Int.* **2015**, *2015*, 794632.
(263) Knyazer, A.; Bunu, G.; Toren, D.; Mracica, T. B.; Segev, Y.; Wolfson, M.; Muradian, K. K.; Tacutu, R.; Fraifeld, V. E. Small Molecules for Cell Reprogramming: A Systems Biology Analysis. *Aging (Albany. NY)* **2021**, *13*, 25739−25762.
(264) Kim, Y.; Jeong, J.; Choi, D. Small-Molecule-Mediated Reprogramming: A Silver Lining for Regenerative Medicine. *Exp. Mol. Med.* **2020**, *52*, 213−226.
(265) Zhou, J.; Sun, J. A Revolution in Reprogramming: Small Molecules. *Curr. Mol. Med.* **2019**, *19*, 77−90.
(266) Jung, D. W.; Kim, W. H.; Williams, D. R. Reprogram or Reboot: Small Molecule Approaches for the Production of Induced Pluripotent Stem Cells and Direct Cell Reprogramming. *ACS Chem. Biol.* **2014**, *9*, 80−95.
(267) Qin, H.; Zhao, A.; Fu, X. Small Molecules for Reprogramming and Transdifferentiation. *Cell. Mol. Life Sci.* **2017**, *74*, 3553−3575.
(268) Federation, A. J.; Bradner, J. E.; Meissner, A. The Use of Small Molecules in Somatic-Cell Reprogramming. *Trends Cell Biol.* **2014**, *24*, 179−187.

https://doi.org/10.1021/acs.chemrev.2c00212
Chem. Rev. 2022, 122, 14842−14880

(269) Li, W.; Ding, S. Small Molecules That Modulate Embryonic Stem Cell Fate and Somatic Cell Reprogramming. *Trends Pharmacol. Sci.* **2010**, *31*, 36−45.
(270) Qi, Y.; Zhang, X. J.; Renier, N.; Wu, Z.; Atkin, T.; Sun, Z.; Ozair, M. Z.; Tchieu, J.; Zimmer, B.; Fattahi, F.; et al. Combined Small-Molecule Inhibition Accelerates the Derivation of Functional Cortical Neurons from Human Pluripotent Stem Cells. *Nat. Biotechnol.* **2017**, *35*, 154−163.
(271) Hergenreder, E.; Zorina, Y.; Zhao, Z.; Munguba, H.; Calder, L.; Baggiolini, A.; Minotti, A. P.; Walsh, R. M.; Levitz, J.; Garippa, R.; et al. Combined Small Molecule Treatment Accelerates Timing of Maturation in Human Pluripotent Stem Cell-Derived Neurons. *bioRxiv* **2022**, 2022.06.02.494616, DOI: DOI: 10.1101/2022.06.02.494616.
(272) Limone, F.; Mitchell, J. M.; San Juan, I. G.; Smith, J. L. M.; Raghunathan, K.; Couto, A.; Ghosh, S. D.; Meyer, D.; Mello, C. J.; Nemesh, J.; et al. Efficient Generation of Lower Induced Motor Neurons by Coupling Ngn2 Expression with Developmental Cues. *bioRxiv* **2022**, 2022.01.12.476020, DOI: DOI: 10.1101/2022.01.12.476020.
(273) Napolitano, F.; Rapakoulia, T.; Annunziata, P.; Hasegawa, A.; Cardon, M.; Napolitano, S.; Vaccaro, L.; Iuliano, A.; Wanderlingh, L. G.; Kasukawa, T.; et al. Automatic Identification of Small Molecules That Promote Cell Conversion and Reprogramming. *Stem Cell Reports* **2021**, *16*, 1381−1390.
(274) Cheng, L.; Gao, L.; Guan, W.; Mao, J.; Hu, W.; Qiu, B.; Zhao, J.; Yu, Y.; Pei, G. Direct Conversion of Astrocytes into Neuronal Cells by Drug Cocktail. *Cell Res.* **2015**, *25*, 1269−1272.
(275) Hu, W.; Qiu, B.; Guan, W.; Wang, Q.; Wang, M.; Li, W.; Gao, L.; Shen, L.; Huang, Y.; Xie, G.; et al. Direct Conversion of Normal and Alzheimer's Disease Human Fibroblasts into Neuronal Cells by Small Molecules. *Cell Stem Cell* **2015**, *17*, 204−212.
(276) Hou, P.; Li, Y.; Zhang, X.; Liu, C.; Guan, J.; Li, H.; Zhao, T.; Ye, J.; Yang, W.; Liu, K.; et al. Pluripotent Stem Cells Induced from Mouse Somatic Cells by Small-Molecule Compounds. *Science* **2013**, *341*, 651−654.
(277) Millet, L. J.; Stewart, M. E.; Nuzzo, R. G.; Gillette, M. U. Guiding Neuron Development with Planar Surface Gradients of Substrate Cues Deposited Using Microfluidic Devices. *Lab Chip* **2010**, *10*, 1525−1535.
(278) Dertinger, S. K. W.; Jiang, X.; Li, Z.; Murthy, V. N.; Whitesides, G. M. Gradients of Substrate-Bound Laminin Orient Axonal Specification of Neurons. *Proc. Natl. Acad. Sci. U. S. A.* **2002**, *99*, 12542−12547.
(279) Kunze, A.; Valero, A.; Zosso, D.; Renaud, P. Synergistic Ngf/B27 Gradients Position Synapses Heterogeneously in 3d Micropatterned Neural Cultures. *PLoS One* **2011**, *6*, No. e26187.
(280) Kunze, A.; Bertsch, A.; Giugliano, M.; Renaud, P. Microfluidic Hydrogel Layers with Multiple Gradients to Stimulate and Perfuse Three-Dimensional Neuronal Cell Cultures. *Procedia Chem.* **2009**, *1*, 369−372.
(281) Knowlton, S.; Cho, Y.; Li, X. J.; Khademhosseini, A.; Tasoglu, S. Utilizing Stem Cells for Three-Dimensional Neural Tissue Engineering. *Biomater. Sci.* **2016**, *4*, 768−784.
(282) Wang, X.; Wang, Z.; Zhai, W.; Wang, F.; Ge, Z.; Yu, H.; Yang, W. Engineering Biological Tissues from the Bottom-Up: Recent Advances and Future Prospects. *Micromachines* **2022**, *13*, 75.
(283) Matsui, T. K.; Tsuru, Y.; Kuwako, K. I. Challenges in Modeling Human Neural Circuit Formation via Brain Organoid Technology. *Front. Cell. Neurosci.* **2020**, *14*, 607399.
(284) Stiles, J.; Jernigan, T. L. The Basics of Brain Development. *Neuropsychol. Rev.* **2010**, *20*, 327−348.
(285) Stiles, J. Brain Development and the Nature versus Nurture Debate. In *Progress in Brain Research*; Elsevier, 2011; Vol. *189*, pp 3−22, DOI: DOI: 10.1016/B978-0-444-53884-0.00015-4.
(286) Fedorchak, N. J.; Iyer, N.; Ashton, R. S. Bioengineering Tissue Morphogenesis and Function in Human Neural Organoids. *Semin. Cell Dev. Biol.* **2021**, *111*, 52−59.
(287) Thomas, M.; Willerth, S. M. 3-D Bioprinting of Neural Tissue for Applications in Cell Therapy and Drug Screening. *Front. Bioeng. Biotechnol.* **2017**, *5*, 69.
(288) Brofiga, M.; Pisano, M.; Tedesco, M.; Raiteri, R.; Massobrio, P. Three-Dimensionality Shapes the Dynamics of Cortical Interconnected to Hippocampal Networks. *J. Neural Eng.* **2020**, *17*, 056044.
(289) Kelava, I.; Lancaster, M. A. Stem Cell Models of Human Brain Development. *Cell Stem Cell* **2016**, *18*, 736−748.
(290) Forro, C.; Caron, D.; Angotzi, G. N.; Gallo, V.; Berdondini, L.; Santoro, F.; Palazzolo, G.; Panuccio, G. Electrophysiology Read-out Tools for Brain-on-Chip Biotechnology. *Micromachines* **2021**, *12*, 124.
(291) Zhao, Y.; Demirci, U.; Chen, Y.; Chen, P. Multiscale Brain Research on a Microfluidic Chip. *Lab Chip* **2020**, *20*, 1531−1543.
(292) Kamudzandu, M.; Köse-Dunn, M.; Evans, M. G.; Fricker, R. A.; Roach, P. A Micro-Fabricated in Vitro Complex Neuronal Circuit Platform. *Biomed. Phys. Eng. Express* **2019**, *5*, 045016.
(293) Budday, S.; Steinmann, P.; Kuhl, E. Physical Biology of Human Brain Development. *Front. Cell. Neurosci.* **2015**, *9*, 267.
(294) Silbereis, J. C.; Pochareddy, S.; Zhu, Y.; Li, M.; Sestan, N. The Cellular and Molecular Landscapes of the Developing Human Central Nervous System. *Neuron* **2016**, *89*, 248−268.
(295) Riccomagno, M. M.; Kolodkin, A. L. Sculpting Neural Circuits by Axon and Dendrite Pruning. *Annu. Rev. Cell Dev. Biol.* **2015**, *31*, 779−805.
(296) Foubet, O.; Trejo, M.; Toro, R. Mechanical Morphogenesis and the Development of Neocortical Organisation. *Cortex* **2019**, *118*, 315−326.
(297) Jiang, X.; Nardelli, J. Cellular and Molecular Introduction to Brain Development. *Neurobiol. Dis.* **2016**, *92*, 3−17.
(298) Bystron, I.; Blakemore, C.; Rakic, P. Development of the Human Cerebral Cortex: Boulder Committee Revisited. *Nat. Rev. Neurosci.* **2008**, *9*, 110−122.
(299) Raybaud, C.; Ahmad, T.; Rastegar, N.; Shroff, M.; Al Nassar, M. The Premature Brain: Developmental and Lesional Anatomy. *Neuroradiology* **2013**, *55*, 23−40.
(300) Agirman, G.; Broix, L.; Nguyen, L. Cerebral Cortex Development: An Outside-in Perspective. *FEBS Lett.* **2017**, *591*, 3978−3992.
(301) Lancaster, M. A.; Corsini, N. S.; Wolfinger, S.; Gustafson, E. H.; Phillips, A. W.; Burkard, T. R.; Otani, T.; Livesey, F. J.; Knoblich, J. A. Guided Self-Organization and Cortical Plate Formation in Human Brain Organoids. *Nat. Biotechnol.* **2017**, *35*, 659−666.
(302) Molnár, Z.; Clowry, G. J.; Šestan, N.; Alzu'bi, A.; Bakken, T.; Hevner, R. F.; Hüppi, P. S.; Kostović, I.; Rakic, P.; Anton, E. S.; et al. New Insights into the Development of the Human Cerebral Cortex. *J. Anat.* **2019**, *235*, 432−451.
(303) Van Essen, D. C.; Donahue, C. J.; Glasser, M. F. Development and Evolution of Cerebral and Cerebellar Cortex. *Brain. Behav. Evol.* **2018**, *91*, 158−169.
(304) Howard, B. M.; Mo, Z.; Filipovic, R.; Moore, A. R.; Antic, S. D.; Zecevic, N. Radial Glia Cells in the Developing Human Brain. *Neuroscientist* **2008**, *14*, 459−473.
(305) Jakovcevski, I.; Filipovic, R.; Mo, Z.; Rakic, S.; Zecevic, N. Oligodendrocyte Development and the Onset of Myelination in the Human Fetal Brain. *Front. Neuroanat.* **2009**, *3*, 5.
(306) Huttenlocher, P. R. Synaptic Density in Human Frontal Cortex - Developmental Changes and Effects of Aging. *Brain Res.* **1979**, *163*, 195−205.
(307) Craik, F. I. M.; Bialystok, E. Cognition through the Lifespan: Mechanisms of Change. *Trends Cogn. Sci.* **2006**, *10*, 131−138.
(308) Craig, A. M.; Graf, E. R.; Linhoff, M. W. How to Build a Central Synapse: Clues from Cell Culture. *Trends Neurosci.* **2006**, *29*, 8−20.
(309) Kirwan, P.; Turner-Bridger, B.; Peter, M.; Momoh, A.; Arambepola, D.; Robinson, H. P. C.; Livesey, F. J. Development and Function of Human Cerebral Cortex Neural Networks from Pluripotent Stem Cells in Vitro. *Dev.* **2015**, *142*, 3178−3187.
(310) Shi, Y.; Kirwan, P.; Smith, J.; Robinson, H. P. C.; Livesey, F. J. Human Cerebral Cortex Development from Pluripotent Stem Cells to Functional Excitatory Synapses. *Nat. Neurosci.* **2012**, *15*, 477−486.

(311) Vasung, L.; Abaci Turk, E.; Ferradal, S. L.; Sutin, J.; Stout, J. N.; Ahtam, B.; Lin, P. Y.; Grant, P. E. Exploring Early Human Brain Development with Structural and Physiological Neuroimaging. *Neuroimage* **2019**, *187*, 226−254.
(312) Robinson, H. P. C.; Kawahara, M.; Jimbo, Y.; Torimitsu, K.; Kuroda, Y.; Kawana, A. Periodic Synchronized Bursting and Intracellular Calcium Transients Elicited by Low Magnesium in Cultured Cortical Neurons. *J. Neurophysiol.* **1993**, *70*, 1606−1616.
(313) Corlew, R.; Bosma, M. M.; Moody, W. J. Spontaneous, Synchronous Electrical Activity in Neonatal Mouse Cortical Neurones. *J. Physiol.* **2004**, *560*, 377−390.
(314) Yuste, R.; Peinado, A.; Katz, L. C. Neuronal Domains in Developing Neocortex. *Science* **1992**, *257*, 665−669.
(315) Kilb, W.; Kirischuk, S.; Luhmann, H. J. Electrical Activity Patterns and the Functional Maturation of the Neocortex. *Eur. J. Neurosci.* **2011**, *34*, 1677−1686.
(316) Leinekugel, X.; Khazipov, R.; Cannon, R.; Hirase, H.; Ben-Ari, Y.; Buzsáki, G. Correlated Bursts of Activity in the Neonatal Hippocampus in Vivo. *Science* **2002**, *296*, 2049−2052.
(317) Moore, A. R.; Zhou, W. L.; Jakovcevski, I.; Zecevic, N.; Antic, S. D. Spontaneous Electrical Activity in the Human Fetal Cortex in Vitro. *J. Neurosci.* **2011**, *31*, 2391−2398.
(318) Tolonen, M.; Palva, J. M.; Andersson, S.; Vanhatalo, S. Development of the Spontaneous Activity Transients and Ongoing Cortical Activity in Human Preterm Babies. *Neuroscience* **2007**, *145*, 997−1006.
(319) Khazipov, R.; Luhmann, H. J. Early Patterns of Electrical Activity in the Developing Cerebral Cortex of Humans and Rodents. *Trends Neurosci.* **2006**, *29*, 414−418.
(320) Lamblin, M. D.; André, M.; Challamel, M. J.; Curzi-Dascalova, L.; D'Allest, A. M.; De Giovanni, E.; Moussalli-Salefranque, F.; Navelet, Y.; Plouin, P.; Radvanyi-Bouvet, M. F.; et al. EEG in premature and full-term newborns. Maturation and glossary. *Neurophysiol. Clin.* **1999**, *29*, 123−219.
(321) Ronchi, S.; Buccino, A. P.; Prack, G.; Kumar, S. S.; Schröter, M.; Fiscella, M.; Hierlemann, A. Electrophysiological Phenotype Characterization of Human IPSC-Derived Neuronal Cell Lines by Means of High-Density Microelectrode Arrays. *Adv. Biol.* **2021**, *5*, 2000223.
(322) Sasaki, T.; Suzuki, I.; Yokoi, R.; Sato, K.; Ikegaya, Y. Synchronous Spike Patterns in Differently Mixed Cultures of Human IPSC-Derived Glutamatergic and GABAergic Neurons. *Biochem. Biophys. Res. Commun.* **2019**, *513*, 300−305.
(323) Odawara, A.; Saitoh, Y.; Alhebshi, A. H.; Gotoh, M.; Suzuki, I. Long-Term Electrophysiological Activity and Pharmacological Response of a Human Induced Pluripotent Stem Cell-Derived Neuron and Astrocyte Co-Culture. *Biochem. Biophys. Res. Commun.* **2014**, *443*, 1176−1181.
(324) Schmieder, F.; Habibey, R.; Busskamp, V.; Büttner, L.; Czarske, J. W. Investigation of in Vitro Human IPSC-Derived Neuronal Networks Using Holographic Stimulation (Conference Presentation). *Proc. SPIE* **2020**, *2020*, 11227.
(325) Aebersold, M. J.; Dermutz, H.; Forró, C.; Weydert, S.; Thompson-Steckel, G.; Vörös, J.; Demkó, L. Brains on a Chip": Towards Engineered Neural Networks. *TrAC - Trends Anal. Chem.* **2016**, *78*, 60−69.
(326) Chen, H. I.; Wolf, J. A.; Smith, D. H. Multichannel Activity Propagation across an Engineered Axon Network. *J. Neural Eng.* **2017**, *14*, 026016.
(327) DeMarse, T. B.; Pan, L.; Alagapan, S.; Brewer, G. J.; Wheeler, B. C. Feed-Forward Propagation of Temporal and Rate Information between Cortical Populations during Coherent Activation in Engineered in Vitro Networks. *Front. Neural Circuits.* **2016**, *10*, 32.
(328) Obien, M. E. J.; Deligkaris, K.; Bullmann, T.; Bakkum, D. J.; Frey, U. Revealing Neuronal Function through Microelectrode Array Recordings. *Front. Neurosci.* **2015**, *8*, 423.
(329) Dragas, J.; Viswam, V.; Shadmani, A.; Chen, Y.; Bounik, R.; Stettler, A.; Radivojevic, M.; Geissler, S.; Obien, M. E. J.; Müller, J.; et al. In Vitro Multi-Functional Microelectrode Array Featuring 59 760 Electrodes, 2048 Electrophysiology Channels, Stimulation, Impedance Measurement, and Neurotransmitter Detection Channels. *IEEE J. Solid-State Circuits* **2017**, *52*, 1576−1590.
(330) Nam, Y.; Wheeler, B. C. In Vitro Microelectrode Array Technology and Neural Recordings. *Crit. Rev. Biomed. Eng.* **2011**, *39*, 45−61.
(331) Lewandowska, M. K.; Bakkum, D. J.; Rompani, S. B.; Hierlemann, A. Recording Large Extracellular Spikes in Microchannels along Many Axonal Sites from Individual Neurons. *PLoS One* **2015**, *10*, No. e0118514.
(332) Wilk, N.; Habibey, R.; Golabchi, A.; Latifi, S.; Ingebrandt, S.; Blau, A. Selective Comparison of Gelling Agents as Neural Cell Culture Matrices for Long-Term Microelectrode Array Electrophysiology. *OCL* **2016**, *23*, D117.
(333) Müller, J.; Ballini, M.; Livi, P.; Chen, Y.; Radivojevic, M.; Shadmani, A.; Viswam, V.; Jones, I. L.; Fiscella, M.; Diggelmann, R.; et al. High-Resolution CMOS MEA Platform to Study Neurons at Subcellular, Cellular, and Network Levels. *Lab Chip* **2015**, *15*, 2767−2780.
(334) Bakkum, D. J.; Frey, U.; Radivojevic, M.; Russell, T. L.; Müller, J.; Fiscella, M.; Takahashi, H.; Hierlemann, A. Tracking Axonal Action Potential Propagation on a High-Density Microelectrode Array across Hundreds of Sites. *Nat. Commun.* **2013**, *4*, 2181.
(335) Sahu, M. P.; Nikkilä, O.; Lågas, S.; Kolehmainen, S.; Castrén, E. Culturing Primary Neurons from Rat Hippocampus and Cortex. *Neuronal Signal.* **2019**, *3*, NS20180207.
(336) Barnes, D. W.; Murayama, K.; Singh, N. N.; Helmrich, A. Neural Cell Lines. In *Protocols for Neural Cell Culture*; Fedoroff, S., Richardson, A., Eds.; Humana Press: Totowa, NJ, 2003; pp 219−228, DOI: DOI: 10.1385/1-59259-207-4:219.
(337) Gottlieb, D. I. Large-Scale Sources of Neural Stem Cells. *Annu. Rev. Neurosci.* **2002**, *25*, 381−407.
(338) Ma, D. K.; Bonaguidi, M. A.; Ming, G. L.; Song, H. Adult Neural Stem Cells in the Mammalian Central Nervous System. *Cell Res.* **2009**, *19*, 672−682.
(339) Lange, S. C.; Bak, L. K.; Waagepetersen, H. S.; Schousboe, A.; Norenberg, M. D. Primary Cultures of Astrocytes: Their Value in Understanding Astrocytes in Health and Disease. *Neurochem. Res.* **2012**, *37*, 2569−2588.
(340) Blain, M.; Miron, V. E.; Lambert, C.; Darlington, P. J.; Cui, Q.-L.; Saikali, P.; Yong, V. W.; Antel, J. P. *Isolation and Culture of Primary Human CNS Neural Cells*; Doering, L. C., Ed.; Humana Press: Totowa, NJ, 2009; pp 87−104, DOI: DOI: 10.1007/978-1-60761-292-6_5.
(341) Gross, P. G.; Kartalov, E. P.; Scherer, A.; Weiner, L. P. Applications of Microfluidics for Neuronal Studies. *J. Neurol. Sci.* **2007**, *252*, 135−143.
(342) Mccaughey-Chapman, A.; Connor, B. Human Cortical Neuron Generation Using Cell Reprogramming: A Review of Recent Advances. *Stem Cells Dev.* **2018**, *27*, 1674−1692.
(343) Fantuzzo, J. A.; De Filippis, L.; McGowan, H.; Yang, N.; Ng, Y.-H.; Halikere, A.; Liu, J.-J.; Hart, R. P.; Wernig, M.; Zahn, J. D.; et al. MNeurocircuitry: Establishing in Vitro Models of Neurocircuits with Human Neurons. *Technology* **2017**, *05*, 87−97.
(344) Habibey, R.; Sharma, K.; Swiersy, A.; Busskamp, V. Optogenetics for Neural Transplant Manipulation and Functional Analysis. *Biochem. Biophys. Res. Commun.* **2020**, *527*, 343−349.
(345) Hartlaub, A. M.; McElroy, C. A.; Maitre, N. L.; Hester, M. E. Modeling Human Brain Circuitry Using Pluripotent Stem Cell Platforms. *Front. Pediatr.* **2019**, *7*, 57.
(346) Hyman, S. E. Back to Basics: Luring Industry Back into Neuroscience. *Nat. Neurosci.* **2016**, *19*, 1383−1384.
(347) Ilic, D.; Ogilvie, C. Concise Review: Human Embryonic Stem Cells—What Have We Done? What Are We Doing? Where Are We Going? *Stem Cells* **2017**, *35*, 17−25.
(348) Silva, M. C.; Haggarty, S. J. Human Pluripotent Stem Cell−Derived Models and Drug Screening in CNS Precision Medicine. *Ann. N.Y. Acad. Sci.* **2020**, *1471*, 18−56.
(349) Stoeckli, E. T. Understanding Axon Guidance: Are We Nearly There Yet? *Development* **2018**, *145*, dev151415.

https://doi.org/10.1021/acs.chemrev.2c00212
Chem. Rev. 2022, 122, 14842−14880

(350) Stoeckli, E. Where Does Axon Guidance Lead Us? *F1000Research* **2017**, *6*, 78.
(351) Taylor, A. M.; Blurton-Jones, M.; Rhee, S. W.; Cribbs, D. H.; Cotman, C. W.; Jeon, N. L. A Microfluidic Culture Platform for CNS Axonal Injury, Regeneration and Transport. *Nat. Methods* **2005**, *2*, 599−605.
(352) Taylor, A. M.; Jeon, N. L. Microfluidic and Compartmentalized Platforms for Neurobiological Research. *Crit. Rev. Biomed. Eng.* **2011**, *39*, 185−200.
(353) Habibey, R.; Golabchi, A.; Latifi, S.; Difato, F.; Blau, A. A Microchannel Device Tailored to Laser Axotomy and Long-Term Microelectrode Array Electrophysiology of Functional Regeneration. *Lab Chip* **2015**, *15*, 4578−4590.
(354) Moutaux, E.; Christaller, W.; Scaramuzzino, C.; Genoux, A.; Charlot, B.; Cazorla, M.; Saudou, F. Neuronal Network Maturation Differently Affects Secretory Vesicles and Mitochondria Transport in Axons. *Sci. Rep.* **2018**, *8*, 13429.
(355) Wu, H. I.; Cheng, G. H.; Wong, Y. Y.; Lin, C. M.; Fang, W.; Chow, W. Y.; Chang, Y. C. A Lab-on-a-Chip Platform for Studying the Subcellular Functional Proteome of Neuronal Axons. *Lab Chip* **2010**, *10*, 647−653.
(356) Pan, L.; Alagapan, S.; Franca, E.; Brewer, G. J.; Wheeler, B. C. Propagation of Action Potential Activity in a Predefined Microtunnel Neural Network. *J. Neural Eng.* **2011**, *8*, 046031.
(357) Siddique, R.; Thakor, N. Investigation of Nerve Injury through Microfluidic Devices. *J. R. Soc. Interface* **2014**, *11*, 20130676.
(358) Shrirao, A. B.; Kung, F. H.; Omelchenko, A.; Schloss, R. S.; Boustany, N. N.; Zahn, J. D.; Yarmush, M. L.; Firestein, B. L. Microfluidic Platforms for the Study of Neuronal Injury in Vitro. *Biotechnol. Bioeng.* **2018**, *115*, 815−830.
(359) Hosmane, S.; Fournier, A.; Wright, R.; Rajbhandari, L.; Siddique, R.; Yang, I. H.; Ramesh, K. T.; Venkatesan, A.; Thakor, N. Valve-Based Microfluidic Compression Platform: Single Axon Injury and Regrowth. *Lab Chip* **2011**, *11*, 3888−3895.
(360) Jain, A.; Gillette, M. U. Development of Microfluidic Devices for the Manipulation of Neuronal Synapses. In *Microfluidic and Compartmentalized Platforms for Neurobiological Research*; Biffi, E., Ed.; Springer: New York, 2015; pp 127−137, DOI: DOI: 10.1007/978-1-4939-2510-0_7.
(361) Favuzzi, E.; Rico, B. Molecular Diversity Underlying Cortical Excitatory and Inhibitory Synapse Development. *Curr. Opin. Neurobiol.* **2018**, *53*, 8−15.
(362) Taylor, A. M.; Dieterich, D. C.; Ito, H. T.; Kim, S. A.; Schuman, E. M. Microfluidic Local Perfusion Chambers for the Visualization and Manipulation of Synapses. *Neuron* **2010**, *66*, 57−68.
(363) Mahto, S. K.; Song, H.; Rhee, S. W. Functional Synapse Formation between Compartmentalized Cortical Neurons Cultured inside Microfluidic Devices. *Biochip J.* **2011**, *5*, 289−298.
(364) Botzolakis, E. J.; Maheshwari, A.; Feng, H. J.; Lagrange, A. H.; Shaver, J. H.; Kassebaum, N. J.; Venkataraman, R.; Baudenbacher, F.; Macdonald, R. L. Achieving Synaptically Relevant Pulses of Neurotransmitter Using PDMS Microfluidics. *J. Neurosci. Methods* **2009**, *177*, 294−302.
(365) Moutaux, E.; Charlot, B.; Genoux, A.; Saudou, F.; Cazorla, M. An Integrated Microfluidic/Microelectrode Array for the Study of Activity-Dependent Intracellular Dynamics in Neuronal Networks. *Lab Chip* **2018**, *18*, 3425−3435.
(366) Virlogeux, A.; Moutaux, E.; Christaller, W.; Genoux, A.; Bruyère, J.; Fino, E.; Charlot, B.; Cazorla, M.; Saudou, F. Reconstituting Corticostriatal Network On-a-Chip Reveals the Contribution of the Presynaptic Compartment to Huntington's Disease. *Cell Rep.* **2018**, *22*, 110−122.
(367) Vysokov, N.; McMahon, S. B.; Raouf, R. The Role of NaV Channels in Synaptic Transmission after Axotomy in a Microfluidic Culture Platform. *Sci. Rep.* **2019**, *9*, 12915.
(368) Shimba, K.; Sakai, K.; Isomura, T.; Kotani, K.; Jimbo, Y. Axonal Conduction Slowing Induced by Spontaneous Bursting Activity in Cortical Neurons Cultured in a Microtunnel Device. *Integr. Biol. (United Kingdom)* **2015**, *7*, 64−72.
(369) Jang, J. M.; Lee, J.; Kim, H.; Jeon, N. L.; Jung, W. One-Photon and Two-Photon Stimulation of Neurons in a Microfluidic Culture System. *Lab Chip* **2016**, *16*, 1684−1690.
(370) Honegger, T.; Thielen, M. I.; Feizi, S.; Sanjana, N. E.; Voldman, J. Microfluidic Neurite Guidance to Study Structure-Function Relationships in Topologically-Complex Population-Based Neural Networks. *Sci. Rep.* **2016**, *6*, 28384.
(371) Lee, H. U.; Nag, S.; Blasiak, A.; Jin, Y.; Thakor, N.; Yang, I. H. Subcellular Optogenetic Stimulation for Activity-Dependent Myelination of Axons in a Novel Microfluidic Compartmentalized Platform. *ACS Chem. Neurosci.* **2016**, *7*, 1317−1324.
(372) Kamande, J.; Nagendran, T.; Harris, J.; Taylor, A. M. Multi-Compartment Microfluidic Device Geometry and Covalently Bound Poly-D-Lysine Influence Neuronal Maturation. *Front. Bioeng. Biotechnol.* **2019**, *7*, 84.
(373) Paranjape, S. R.; Nagendran, T.; Poole, V.; Harris, J.; Taylor, A. M. Compartmentalization of Human Stem Cell-Derived Neurons within Pre- Assembled Plastic Microfluidic Chips. *J. Vis. Exp.* **2019**, *2019*, 59250.
(374) Wieringa, P. A.; Wiertz, R. W. F.; De Weerd, E.; Rutten, W. L. C. Bifurcating Microchannels as a Scaffold to Induce Separation of Regenerating Neurites. *J. Neural Eng.* **2010**, *7*, 016001.
(375) Zhang, K.; Osakada, Y.; Vrljic, M.; Chen, L.; Mudrakola, H. V.; Cui, B. Single-Molecule Imaging of NGF Axonal Transport in Microfluidic Devices. *Lab Chip* **2010**, *10*, 2566−2573.
(376) Coquinco, A.; Kojic, L.; Wen, W.; Wang, Y. T.; Jeon, N. L.; Milnerwood, A. J.; Cynader, M. A Microfluidic Based in Vitro Model of Synaptic Competition. *Mol. Cell. Neurosci.* **2014**, *60*, 43−52.
(377) Shi, P.; Scott, M. A.; Ghosh, B.; Wan, D.; Wissner-Gross, Z.; Mazitschek, R.; Haggarty, S. J.; Yanik, M. F. Synapse Microarray Identification of Small Molecules That Enhance Synaptogenesis. *Nat. Commun.* **2011**, *2*, 510.
(378) Cohen, M. S.; Orth, C. B.; Kim, H. J.; Jeon, N. L.; Jaffrey, S. R. Neurotrophin-Mediated Dendrite-to-Nucleus Signaling Revealed by Microfluidic Compartmentalization of Dendrites. *Proc. Natl. Acad. Sci. U. S. A.* **2011**, *108*, 11246−11251.
(379) Triesch, J.; Vo, A. D.; Hafner, A. S. Competition for Synaptic Building Blocks Shapes Synaptic Plasticity. *Elife* **2018**, *7*, No. e37836.
(380) Morin, F.; Nishimura, N.; Griscom, L.; LePioufle, B.; Fujita, H.; Takamura, Y.; Tamiya, E. Constraining the Connectivity of Neuronal Networks Cultured on Microelectrode Arrays with Microfluidic Techniques: A Step towards Neuron-Based Functional Chips. *Biosens. Bioelectron.* **2006**, *21*, 1093−1100.
(381) Wheeler, B. C.; Brewer, G. J. Designing Neural Networks in Culture. *Proc. IEEE* **2010**, *98*, 398−406.
(382) Peyrin, J. M.; Deleglise, B.; Saias, L.; Vignes, M.; Gougis, P.; Magnifico, S.; Betuing, S.; Pietri, M.; Caboche, J.; Vanhoutte, P.; et al. Axon Diodes for the Reconstruction of Oriented Neuronal Networks in Microfluidic Chambers. *Lab Chip* **2011**, *11*, 3663−3673.
(383) Gladkov, A.; Pigareva, Y.; Kutyina, D.; Kolpakov, V.; Bukatin, A.; Mukhina, I.; Kazantsev, V.; Pimashkin, A. Design of Cultured Neuron Networks in Vitro with Predefined Connectivity Using Asymmetric Microfluidic Channels. *Sci. Rep.* **2017**, *7*, 15625.
(384) Renault, R.; Durand, J. B.; Viovy, J. L.; Villard, C. Asymmetric Axonal Edge Guidance: A New Paradigm for Building Oriented Neuronal Networks. *Lab Chip* **2016**, *16*, 2188−2191.
(385) Pan, L.; Alagapan, S.; Franca, E.; Leondopulos, S. S.; DeMarse, T. B.; Brewer, G. J.; Wheeler, B. C. An in Vitro Method to Manipulate the Direction and Functional Strength between Neural Populations. *Front. Neural Circuits.* **2015**, *9*, 32.
(386) Kim, H.; Lee, I. K.; Taylor, K.; Richters, K.; Baek, D. H.; Ryu, J. H.; Cho, S. J.; Jung, Y. H.; Park, D. W.; Novello, J.; et al. Single-Neuronal Cell Culture and Monitoring Platform Using a Fully Transparent Microfluidic DEP Device. *Sci. Rep.* **2018**, *8*, 13194.
(387) Li, W.; Xu, Z.; Huang, J.; Lin, X.; Luo, R.; Chen, C. H.; Shi, P. NeuroArray: A Universal Interface for Patterning and Interrogating Neural Circuitry with Single Cell Resolution. *Sci. Rep.* **2015**, *4*, 4784.

(388) Zhang, K.; Chou, C. K.; Xia, X.; Hung, M. C.; Qin, L. Block-Cell-Printing for Live Single-Cell Printing. *Proc. Natl. Acad. Sci. U. S. A.* **2014**, *111*, 2948−2953.
(389) Narula, U.; Ruiz, A.; McQuaide, M.; DeMarse, T. B.; Wheeler, B. C.; Brewer, G. J. Narrow Microtunnel Technology for the Isolation and Precise Identification of Axonal Communication among Distinct Hippocampal Subregion Networks. *PLoS One* **2017**, *12*, No. e0176868.
(390) Kanagasabapathi, T. T.; Ciliberti, D.; Martinoia, S.; Wadman, W. J.; Decré, M. M. J. Dual-Compartment Neurofluidic System for Electrophysiological Measurements in Physically Segregated and Functionally Connected Neuronal Cell Culture. *Front. Neuroeng.* **2011**, *4*, 13.
(391) Kanagasabapathi, T. T.; Massobrio, P.; Barone, R. A.; Tedesco, M.; Martinoia, S.; Wadman, W. J.; Decré, M. M. J. Functional Connectivity and Dynamics of Cortical-Thalamic Networks Co-Cultured in a Dual Compartment Device. *J. Neural Eng.* **2012**, *9*, 036010.
(392) Poli, D.; Demarse, T. B.; Wheeler, B. C.; Brewer, G. J. Specific CA3 Neurons Decode Neural Information of Dentate Granule Cells Evoked by Paired-Pulse Stimulation in Co-Cultured Networks. In *Proceedings of the Annual International Conference of the IEEE Engineering in Medicine and Biology Society, EMBS*; 2017; pp 3628−3631, DOI: DOI: 10.1109/EMBC.2017.8037643.
(393) Poli, D.; Wheeler, B. C.; Demarse, T. B.; Brewer, G. J. Pattern Separation and Completion of Distinct Axonal Inputs Transmitted via Micro-Tunnels between Co-Cultured Hippocampal Dentate, CA3, CA1 and Entorhinal Cortex Networks. *J. Neural Eng.* **2018**, *15*, 046009.
(394) van de Wijdeven, R.; Ramstad, O. H.; Bauer, U. S.; Halaas, Ø.; Sandvig, A.; Sandvig, I. Structuring a Multi-Nodal Neural Network in Vitro within a Novel Design Microfluidic Chip. *Biomed. Microdevices* **2018**, *20*, 9.
(395) Sarkar, A.; Mei, A.; Paquola, A. C. M.; Stern, S.; Bardy, C.; Klug, J. R.; Kim, S.; Neshat, N.; Kim, H. J.; Ku, M.; et al. Efficient Generation of CA3 Neurons from Human Pluripotent Stem Cells Enables Modeling of Hippocampal Connectivity In Vitro. *Cell Stem Cell* **2018**, *22*, 684.
(396) Fantuzzo, J. A.; Robles, D. A.; Mirabella, V. R.; Hart, R. P.; Pang, Z. P.; Zahn, J. D. Development of a High-Throughput Arrayed Neural Circuitry Platform Using Human Induced Neurons for Drug Screening Applications. *Lab Chip* **2020**, *20*, 1140−1152.
(397) Markov, N. T.; Vezoli, J.; Chameau, P.; Falchier, A.; Quilodran, R.; Huissoud, C.; Lamy, C.; Misery, P.; Giroud, P.; Ullman, S.; et al. Anatomy of Hierarchy: Feedforward and Feedback Pathways in Macaque Visual Cortex. *J. Comp. Neurol.* **2014**, *522*, 225−259.
(398) Pessoa, L. Understanding Brain Networks and Brain Organization. *Phys. Life Rev.* **2014**, *11*, 400−435.
(399) Holland, S. M.; Collura, K. M.; Ketschek, A.; Noma, K.; Ferguson, T. A.; Jin, Y.; Gallo, G.; Thomas, G. M. Palmitoylation Controls DLK Localization, Interactions and Activity to Ensure Effective Axonal Injury Signaling. *Proc. Natl. Acad. Sci. U. S. A.* **2016**, *113*, 763−768.
(400) Poli, D.; Thiagarajan, S.; DeMarse, T. B.; Wheeler, B. C.; Brewer, G. J. Sparse and Specific Coding during Information Transmission between Co-Cultured Dentate Gyrus and CA3 Hippocampal Networks. *Front. Neural Circuits* **2017**, *11*, 13.
(401) Su, P. J.; Liu, Z.; Zhang, K.; Han, X.; Saito, Y.; Xia, X.; Yokoi, K.; Shen, H.; Qin, L. Retinal Synaptic Regeneration via Microfluidic Guiding Channels. *Sci. Rep.* **2015**, *5*, 13591.
(402) Barral, J.; Wang, X. J.; Reyes, A. D. Propagation of Temporal and Rate Signals in Cultured Multilayer Networks. *Nat. Commun.* **2019**, *10*, 3969.
(403) Park, J.; Koito, H.; Li, J.; Han, A. Microfluidic Compartmentalized Co-Culture Platform for CNS Axon Myelination Research. *Biomed. Microdevices* **2009**, *11*, 1145−1153.
(404) Lassus, B.; Naudé, J.; Faure, P.; Guedin, D.; Von Boxberg, Y.; Mannoury la Cour, C.; Millan, M. J.; Peyrin, J. M. Glutamatergic and Dopaminergic Modulation of Cortico-Striatal Circuits Probed by Dynamic Calcium Imaging of Networks Reconstructed in Microfluidic Chips. *Sci. Rep.* **2018**, *8*, 17461.
(405) Bhattacharya, A.; Desai, H.; DeMarse, T. B.; Wheeler, B. C.; Brewer, G. J. Repeating Spatial-Temporal Motifs of CA3 Activity Dependent on Engineered Inputs from Dentate Gyrus Neurons in Live Hippocampal Networks. *Front. Neural Circuits* **2016**, *10*, 45.
(406) Brewer, G. J.; Boehler, M. D.; Leondopulos, S.; Pan, L.; Alagapan, S.; DeMarse, T. B.; Wheeler, B. C. Toward a Self-Wired Active Reconstruction of the Hippocampal Trisynaptic Loop: DG-CA3. *Front. Neural Circuits* **2013**, *7*, 165.
(407) Isomura, T.; Shimba, K.; Takayama, Y.; Takeuchi, A.; Kotani, K.; Jimbo, Y. Signal Transfer within a Cultured Asymmetric Cortical Neuron Circuit. *J. Neural Eng.* **2015**, *12*, 066023.
(408) Holloway, P. M.; Hallinan, G. I.; Hegde, M.; Lane, S. I. R.; Deinhardt, K.; West, J. Asymmetric Confinement for Defining Outgrowth Directionality. *Lab Chip* **2019**, *19*, 1484−1489.
(409) Le Feber, J.; Postma, W.; de Weerd, E.; Weusthof, M.; Rutten, W. L. C. Barbed Channels Enhance Unidirectional Connectivity between Neuronal Networks Cultured on Multi Electrode Arrays. *Front. Neurosci.* **2015**, *9*, 412.
(410) Levy, O.; Ziv, N. E.; Marom, S. Enhancement of Neural Representation Capacity by Modular Architecture in Networks of Cortical Neurons. *Eur. J. Neurosci.* **2012**, *35*, 1753−1760.
(411) Jokinen, V.; Sakha, P.; Suvanto, P.; Rivera, C.; Franssila, S.; Lauri, S. E.; Huttunen, H. J. A Microfluidic Chip for Axonal Isolation and Electrophysiological Measurements. *J. Neurosci. Methods* **2013**, *212*, 276−282.
(412) Feinerman, O.; Rotem, A.; Moses, E. Reliable Neuronal Logic Devices from Patterned Hippocampal Cultures. *Nat. Phys.* **2008**, *4*, 967−973.
(413) Feinerman, O.; Moses, E. Transport of Information along Unidimensional Layered Networks of Dissociated Hippocampal Neurons and Implications for Rate Coding. *J. Neurosci.* **2006**, *26*, 4526−4534.
(414) Albers, J.; Offenhäusser, A. Signal Propagation between Neuronal Populations Controlled by Micropatterning. *Front. Bioeng. Biotechnol.* **2016**, *4*, 46.
(415) Renault, R.; Sukenik, N.; Descroix, S.; Malaquin, L.; Viovy, J. L.; Peyrin, J. M.; Bottani, S.; Monceau, P.; Moses, E.; Vignes, M. Combining Microfluidics, Optogenetics and Calcium Imaging to Study Neuronal Communication in Vitro. *PLoS One* **2015**, *10*, No. e0120680.
(416) Korhonen, P.; Malm, T.; White, A. R. 3D Human Brain Cell Models: New Frontiers in Disease Understanding and Drug Discovery for Neurodegenerative Diseases. *Neurochem. Int.* **2018**, *120*, 191−199.
(417) Hopkins, A. M.; DeSimone, E.; Chwalek, K.; Kaplan, D. L. 3D in Vitro Modeling of the Central Nervous System. *Prog. Neurobiol.* **2015**, *125*, 1−25.
(418) Hsieh, F. Y.; Lin, H. H.; Hsu, S. 3D Bioprinting of Neural Stem Cell-Laden Thermoresponsive Biodegradable Polyurethane Hydrogel and Potential in Central Nervous System Repair. *Biomaterials* **2015**, *71*, 48−57.
(419) Zhuang, P.; Sun, A. X.; An, J.; Chua, C. K.; Chew, S. Y. 3D Neural Tissue Models: From Spheroids to Bioprinting. *Biomaterials* **2018**, *154*, 113−133.
(420) Murphy, A. R.; Laslett, A.; O'Brien, C. M.; Cameron, N. R. Scaffolds for 3D in Vitro Culture of Neural Lineage Cells. *Acta Biomater.* **2017**, *54*, 1−20.
(421) Sensharma, P.; Madhumathi, G.; Jayant, R. D.; Jaiswal, A. K. Biomaterials and Cells for Neural Tissue Engineering: Current Choices. *Mater. Sci. Eng., C* **2017**, *77*, 1302−1315.
(422) Shimba, K.; Chang, C. H.; Asahina, T.; Moriya, F.; Kotani, K.; Jimbo, Y.; Gladkov, A.; Antipova, O.; Pigareva, Y.; Kolpakov, V.; et al. Functional Scaffolding for Brain Implants: Engineered Neuronal Network by Microfabrication and IPSC Technology. *Front. Neurosci.* **2019**, *13*, 890.
(423) Kato-Negishi, M.; Morimoto, Y.; Onoe, H.; Takeuchi, S. Millimeter-Sized Neural Building Blocks for 3D Heterogeneous Neural Network Assembly. *Adv. Healthc. Mater.* **2013**, *2*, 1564−1570.
(424) Odawara, A.; Gotoh, M.; Suzuki, I. A Three-Dimensional Neuronal Culture Technique That Controls the Direction of Neurite

Elongation and the Position of Soma to Mimic the Layered Structure of the Brain. *RSC Adv.* **2013**, *3*, 23620−23630.
(425) Bang, S.; Na, S.; Jang, J. M.; Kim, J.; Jeon, N. L. Engineering-Aligned 3D Neural Circuit in Microfluidic Device. *Adv. Healthc. Mater.* **2016**, *5*, 159−166.
(426) Kim, S. H.; Im, S. K.; Oh, S. J.; Jeong, S.; Yoon, E. S.; Lee, C. J.; Choi, N.; Hur, E. M. Anisotropically Organized Three-Dimensional Culture Platform for Reconstruction of a Hippocampal Neural Network. *Nat. Commun.* **2017**, *8*, 14346.
(427) Fennema, E.; Rivron, N.; Rouwkema, J.; van Blitterswijk, C.; De Boer, J. Spheroid Culture as a Tool for Creating 3D Complex Tissues. *Trends Biotechnol.* **2013**, *31*, 108−115.
(428) Clevers, H. Modeling Development and Disease with Organoids. *Cell* **2016**, *165*, 1586−1597.
(429) Sharma, K.; Krohne, T. U.; Busskamp, V. The Rise of Retinal Organoids for Vision Research. *Int. J. Mol. Sci.* **2020**, *21*, 8484.
(430) Qian, X.; Nguyen, H. N.; Song, M. M.; Hadiono, C.; Ogden, S. C.; Hammack, C.; Yao, B.; Hamersky, G. R.; Jacob, F.; Zhong, C.; et al. Brain-Region-Specific Organoids Using Mini-Bioreactors for Modeling ZIKV Exposure. *Cell* **2016**, *165*, 1238−1254.
(431) Qian, X.; Song, H.; Ming, G. L. Brain Organoids: Advances, Applications and Challenges. *Dev.* **2019**, *146*, dev166074.
(432) Kadoshima, T.; Sakaguchi, H.; Nakano, T.; Soen, M.; Ando, S.; Eiraku, M.; Sasai, Y. Self-Organization of Axial Polarity, inside-out Layer Pattern, and Species-Specific Progenitor Dynamics in Human ES Cell-Derived Neocortex. *Proc. Natl. Acad. Sci. U. S. A.* **2013**, *110*, 20284−20289.
(433) Dehorter, N.; Del Pino, I. Shifting Developmental Trajectories During Critical Periods of Brain Formation. *Front. Cell Neurosci.* **2020**, *14*, 283.
(434) Jo, J.; Xiao, Y.; Sun, A. X.; Cukuroglu, E.; Tran, H. D.; Göke, J.; Tan, Z. Y.; Saw, T. Y.; Tan, C. P.; Lokman, H.; et al. Midbrain-like Organoids from Human Pluripotent Stem Cells Contain Functional Dopaminergic and Neuromelanin-Producing Neurons. *Cell Stem Cell* **2016**, *19*, 248−257.
(435) Yoon, S. J.; Elahi, L. S.; Paşca, A. M.; Marton, R. M.; Gordon, A.; Revah, O.; Miura, Y.; Walczak, E. M.; Holdgate, G. M.; Fan, H. C.; et al. Reliability of Human Cortical Organoid Generation. *Nat. Methods* **2019**, *16*, 75−78.
(436) Muguruma, K.; Nishiyama, A.; Kawakami, H.; Hashimoto, K.; Sasai, Y. Self-Organization of Polarized Cerebellar Tissue in 3D Culture of Human Pluripotent Stem Cells. *Cell Rep.* **2015**, *10*, 537−550.
(437) Sakaguchi, H.; Kadoshima, T.; Soen, M.; Narii, N.; Ishida, Y.; Ohgushi, M.; Takahashi, J.; Eiraku, M.; Sasai, Y. Generation of Functional Hippocampal Neurons from Self-Organizing Human Embryonic Stem Cell-Derived Dorsomedial Telencephalic Tissue. *Nat. Commun.* **2015**, *6*, 8896.
(438) Xiang, Y.; Tanaka, Y.; Patterson, B.; Kang, Y. J.; Govindaiah, G.; Roselaar, N.; Cakir, B.; Kim, K. Y.; Lombroso, A. P.; Hwang, S. M.; et al. Fusion of Regionally Specified HPSC-Derived Organoids Models Human Brain Development and Interneuron Migration. *Cell Stem Cell* **2017**, *21*, 383.
(439) Birey, F.; Andersen, J.; Makinson, C. D.; Islam, S.; Wei, W.; Huber, N.; Fan, H. C.; Metzler, K. R. C.; Panagiotakos, G.; Thom, N.; et al. Assembly of Functionally Integrated Human Forebrain Spheroids. *Nature* **2017**, *545*, 54−59.
(440) Bagley, J. A.; Reumann, D.; Bian, S.; Lévi-Strauss, J.; Knoblich, J. A. Fused Cerebral Organoids Model Interactions between Brain Regions. *Nat. Methods* **2017**, *14*, 743−751.
(441) Panoutsopoulos, A.; Organoids, A. Assembloids, and Novel Biotechnology: Steps Forward in Developmental and Disease-Related Neuroscience. *Neuroscientist* **2021**, *27*, 463−472.
(442) Andersen, J.; Revah, O.; Miura, Y.; Thom, N.; Amin, N. D.; Kelley, K. W.; Singh, M.; Chen, X.; Thete, M. V.; Walczak, E. M.; et al. Generation of Functional Human 3D Cortico-Motor Assembloids. *Cell* **2020**, *183*, 1913.
(443) Xiang, Y.; Tanaka, Y.; Cakir, B.; Patterson, B.; Kim, K. Y.; Sun, P.; Kang, Y. J.; Zhong, M.; Liu, X.; Patra, P.; et al. HESC-Derived Thalamic Organoids Form Reciprocal Projections When Fused with Cortical Organoids. *Cell Stem Cell* **2019**, *24*, 487.
(444) Mansour, A. A.; Gonçalves, J. T.; Bloyd, C. W.; Li, H.; Fernandes, S.; Quang, D.; Johnston, S.; Parylak, S. L.; Jin, X.; Gage, F. H. An in Vivo Model of Functional and Vascularized Human Brain Organoids. *Nat. Biotechnol.* **2018**, *36*, 432−441.
(445) Cai, H.; Ao, Z.; Wu, Z.; Song, S.; Mackie, K.; Guo, F. Intelligent Acoustofluidics Enabled Mini-Bioreactors for Human Brain Organoids. *Lab Chip* **2021**, *21*, 2194−2205.
(446) Shou, Y.; Liang, F.; Xu, S.; Li, X. The Application of Brain Organoids: From Neuronal Development to Neurological Diseases. *Front. Cell Dev. Biol.* **2020**, *8*, 579659.
(447) Liu, H.; Wang, Y.; Wang, H.; Zhao, M.; Tao, T.; Zhang, X.; Qin, J. A Droplet Microfluidic System to Fabricate Hybrid Capsules Enabling Stem Cell Organoid Engineering. *Adv. Sci.* **2020**, *7*, 1903739.
(448) Shi, Y.; Sun, L.; Wang, M.; Liu, J.; Zhong, S.; Li, R.; Li, P.; Guo, L.; Fang, A.; Chen, R.; et al. Vascularized Human Cortical Organoids (VOrganoids) Model Cortical Development in Vivo. *PLoS Biol.* **2020**, *18*, No. e3000705.
(449) Park, J.; Lee, B. K.; Jeong, G. S.; Hyun, J. K.; Lee, C. J.; Lee, S. H. Three-Dimensional Brain-on-a-Chip with an Interstitial Level of Flow and Its Application as an in Vitro Model of Alzheimer's Disease. *Lab Chip* **2015**, *15*, 141−150.
(450) Wang, Y.; Wang, L.; Guo, Y.; Zhu, Y.; Qin, J. Engineering Stem Cell-Derived 3D Brain Organoids in a Perfusable Organ-on-a-Chip System. *RSC Adv.* **2018**, *8*, 1677−1685.
(451) Cho, A. N.; Jin, Y.; An, Y.; Kim, J.; Choi, Y. S.; Lee, J. S.; Kim, J.; Choi, W. Y.; Koo, D. J.; Yu, W.; et al. Microfluidic Device with Brain Extracellular Matrix Promotes Structural and Functional Maturation of Human Brain Organoids. *Nat. Commun.* **2021**, *12*, 4730.
(452) Uzel, S. G. M.; Platt, R. J.; Subramanian, V.; Pearl, T. M.; Rowlands, C. J.; Chan, V.; Boyer, L. A.; So, P. T. C.; Kamm, R. D. Microfluidic Device for the Formation of Optically Excitable, Three-Dimensional, Compartmentalized Motor Units. *Sci. Adv.* **2016**, *2*, No. e1501429.
(453) Osaki, T.; Uzel, S. G. M.; Kamm, R. D. Microphysiological 3D Model of Amyotrophic Lateral Sclerosis (ALS) from Human IPS-Derived Muscle Cells and Optogenetic Motor Neurons. *Sci. Adv.* **2018**, *4*, eaat5847−eaat5847.
(454) de Jongh, R.; Spijkers, X. M.; Pasteuning-Vuhman, S.; Vulto, P.; Pasterkamp, R. J. Neuromuscular Junction-on-a-Chip: ALS Disease Modeling and Read-out Development in Microfluidic Devices. *J. Neurochem.* **2021**, *157*, 393−412.
(455) Osaki, T.; Sivathanu, V.; Kamm, R. D. Engineered 3D Vascular and Neuronal Networks in a Microfluidic Platform. *Sci. Rep.* **2018**, *8*, 5168.
(456) Oddo, A.; Peng, B.; Tong, Z.; Wei, Y.; Tong, W. Y.; Thissen, H.; Voelcker, N. H. Advances in Microfluidic Blood−Brain Barrier (BBB) Models. *Trends Biotechnol.* **2019**, *37*, 1295−1314.
(457) Jiang, L.; Li, S.; Zheng, J.; Li, Y.; Huang, H. Recent Progress in Microfluidic Models of the Blood-Brain Barrier. *Micromachines* **2019**, *10*, 375.
(458) Adriani, G.; Ma, D.; Pavesi, A.; Kamm, R. D.; Goh, E. L. K. A 3D Neurovascular Microfluidic Model Consisting of Neurons, Astrocytes and Cerebral Endothelial Cells as a Blood-Brain Barrier. *Lab Chip* **2017**, *17*, 448−459.
(459) Lee, S. R.; Hyung, S.; Bang, S.; Lee, Y.; Ko, J.; Lee, S.; Kim, H. J.; Jeon, N. L. Modeling Neural Circuit, Blood-Brain Barrier, and Myelination on a Microfluidic 96 Well Plate. *Biofabrication* **2019**, *11*, 035013.
(460) Del Dosso, A.; Urenda, J. P.; Nguyen, T.; Quadrato, G. Upgrading the Physiological Relevance of Human Brain Organoids. *Neuron* **2020**, *107*, 1014−1028.
(461) Bergmann, S.; Schindler, M.; Munger, C.; Penfold, C. A.; Boroviak, T. E. Building a Stem Cell-Based Primate Uterus. *Commun. Biol.* **2021**, *4*, 749.
(462) Qiao, H.; Zhang, Y. S.; Chen, P. Commentary: Human Brain Organoid-on-a-Chip to Model Prenatal Nicotine Exposure. *Front. Bioeng. Biotechnol.* **2018**, *6*, 138.

https://doi.org/10.1021/acs.chemrev.2c00212
Chem. Rev. 2022, 122, 14842−14880

(463) Achberger, K.; Probst, C.; Haderspeck, J. C.; Bolz, S.; Rogal, J.; Chuchuy, J.; Nikolova, M.; Cora, V.; Antkowiak, L.; Haq, W.; et al. Merging Organoid and Organ-on-a-Chip Technology to Generate Complex Multi-Layer Tissue Models in a Human Retina-on-a-Chip Platform. *Elife* **2019**, *8*, No. e46188.
(464) Akhtar, A. A.; Sances, S.; Barrett, R.; Breunig, J. J. Organoid and Organ-on-a-Chip Systems: New Paradigms for Modeling Neurological and Gastrointestinal Disease. *Curr. Stem Cell Rep.* **2017**, *3*, 98−111.
(465) Marton, R. M.; Paşca, S. P. Organoid and Assembloid Technologies for Investigating Cellular Crosstalk in Human Brain Development and Disease. *Trends Cell Biol.* **2020**, *30*, 133−143.
(466) Sloan, S. A.; Andersen, J.; Paşca, A. M.; Birey, F.; Paşca, S. P. Generation and Assembly of Human Brain Region−Specific Three-Dimensional Cultures. *Nat. Protoc.* **2018**, *13*, 2062−2085.
(467) Tanaka, Y.; Park, I. H. Regional Specification and Complementation with Non-Neuroectodermal Cells in Human Brain Organoids. *J. Mol. Med.* **2021**, *99*, 489−500.
(468) Saalfrank, D.; Konduri, A. K.; Latifi, S.; Habibey, R.; Golabchi, A.; Martiniuc, A. V.; Knoll, A.; Ingebrandt, S.; Blau, A. Incubator-Independent Cell-Culture Perfusion Platform for Continuous Long-Term Microelectrode Array Electrophysiology and Time-Lapse Imaging. *R. Soc. Open Sci.* **2015**, *2*, 150031.
(469) Hasan, M.; Latifi, S.; Kahn, C. J. F.; Tamayol, A.; Habibey, R.; Passeri, E.; Linder, M.; Arab-Tehrany, E. The Positive Role of Curcumin-Loaded Salmon Nanoliposomes on the Culture of Primary Cortical Neurons. *Mar. Drugs.* **2018**, *16*, 218.
(470) Konduri, A. K.; Deepak, C. S.; Purohit, S.; Narayan, K. S. An Integrated 3D Fluidic Device with Bubble Guidance Mechanism for Long-Term Primary and Secondary Cell Recordings on Multi-Electrode Array Platform. *Biofabrication* **2020**, *12*, 045019.
(471) Kreutzer, J.; Ylä-Outinen, L.; Mäki, A. J.; Ristola, M.; Narkilahti, S.; Kallio, P. Cell Culture Chamber with Gas Supply for Prolonged Recording of Human Neuronal Cells on Microelectrode Array. *J. Neurosci. Methods* **2017**, *280*, 27−35.
(472) Palazzo, G.; Geminiani, A.; Regalia, G.; Ferrigno, G.; Menegon, A.; Pedrocchi, A. Validation of a Bench-Top Culturing and Electrophysiogical Recording Chamber for Neurophysiological Trials. In *MeMeA 2018—2018 IEEE International Symposium on Medical Measurements and Applications, Proceedings*, 2018; pp 1−6, DOI: DOI: 10.1109/MeMeA.2018.8438665.
(473) Shin, H.; Jeong, S.; Lee, J. H.; Sun, W.; Choi, N.; Cho, I. J. 3D High-Density Microelectrode Array with Optical Stimulation and Drug Delivery for Investigating Neural Circuit Dynamics. *Nat. Commun.* **2021**, *12*, 492.
(474) Halldorsson, S.; Lucumi, E.; Gómez-Sjöberg, R.; Fleming, R. M. T. Advantages and Challenges of Microfluidic Cell Culture in Polydimethylsiloxane Devices. *Biosens. Bioelectron.* **2015**, *63*, 218−231.
(475) Wnorowski, A.; Yang, H.; Wu, J. C. Progress, Obstacles, and Limitations in the Use of Stem Cells in Organ-on-a-Chip Models. *Adv. Drug Delivery Rev.* **2019**, *140*, 3−11.
(476) Geraili, A.; Jafari, P.; Hassani, M. S.; Araghi, B. H.; Mohammadi, M. H.; Ghafari, A. M.; Tamrin, S. H.; Modarres, H. P.; Kolahchi, A. R.; Ahadian, S.; et al. Controlling Differentiation of Stem Cells for Developing Personalized Organ-on-Chip Platforms. *Adv. Healthc. Mater.* **2018**, *7*, 1700426.
(477) Alcendor, D. J.; Block, F. E.; Cliffel, D. E.; Daniels, J. S.; Ellacott, K. L. J.; Goodwin, C. R.; Hofmeister, L. H.; Li, D.; Markov, D. A.; May, J. C.; et al. Neurovascular Unit on a Chip: Implications for Translational Applications. *Stem Cell Res. Ther.* **2013**, *4*, S18.

https://doi.org/10.1021/acs.chemrev.2c00212
Chem. Rev. 2022, 122, 14842−14880